AD-A121 600

DRDAR-LCB-TL

MEMORANDUM REPORT ARBRL-MR-03207

BLAST WAVE LOADING OF A TWO-DIMENSIONAL CIRCULAR CYLINDER

George A. Coulter

November 1982

US ARMY ARMAMENT RESEARCH AND DEVELOPMENT COMMAND
BALLISTIC RESEARCH LABORATORY
ABERDEEN PROVING GROUND, MARYLAND

UNCLASSIFIED

SECURITY CLASSIFICATION OF THIS PAGE (When Data Entered)

REPORT DOCUMENTATION PAGE		READ INSTRUCTIONS BEFORE COMPLETING FORM
1. REPORT NUMBER Memorandum Report ARBRL-MR-03207	2. GOVT ACCESSION NO.	3. RECIPIENT'S CATALOG NUMBER
4. TITLE (and Subtitle) BLAST WAVE LOADING OF A TWO-DIMENSIONAL CIRCULAR CYLINDER		5. TYPE OF REPORT & PERIOD COVERED Final
		6. PERFORMING ORG. REPORT NUMBER
7. AUTHOR(s) George A. Coulter		8. CONTRACT OR GRANT NUMBER(s)
9. PERFORMING ORGANIZATION NAME AND ADDRESS USA Ballistic Research Laboratory ATTN: DRDAR-BLT Aberdeen Proving Ground, MD 21005		10. PROGRAM ELEMENT, PROJECT, TASK AREA & WORK UNIT NUMBERS Project No. 1L162618AH80
11. CONTROLLING OFFICE NAME AND ADDRESS US Army Armament Research & Development Command US Army Ballistic Research Laboratory (DRDAR-BL) Aberdeen Proving Ground, MD 21005		12. REPORT DATE November 1982
		13. NUMBER OF PAGES 92
14. MONITORING AGENCY NAME & ADDRESS(if different from Controlling Office)		15. SECURITY CLASS. (of this report) UNCLASSIFIED
		15a. DECLASSIFICATION/DOWNGRADING SCHEDULE

16. DISTRIBUTION STATEMENT (of this Report)

Approved for public release; distribution unlimited

17. DISTRIBUTION STATEMENT (of the abstract entered in Block 20, if different from Report)

18. SUPPLEMENTARY NOTES

19. KEY WORDS (Continue on reverse side if necessary and identify by block number)

Blast Waves
Blast Effects
Diffraction Loading
Model Cylinder
Overpressure
Stagnation Loading

20. ABSTRACT (Continue on reverse side if necessary and identify by block number)

A two-dimensional non-responding cylinder was exposed to decaying shock waves induced in the BRL 57.5 cm shock tube. Pressure-time records are shown for transducer locations spaced at 15° intervals around the cylinder for input side-on overpressure levels of 42.3, 75.9, and 112.2 kPa. Pertinent loading results are listed in tabular form.

DD FORM 1 JAN 73 1473 EDITION OF 1 NOV 65 IS OBSOLETE

UNCLASSIFIED

SECURITY CLASSIFICATION OF THIS PAGE (When Data Entered)

TABLE OF CONTENTS

LIST OF ILLUSTRATIONS

LIST OF ILLUSTRATIONS (cont'd)

LIST OF TABLES

I. INTRODUCTION

Researchers have used a variety of techniques[1-5] to obtain blast loading data in their study of generic shapes. Of these basic shapes; rectangles, cylinders, spheres, and cones have special interest for the Army in that many weapons' systems include one or more of these shapes. The blast loading data were obtained in the studies by means of shadowgraphy, interferometry, pressure-time recording, and with force balances to define the flow fields and drag loading generated by the blast loading from a given weapon.

More recently, two and three dimensional hydrocodes have been developed and are being used[6-8] to predict the flow fields created by blast wave loads. In a sense, the hydrocodes may produce predicted results that summarize the data from the several experimental techniques used to determine blast loads. Wave systems, flow fields, and pressure or density fields may be generated by output from hydrocodes. Integration of the predicted loads over a given target surface may be used to calculate total loads and to generate coefficients of pressure or drag.

---

[1] *S.H. J. Allen and W. G. Vincenti, "Wall Interference in a Two-Dimensional Flow Wind Tunnel with Consideration of the Effect of Compressibility," Nat. Adv. Comm. for Aeronautics Report 782, 1944.*

[2] *R.N. Holbyer and R.E. Duff, "The Effect of Wall Boundary Layer on the Diffraction of Shock Waves around Cylindrical and Rectangular Obstacles," University of Michigan Report 50-2, 1950.*

[3] *W. Bleakney and D.R. White, "Shock Loading of Rectangular Structures," Dept. of Physics Tech. Report II, 11, Princeton Univ., January 1952.*

[4] *N.K. Delany and N.E. Sorensen, "Low Speed Drag of Cylinders of Various Shapes," Nat. Adv. Comm. Aero. Technical Note 3038, Wash., DC, 1953.*

[5] *George A. Coulter and William T. Matthews, "Coefficients of Drag Measured with a Force Balance," BRL Technical Note 1155, December 1954.*

[6] *M.A. Fry and others, "The HULL Hydro-Dynamics Computer Code," AFWL-TR-76-183, U.S. Air Force Weapons Lab, Kirtland Air Force Base, NM, September 1976.*

[7] *Richard E. Lottero, "A Detailed Comparison of 3-D Hydrocodes Computations for Shock Diffraction Loading on an S-280 Electrical Equipment Shelter," BRL Technical Report ARBRL-TR-02334, June 1981.*

[8] *John D. Wortman , "Blast Computations over a Hemicylindrical Aircraft Shelter," BRL Memorandum Report ARBRL-MR-03115, July 1981.*

To build up confidence in a given code or analytical method, point-by-point experimental comparisons are needed. The purpose of the tests reported here is to provide blast loading data for a two-dimensional cylinder which will allow such a comparison. The loading function used is a decaying wave provided by the Ballistic Research Laboratory's (BRL) 57.5 cm shock tube. The next section describes the test procedure used.

II. TEST PROCEDURE

The test procedure is discussed in three parts: the BRL 57.5 cm shock tube, the cylinder, and the instrumentation.

A. BRL 57.5 cm Shock Tube

The BRL 57.5 cm shock tube[9] was modified by installing a 92 cm driver section. Other parameters were left the same. The short driver allowed the rarefaction wave from the driver section to catch up with the shock front[10] and create an exponentially decaying shock wave in the shock tube test section, Figure 1. The pressure-time history, although derived one-dimensionally in the shock tube, simulated quite well a free-field wave. Comparisons between the two types of waves are made in the Analysis Section.

The shock tube was operated in the air-air mode with ambient air present in the test section. The entire downstream test section was open to the outside air. No end plate was used. Driver pressures were chosen to give side-on shock overpressures in the range 42.3 kPa (6.1 psi) to 112.2 kPa (16.3 psi). Shots were repeated until pressure-time histories were recorded for 15° increments of cylinder rotation for the pressure range chosen.

B. Two Dimensional Cylinder

Figure 2 shows the location of the transducers and Figure 3 shows the cylinder in 50.8 cm square test section of the shock tube. Because of transducer-connector length, four transducer locations were chosen at 45° intervals around the model near the center of its length. The remaining 15° intervals were exposed to succeeding repetitive shots of the shock tube. Station 0 was defined to be facing directly into the on-coming shock front, 0°.

---

[9] *George A. Coulter and Brian P. Bertrand, "BRL Shock Tube Facility for the Simulation of Air Blast Effects," BRL Memo Report No. 1685, August 1965.*

[10] *C.W. Lampson, "Résumé of the Theory of Plane Shock and Adiabatic Waves with Applications to the Theory of the Shock Tube," BRL Tech. Note No. 139, March 1950.*

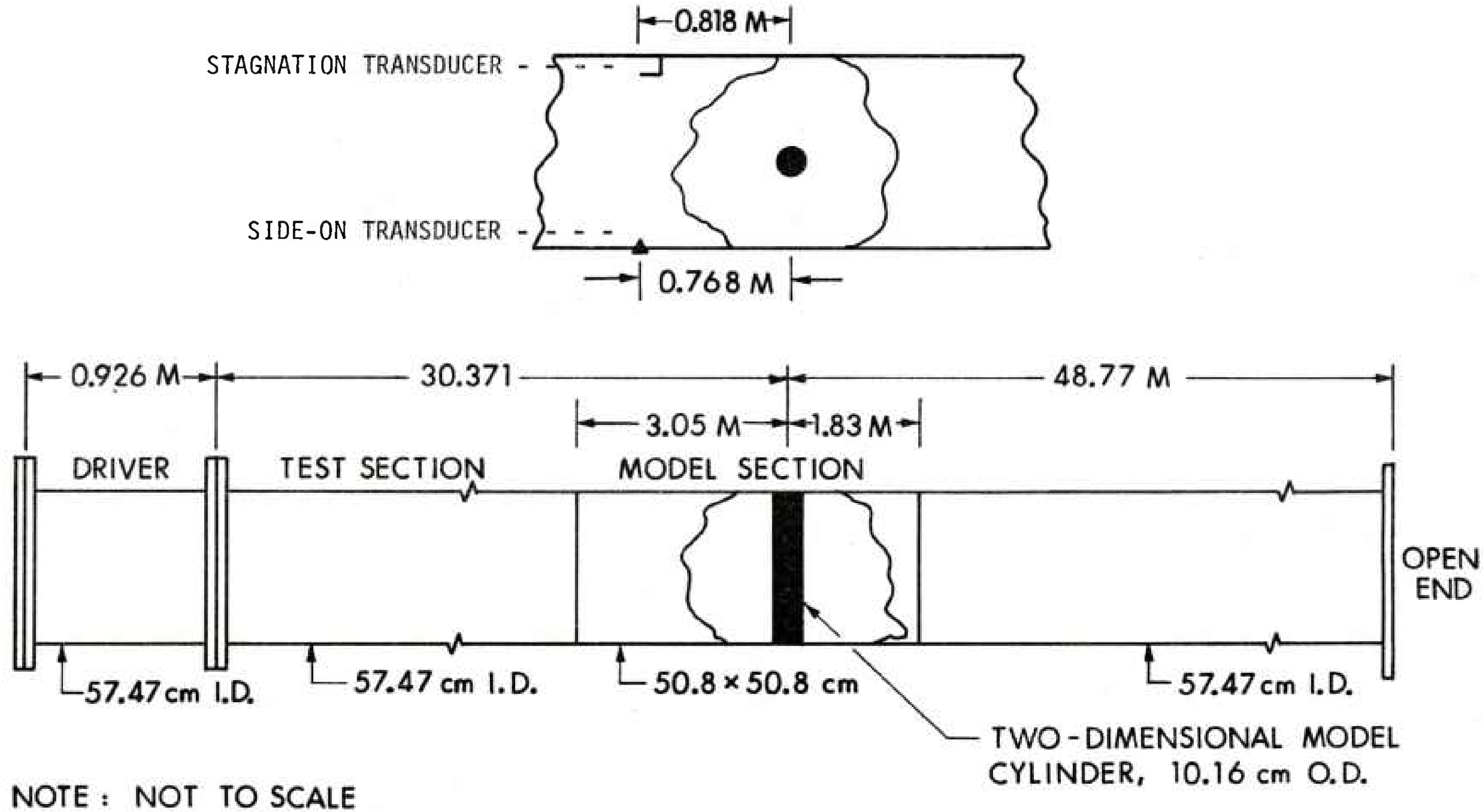

Figure 1. Schematic of BRL 57.5 cm shock tube.

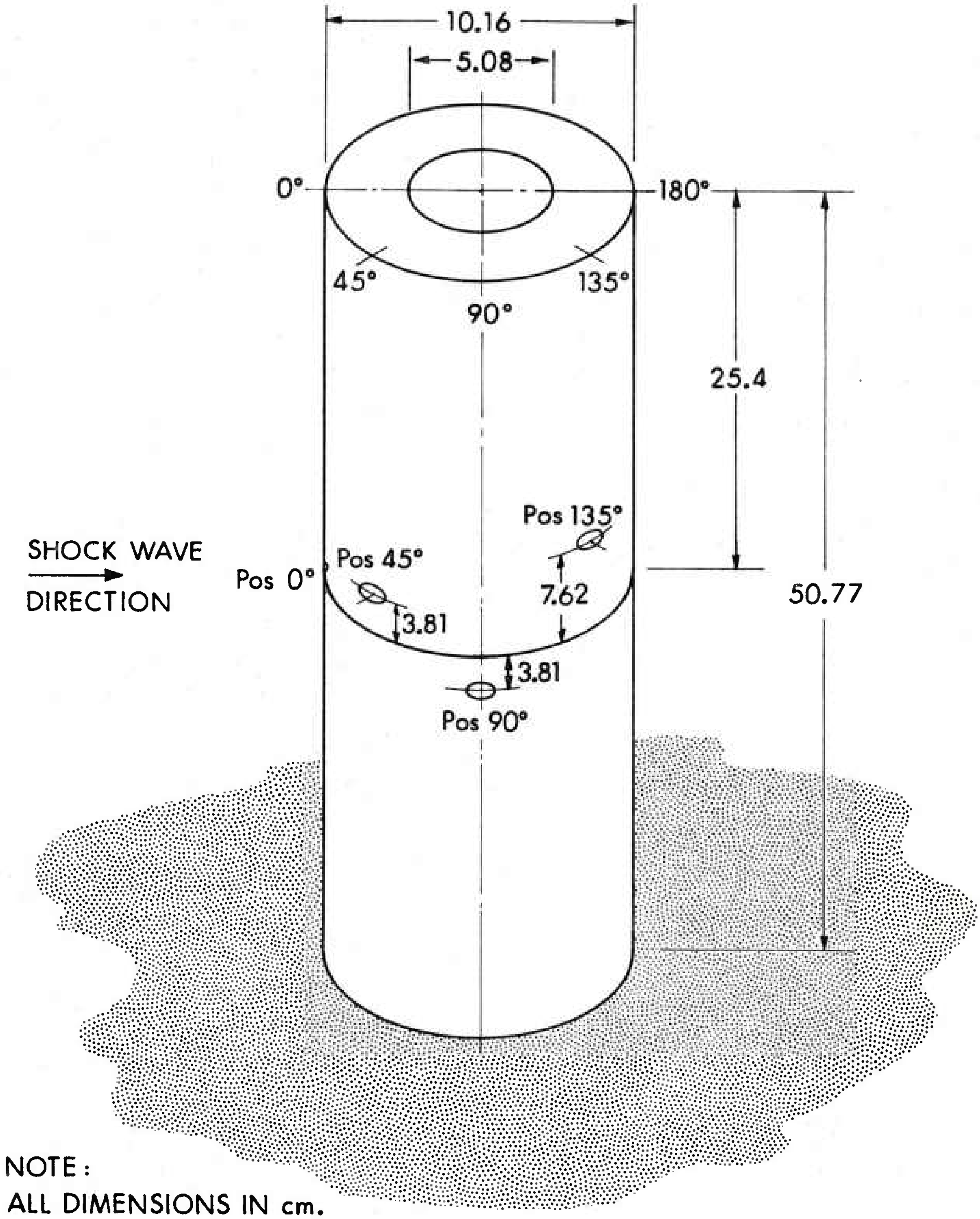

Figure 2. Initial location of transducers.

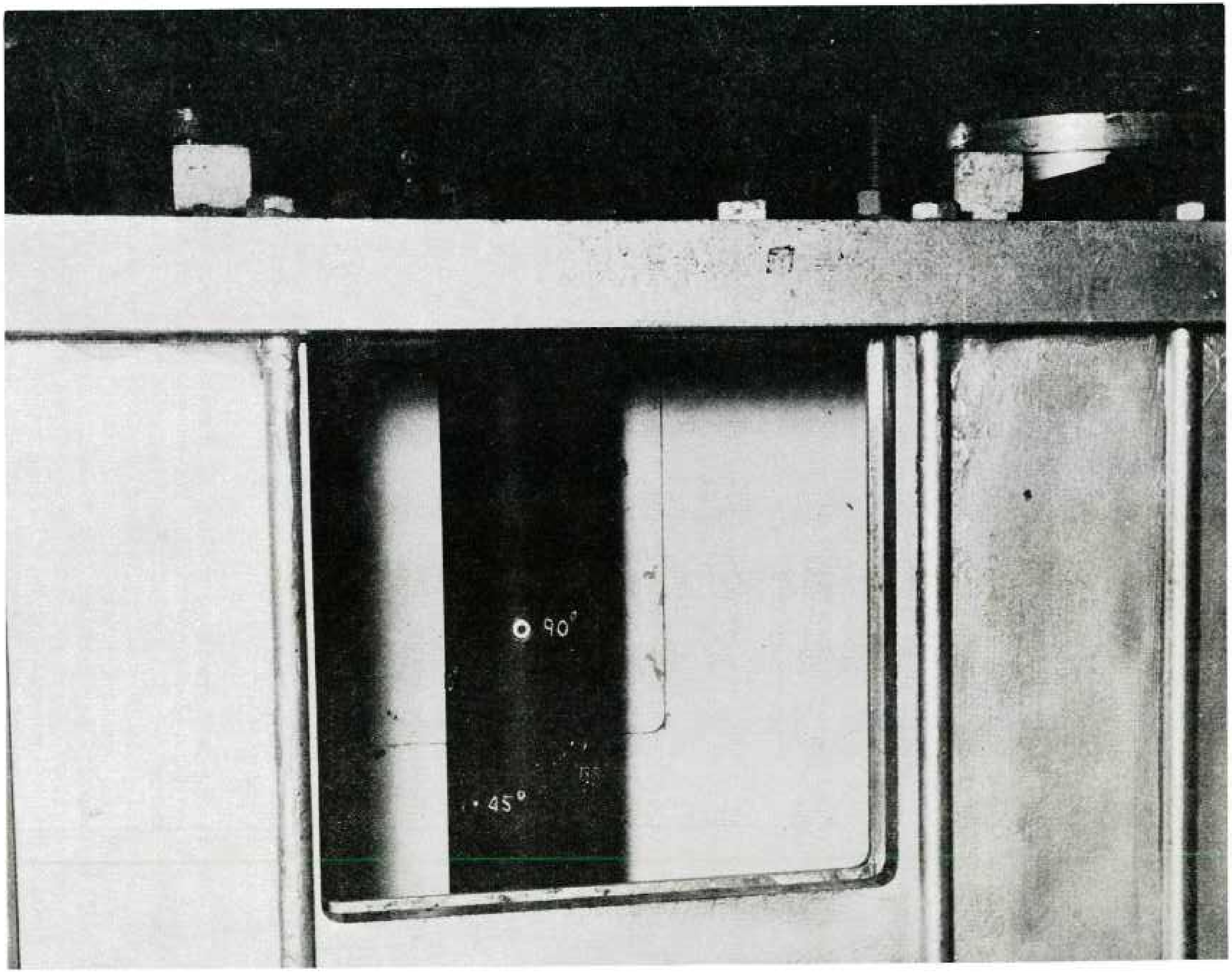

Figure 3. Two-dimensional cylinder installed

The cylinder was fastened to the round access port in the top of the test section. The top of the test section was graduated in degrees so the port could be rotated and matched in rotation (with the cylinder) for the succeeding transducer locations. Appendix A gives details of the test cylinder.

C. Instrumentation

The schematic of Figure 4 summarizes the data acquisition-reduction system. The test cylinder contained four PCB 13A24, quartz element, pressure transducers flush-mounted with surface of the cylinder. Signal conditioners and data amplifiers transferred the pressure-time histories to an FM 7600 Honeywell recorder.

Quick-look data could be obtained by means of the Honeywell 1858 CRT Visicorder. Final data processing was accomplished with a Textronix 4051 computer and related accessories. Final report-ready copies of pressure-time histories with engineering units were made with the data system.

III. RESULTS

Figure 5 shows typical side-on and stagnation pressure records for input pressures of 42.3, 75.9, and 112.2 kPa.

The records were obtained from locations about 0.8 m upstream of the test section (Figure 1) on opposite sides of the shock tube. Ten milliseconds only of the records are shown since this was the test time of interest-through the diffraction phase until flow had been established about the cylinder. The small peaks occurring after about 4 milliseconds are shock reflections from the cylinder and test section walls, and should be ignored. Table 1 is the shot log for the test.

A. Results for Stations 0-30

Pressure-time histories for the period of interest are shown for comparison in Figure 6-18 as a function of transducer location and input side-on shock overpressure. Tables 1 and 2 summarize pertinent shot parameters and test results.

The records are grouped according to increasing input overpressure for each station (transducer location). For example, Station 0 is for 0°, 15 is for 15°, and so on. The records from Stations 0-30 all show initially a peak of reflected pressure which is followed by rarefactions which decay the reflected pressure to the value for stagnation pressure. The small pressure peak at about 1.5 milliseconds is a reflection from the cylinder to the test section wall and back to the transducer. There reflections should be ignored. Similar reflections occur at later times, but are mixed in with the general pressure ocillations and are hard to distinguish.

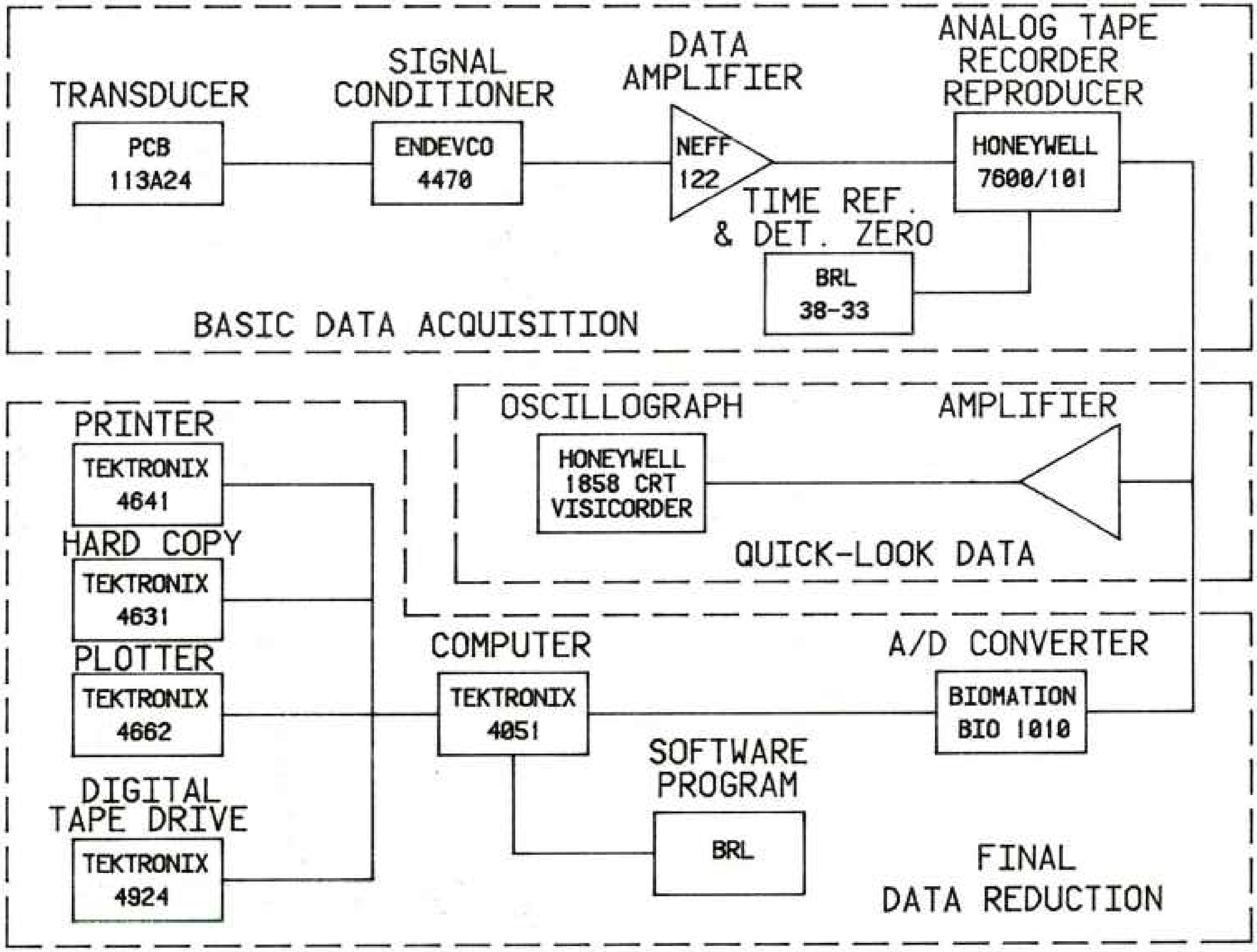

Figure 4. Schematic of data acquisition-reduction system.

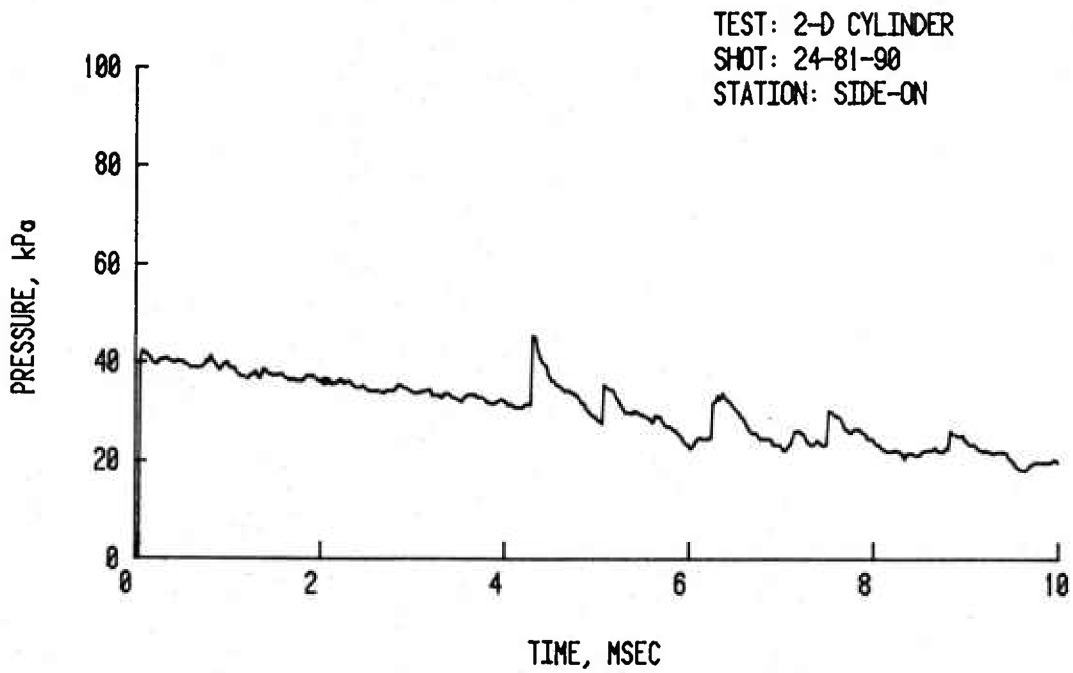

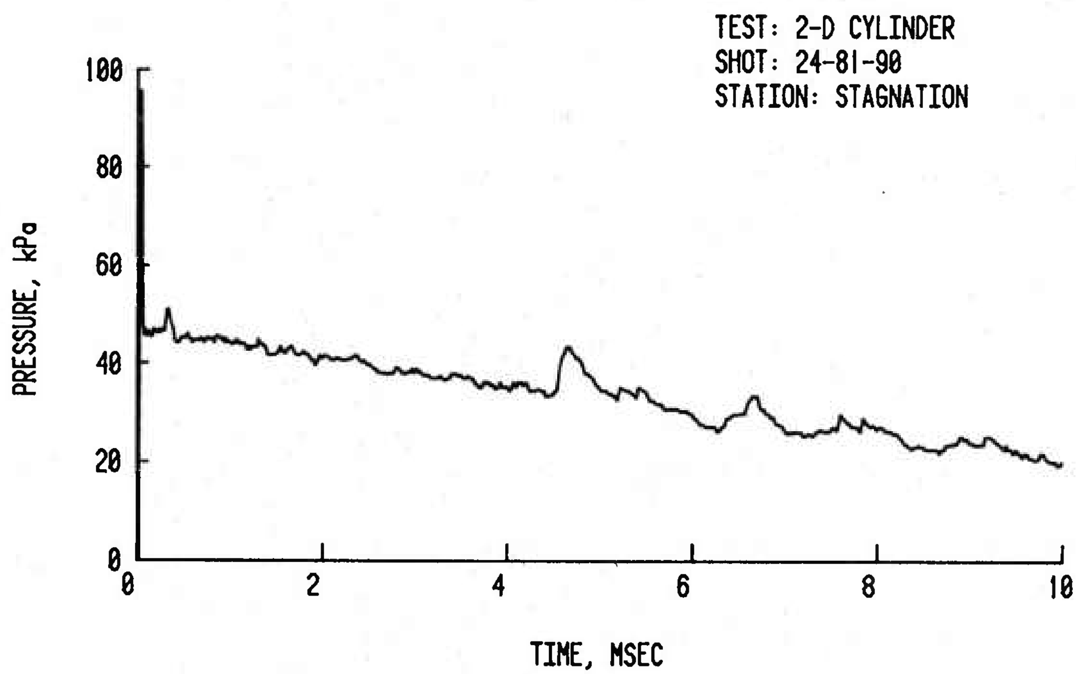

Figure 5. Pressure-time records for input waves.

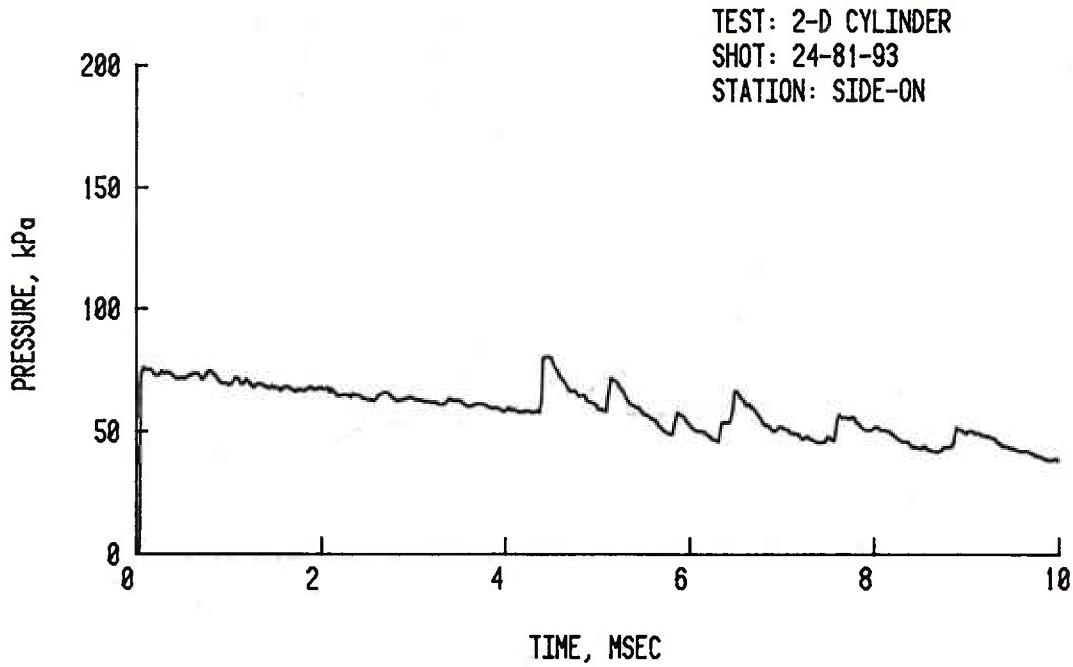

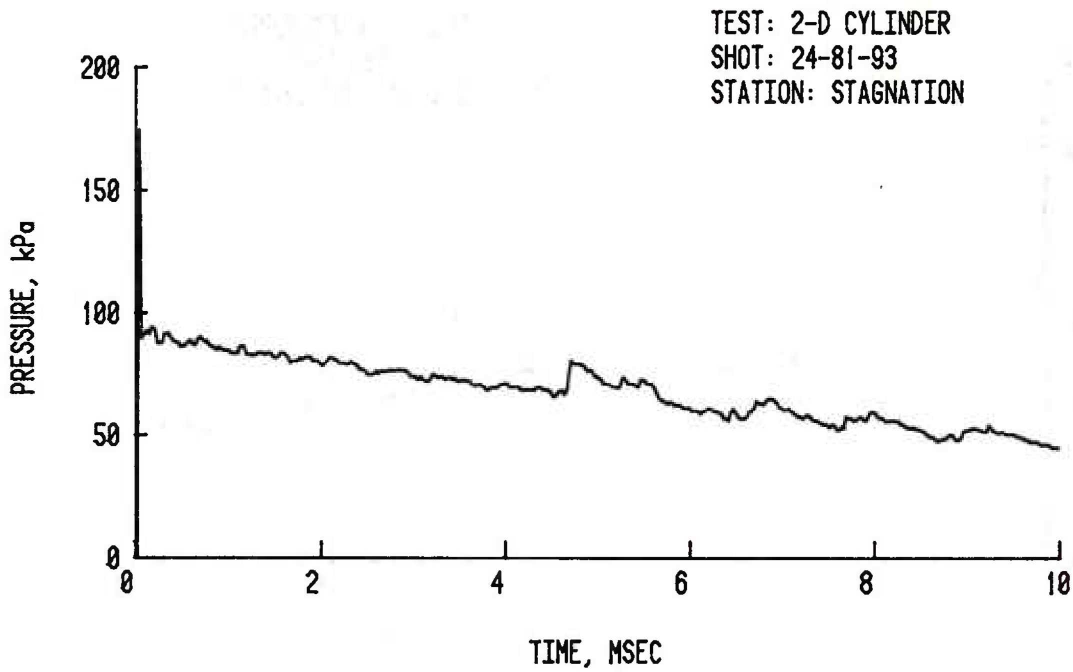

Figure 5. Pressure-time records for input waves. (cont'd)

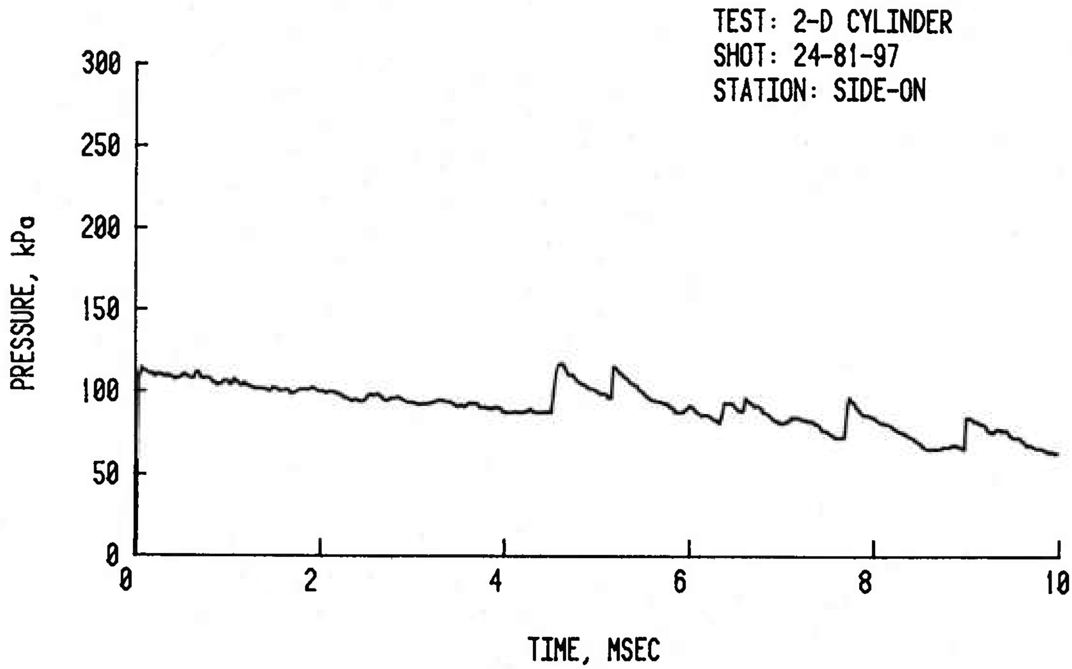

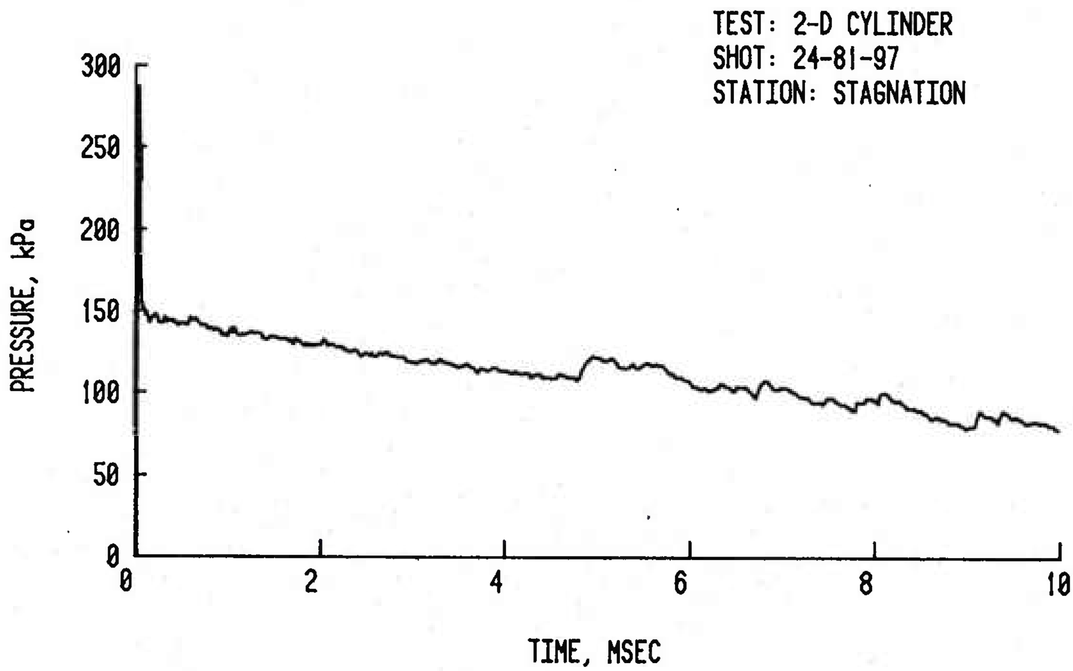

Figure 5. Pressure-time records for input waves. (cont'd)

TABLE 1. LIST OF SHOTS

Shot Number	Input Overpressure kPa	Ambient Pressure kPa	Ambient Temperature °C	Date
24-81-87	43.0	102.86	20.12	29 Sept. 81
24-81-88	41.3	102.73	20.68	29 Sept. 81
24-81-89	42.6	102.66	20.80	29 Sept. 81
24-81-90	42.0	102.66	21.13	29 Sept. 81
24-81-91	42.6	102.66	21.20	29 Sept. 81
24-81-92	42.0	102.66	21.28	29 Sept. 81
24-81-93	75.5	102.86	21.00	30 Sept. 81
24-81-94	75.5	102.86	21.01	30 Sept. 81
24-81-95	76.0	102.86	21.01	30 Sept. 81
24-81-96	76.5	102.86	21.05	30 Sept. 81
24-81-97	112.0	102.86	21.12	30 Sept. 81
24-81-98	114.5	102.86	21.18	30 Sept. 81
24-81-99	112.0	102.86	21.22	30 Sept. 81
24-81-100	110.3	102.86	21.29	30 Sept. 81

TABLE 2. TEST RESULTS

Shot Number	Transducer Position	Initial Overpressure kPa	Positive Duration ms	Positive Impulse* kPa-ms	Negative Pressure kPa
24-81-87	0	96.2	31.5	339.4	
24-81-87	45	81.5	31.3	282.8	
24-81-87	90	51.2	33.7	227.0	
24-81-87	135	27.7	28.9	256.5	
24-81-87	side-on	43.0	32.1	307.8	
24-81-87	stag	-/45.5	31.0	331.7	
24-81-88	0	94.1	32.9	321.7	
24-81-88	45	79.4	32.7	273.0	
24-81-88	90	50.9	31.2	222.9	
24-81-88	135	27.3	32.0	262.4	
24-81-88	side-on	41.3	32.1	294.1	
24-81-88	stag	93.4/45.5	31.8	322.3	
24-81-89	15	87.8	28.2	326.9	
24-81-89	60	----	----	-----	
24-81-89	105	42.4	28.7	251.0	
24-81-89	150	23.6	28.1	265.7	
24-81-89	side-on	42.6	28.4	305.9	
24-81-89	stag	92.0/46.0	27.2	332.6	
24-81-90	15	87.7	31.5	330.3	
24-81-90	60	68.8	31.3	243.8	
24-81-90	105	41.7	33.7	246.4	
24-81-90	150	23.5	28.9	259.2	
24-81-90	side-on	42.0	32.1	303.1	
24-81-90	stag	95.6/47.0	31.0	335.3	
24-81-91	30	88.8	30.6	302.7	
24-81-91	75	61.0	26.2	225.6	
24-81-91	120	33.8	29.2	260.7	
24-81-91	165	20.0	25.9	255.2	
24-81-91	side-on	42.6	28.5	302.2	
24-81-91	stag	95.0/46.3	27.1	332.4	
24-81-92	45	80.0	31.6	267.8	
24-81-92	90	50.1	27.7	219.3	
24-81-92	135	27.0	33.2	265.4	
24-81-92	180	42.6	28.8	270.9	
24-81-92	side-on	42.0	31.9	298.1	
24-81-92	stag	94.7/45.5	30.5	327.9	
24-81-93	0	188.6	40.0	682.9	
24-81-93	45	140.6	35.4	509.6	
24-81-93	90	86.8	43.2	378.7	-10.0
24-81-93	135	49.0	34.1	439.8	
24-81-93	side-on	75.5	42.1	582.3	
24-81-93	stag	174.6/92.0	39.1	675.8	

*Positive impulse given for 10 milliseconds.

TABLE 2. TEST RESULTS (cont'd)

Shot Number	Transducer Position	Initial Overpressure kPa	Positive Duration ms	Positive Impulse* kPa-ms	Negative Pressure kPa
24-81-94	15	185.4	42.1	665.1	
24-81-94	60	127.9	34.1	420.7	
24-81-94	105	71.0	41.9	435.5	-15.0
24-81-94	150	50.0	35.2	436.5	
24-81-94	side-on	75.5	40.2	587.2	
24-81-94	stag	-/93.5	38.5	676.4	
24-81-95	30	172.2	38.8	602.6	
24-81-95	75	96.6	32.7	314.6	
24-81-95	120	59.0	40.7	455.7	-5.0
24-81-95	165	35.5	34.7	454.4	
24-81-95	side-on	76.0	40.8	589.8	
24-81-95	stag	180.0/93.5	38.9	677.2	
24-81-96	45	156.7	40.0	499.2	
24-81-96	90	88.4	33.2	384.1	
24-81-96	135	47.0	40.3	467.3	
24-81-96	180	85.0	33.6	481.0	
24-81-96	side-on	76.5	39.6	587.1	
24-81-96	stag	177.5/93.0	38.7	677.8	
24-81-97	0	297.6	46.7	1,119.4	
24-81-97	45	219.4	35.2	760.0	
24-81-97	90	121.8	39.0	447.3	-23.0
24-81-97	135	73.0	38.8	524.6	-25.0
24-81-97	side-on	112.0	48.5	905.1	
24-81-97	stag	287.6/146.5	47.7	1,112.4	
24-81-98	15	295.1	49.7	1,109.4	
24-81-98	60	193.2	35.0	567.0	
24-81-98	105	104.5	51.6	585.1	-35.0
24-81-98	150	60.0	38.7	558.4	
24-81-98	side-on	114.5	47.5	919.3	
24-81-98	stag	295.9/152.0	46.8	1,127.3	
24-81-99	30	265.1	49.7	952.0	
24-81-99	75	155.3	35.4	409.4	-38.5
24-81-99	120	84.5	53.0	570.7	
24-81-99	165	50.0	38.8	603.9	
24-81-99	side-on	112.0	48.1	902.4	
24-81-99	stag	288.2/146.5	41.5	1,102.4	
24-81-100	45	240.6	44.5	718.8	
24-81-100	90	124.2	35.4	453.4	
24-81-100	135	65.0	51.7	524.1	-40.0
24-81-100	180	124.5	37.4	620.0	
24-81-100	side-on	110.3	50.8	903.1	
24-81-100	stag	281.1/147.0	44.4	1,104.5	

*Positive impulse given for 10 milliseconds.

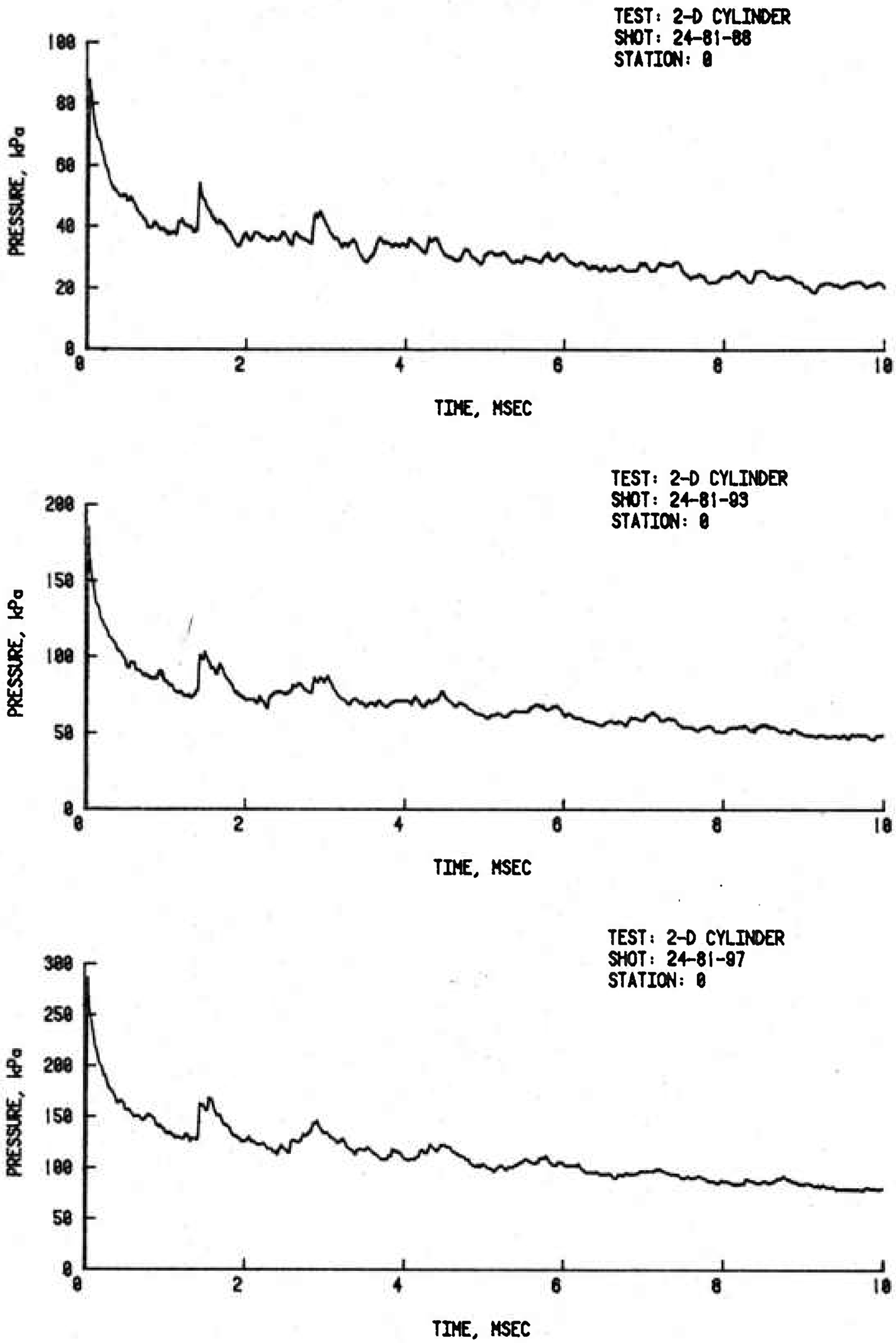

Figure 6. Pressure-time records for 0 degrees.

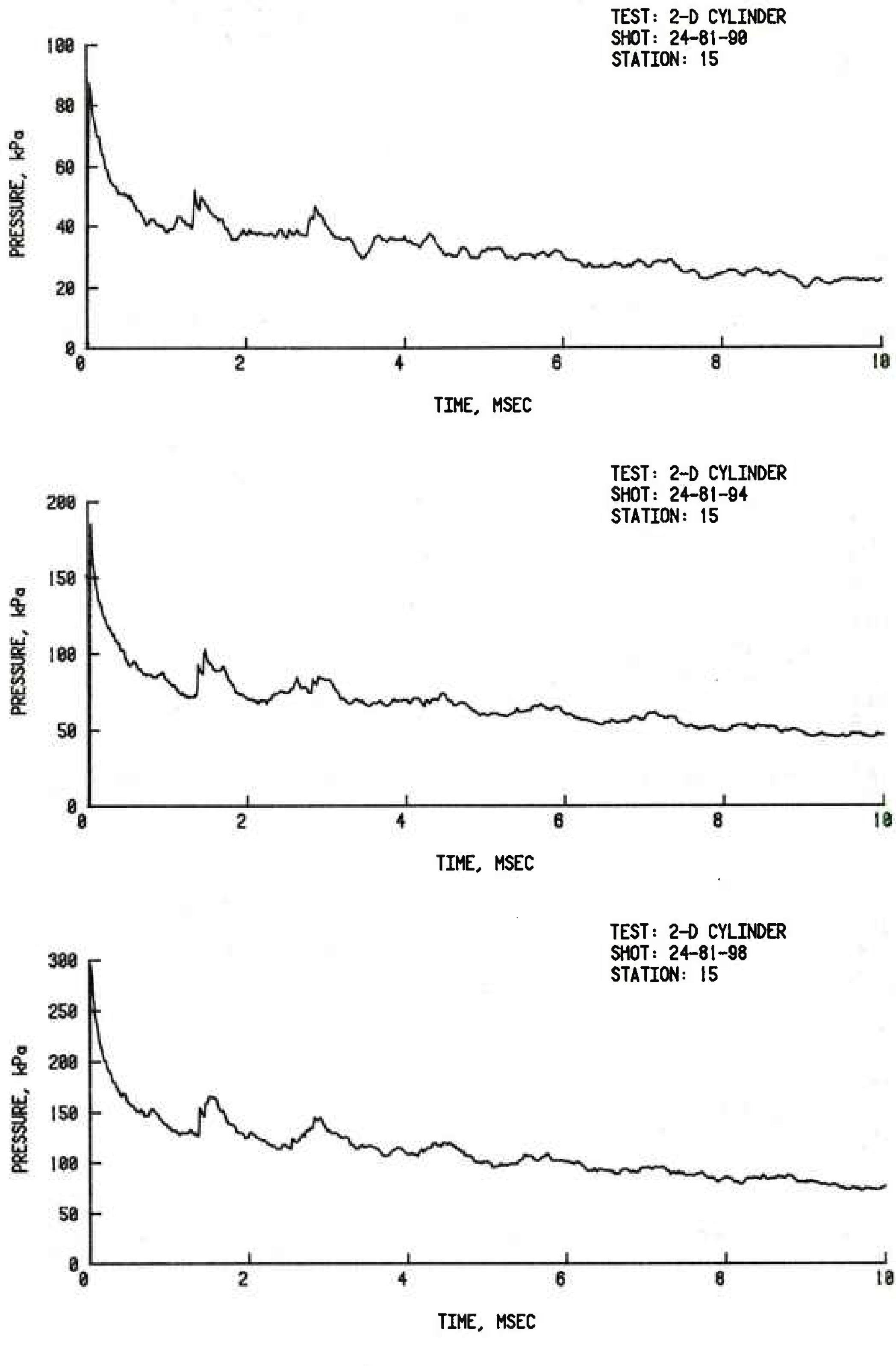

Figure 7. Pressure-time records for 15 degrees.

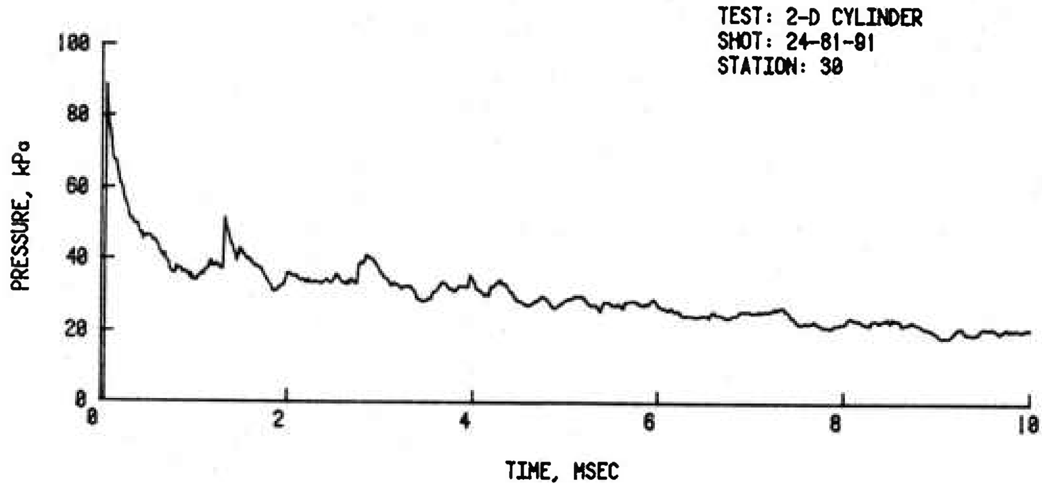

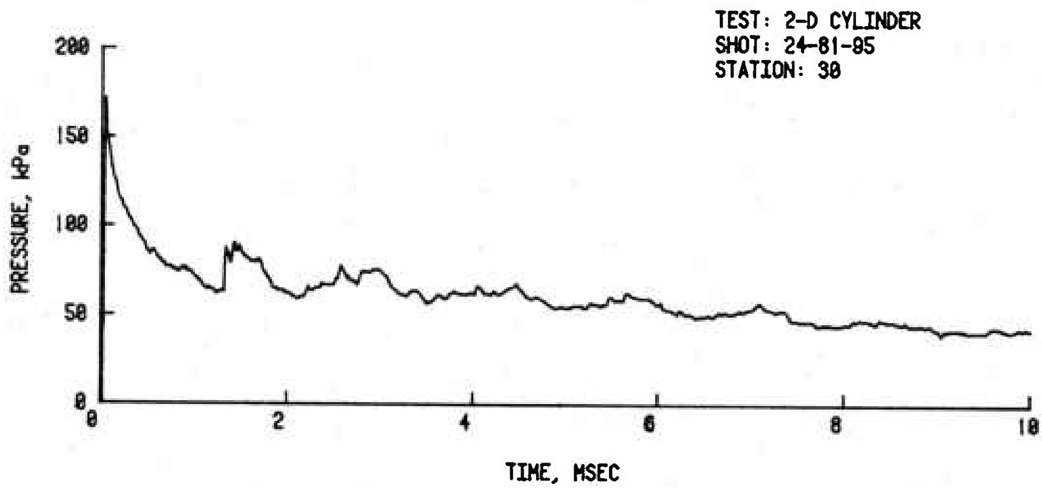

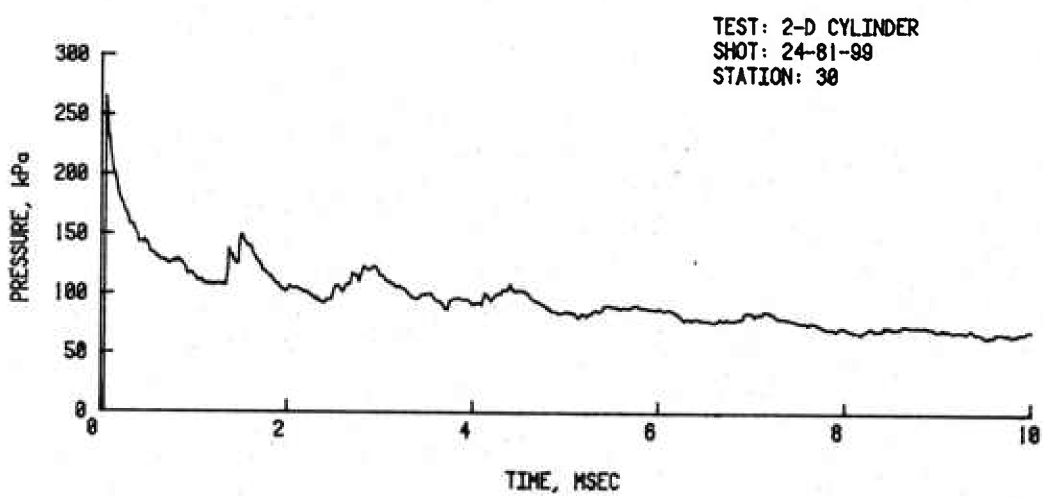

Figure 8. Pressure-time records for 30 degrees.

B. Results for Stations 45-75

Stations for this area of the model show initial peak pressures less than full reflected pressures. The peak value becomes less with increasing station (angle). At Station 75 the initial pressure is 65-75 percent of the initial pressure at Station 45.

The general shape of the records are very similar for all these stations. At Station 75 the peak is followed by rarefactions that began to dip toward zero overpressure. This is seen at the higher two input pressure levels.

C. Results for Stations 90-120

At Station 90, for the 75.9 kPa input level pressure, a negative pressure occurs at about 1 ms. The rarefaction decay plus the vortex action causes this pressure decrease. This has not occurred, however, at the lowest input pressure level. The values for these negative pressures are listed in Table 2.

The initial pressure peak has continued to decrease in amplitude until at Station 120 the initial peak value is no longer the largest value.

D. Results for Stations 135-180

The negative pressure is absent on records from Station 135 at the two lower input pressure levels. At Station 150 the negative pressure is absent at the highest input pressure also. The remaining stations show records that look similar to the side-on input records. The rounded front records, Figure 17, show a two part rise to the maximum value (neglecting the small reflection at about 1 ms). The two parts are caused by different arrival times of the diffracted waves around the cylinder.

For example, the first rise at the 165° position is the initial shock front passing the transducer position. The second rise in pressure is from the interaction of the two parts of the initial shock meeting at 180° and passing back upstream over the 165° position. At Station 180 the arrival times for the two parts of the initial shock (around each side of the cylinder) are equal and a single shock reflection, building up to the rounded maximum, is the result.

Tables 2 and 3 summarize the test results.

IV. ANALYSIS

The analysis will treat three topics. The first section will show a method for determining the free-air, blast equivalent of the shock wave produced by the shock tube for the experimental loading. The second section will describe a way to calculate the coefficient of drag as a function of time for the blast loads measured on the cylinder. The third section will be a presentation of pressure coefficients (P_r/P_s) versus angle of incidence for the three input pressures.

TABLE 3. INPUT SHOCK WAVE PARAMETERS

Shot Number		Peak Side-on Overpressure kPa	Peak Stagnation Overpressure kPa	Side-on Positive Duration ms	Side-on Positive Impulse[a] kPa-ms
24-81-87		43.0	45.5	32.1	307.8
24-81-88		41.3	45.5	32.1	294.1
24-81-89		42.6	46.0	28.4	305.9
24-81-90		42.0	47.0	32.1	303.1
24-81-91		42.6	46.3	28.5	302.2
24-81-92		42.0	45.5	31.9	298.1
	average	42.25	46.00	30.85	301.9
24-81-93		75.5	92.0	42.1	582.3
24-81-94		75.5	93.5	40.2	587.2
24-81-95		76.0	93.5	40.8	589.8
24-81-96		76.5	93.0	39.6	587.1
	average	75.88	93.00	40.68	586.6
24-81-97		112.0	146.5	48.5	905.1
24-81-98		114.5	152.0	46.8	919.3
24-81-99		112.0	146.5	48.1	902.4
24-81-100		110.3	147.0	50.8	903.1
	average	112.2	148.0	48.55	907.5

[a]Positive impulse given for 10 milliseconds.

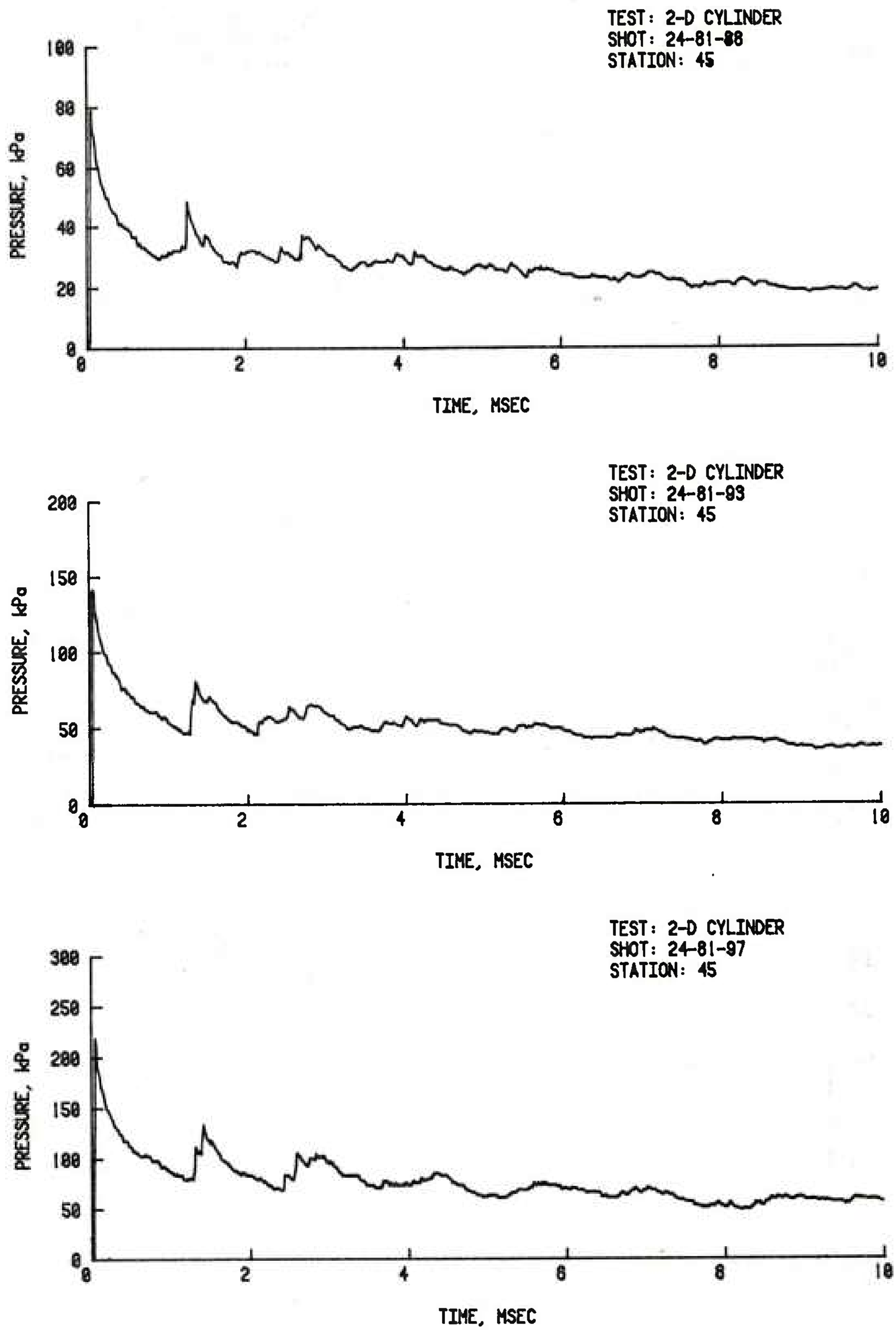

Figure 9. Pressure-time records for 45 degrees.

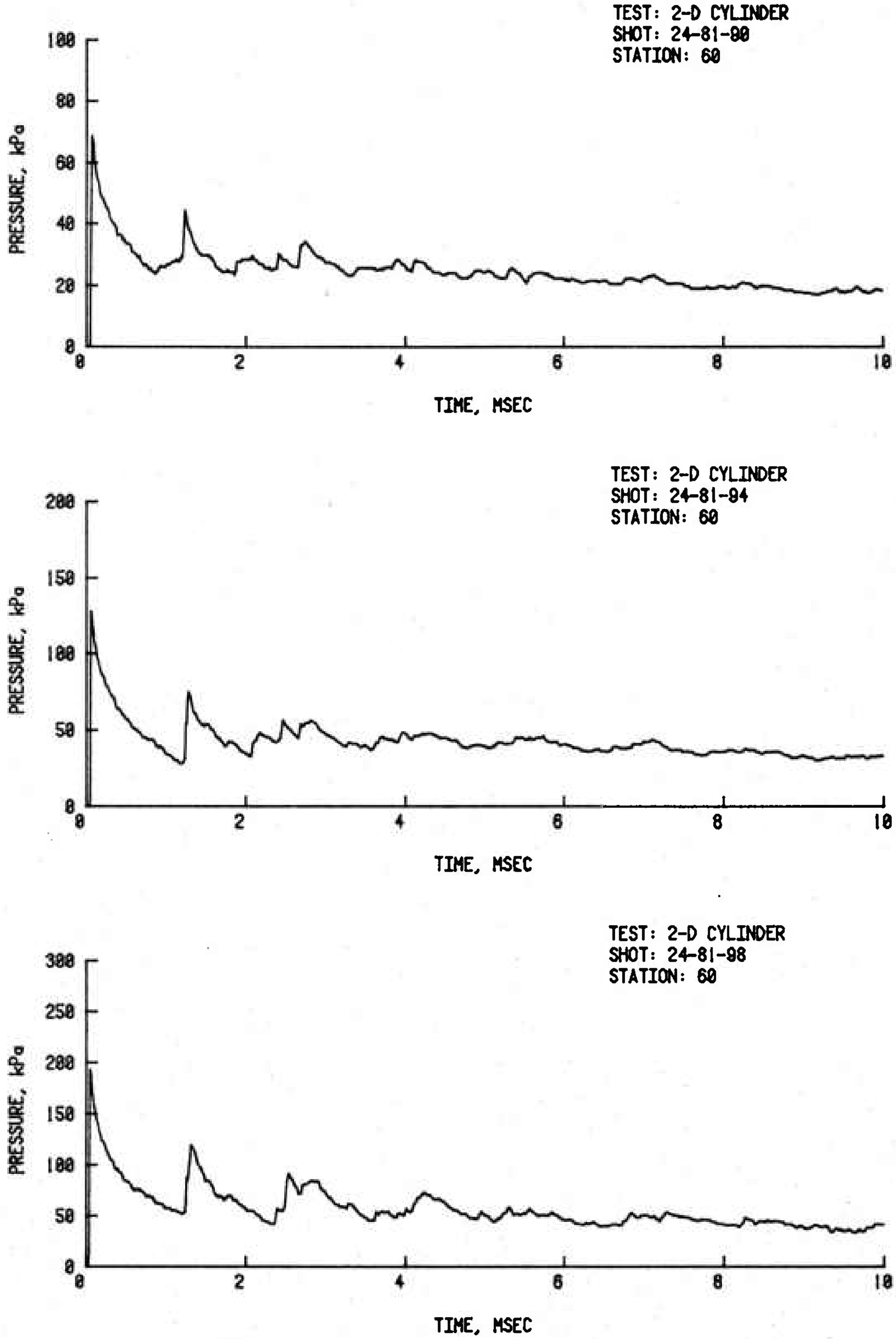

Figure 10. Pressure-time records for 60 degrees.

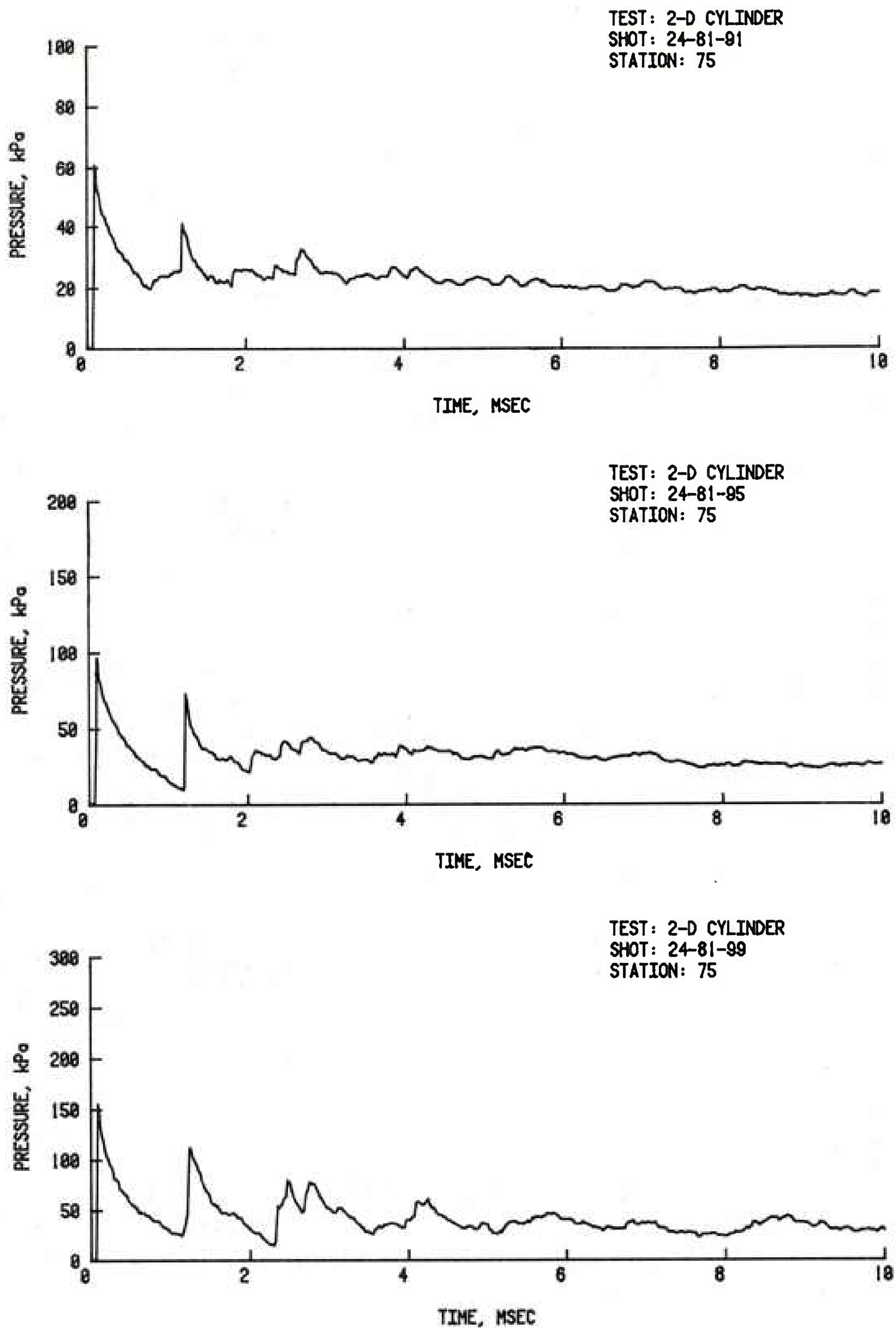

Figure 11. Pressure-time records for 75 degrees.

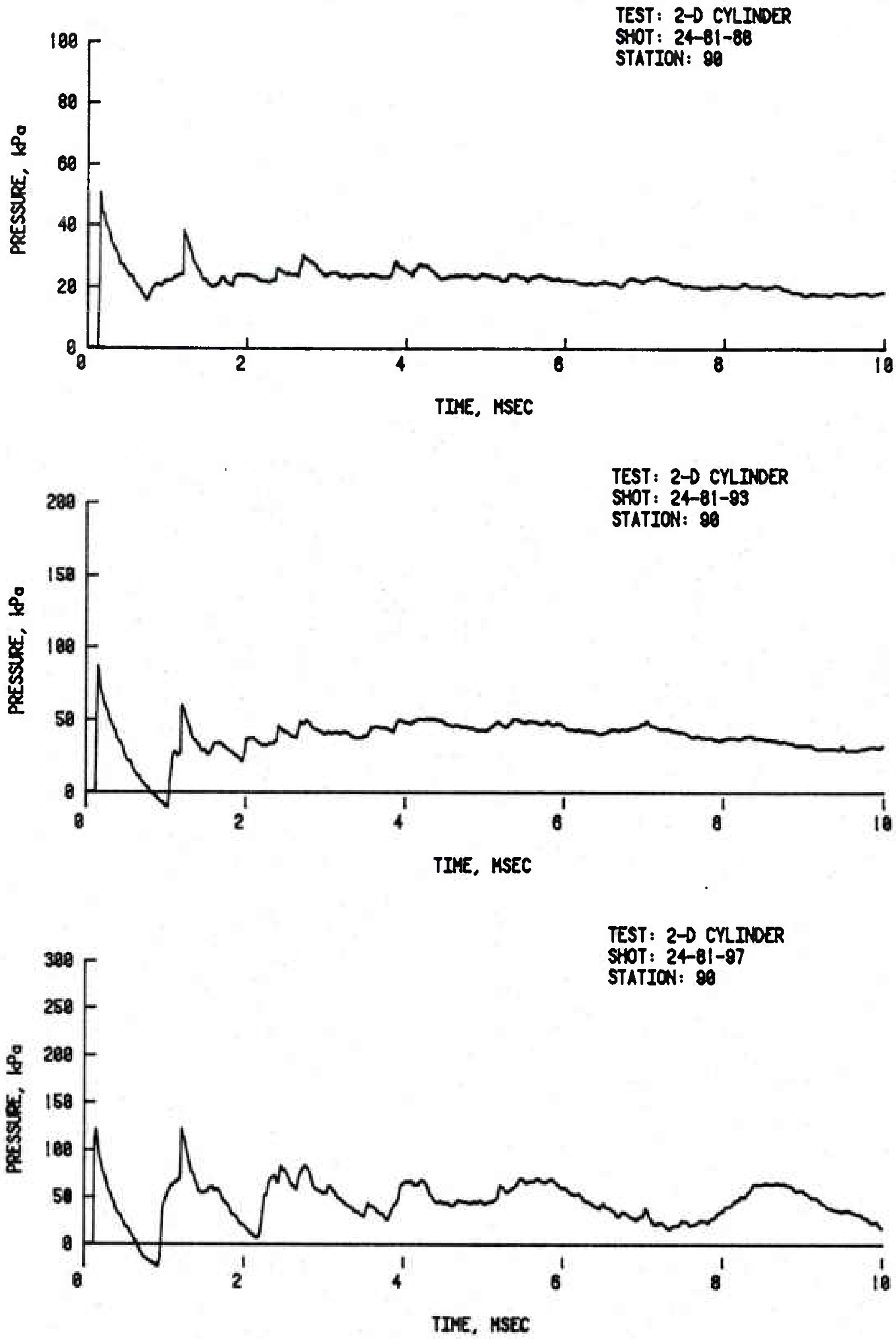

Figure 12. Pressure-time records for 90 degrees.

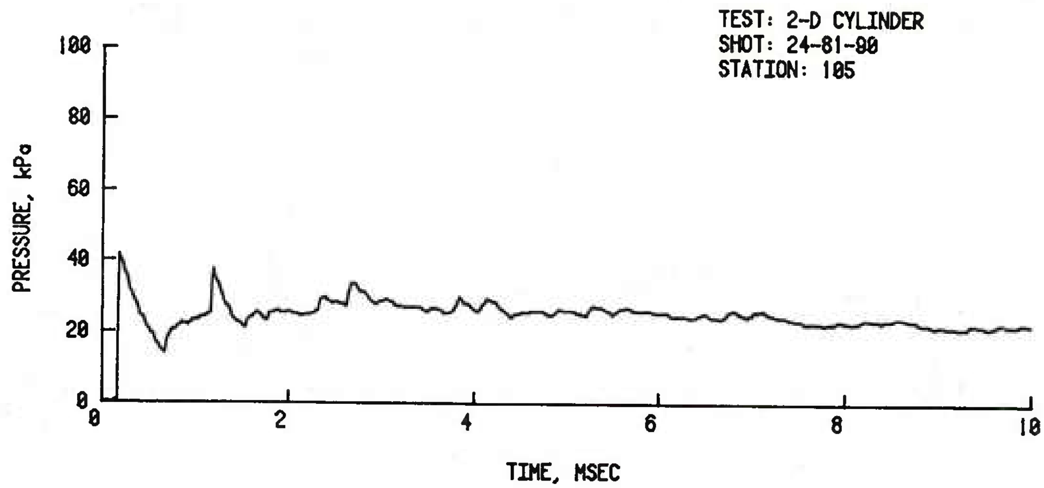

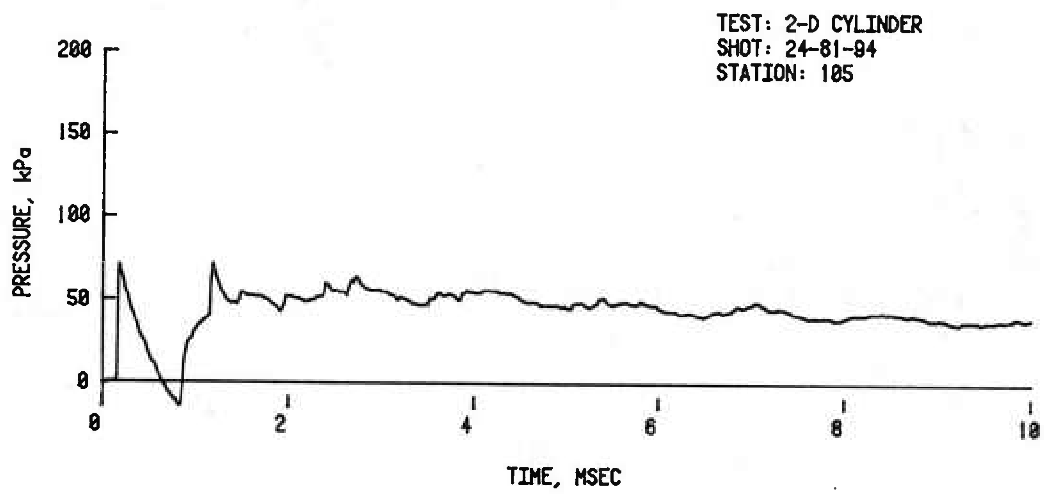

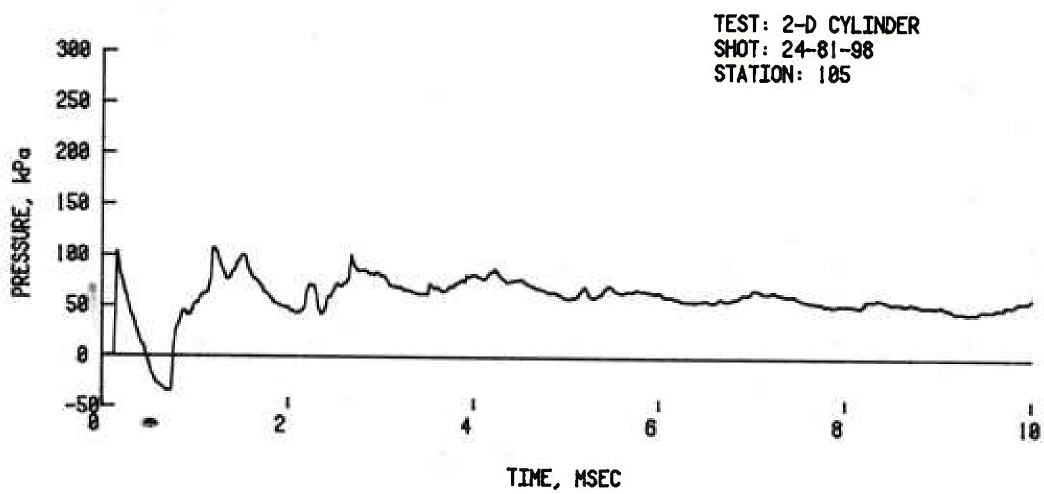

Figure 13. Pressure-time records for 105 degrees.

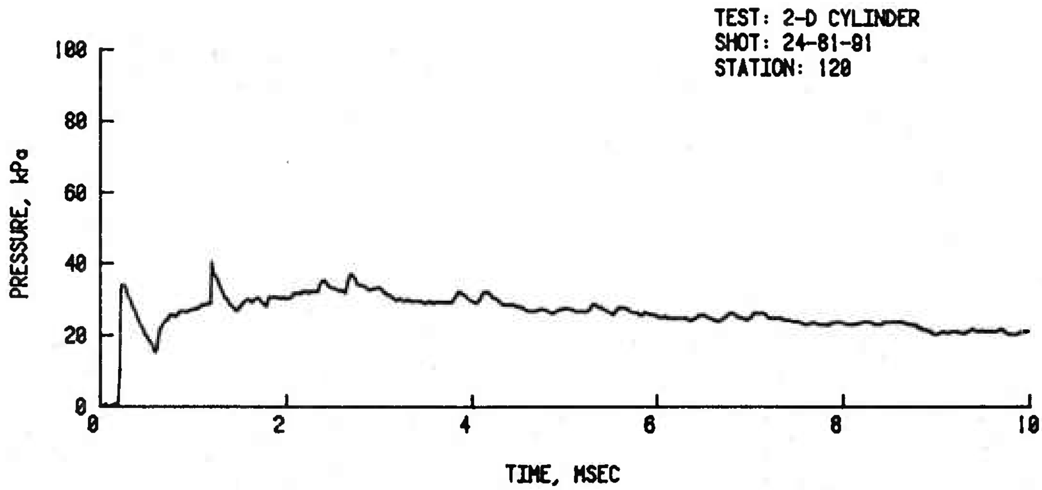

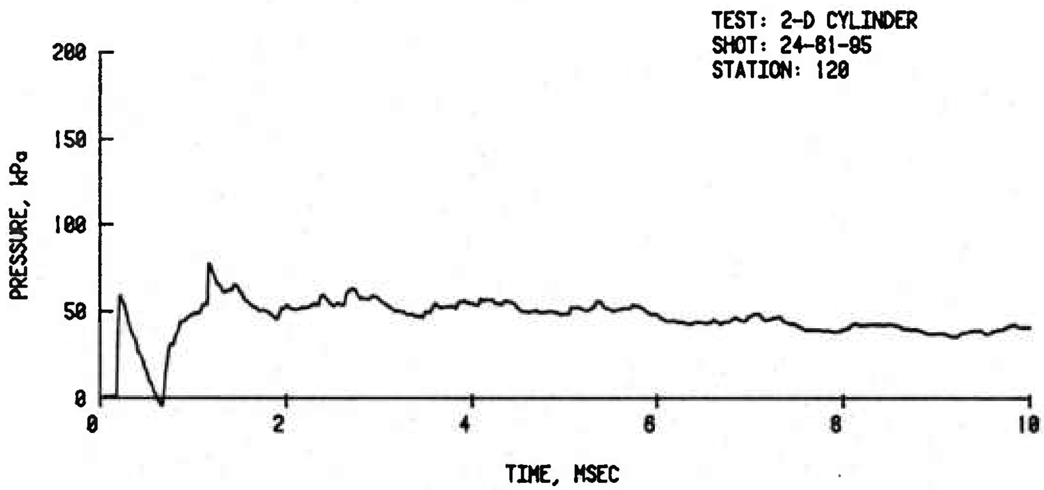

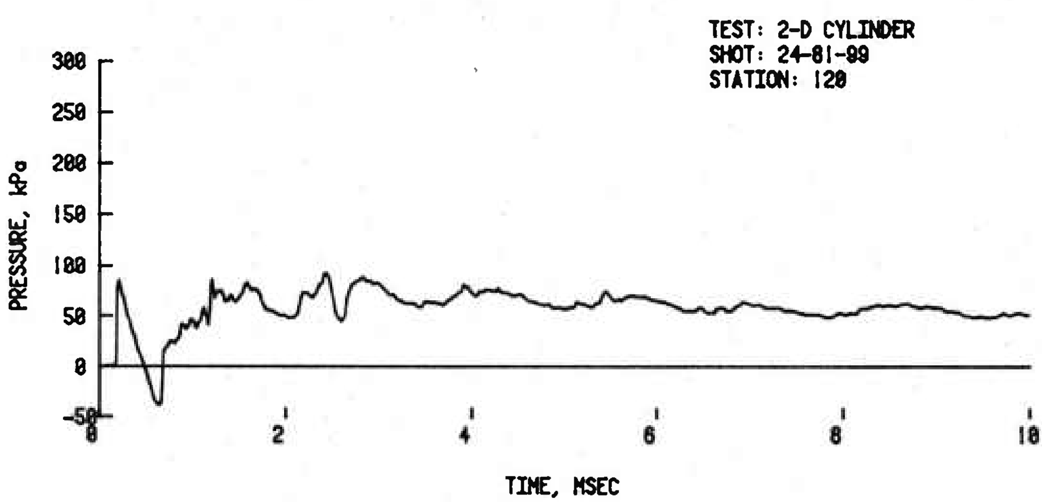

Figure 14. Pressure-time records for 120 degrees.

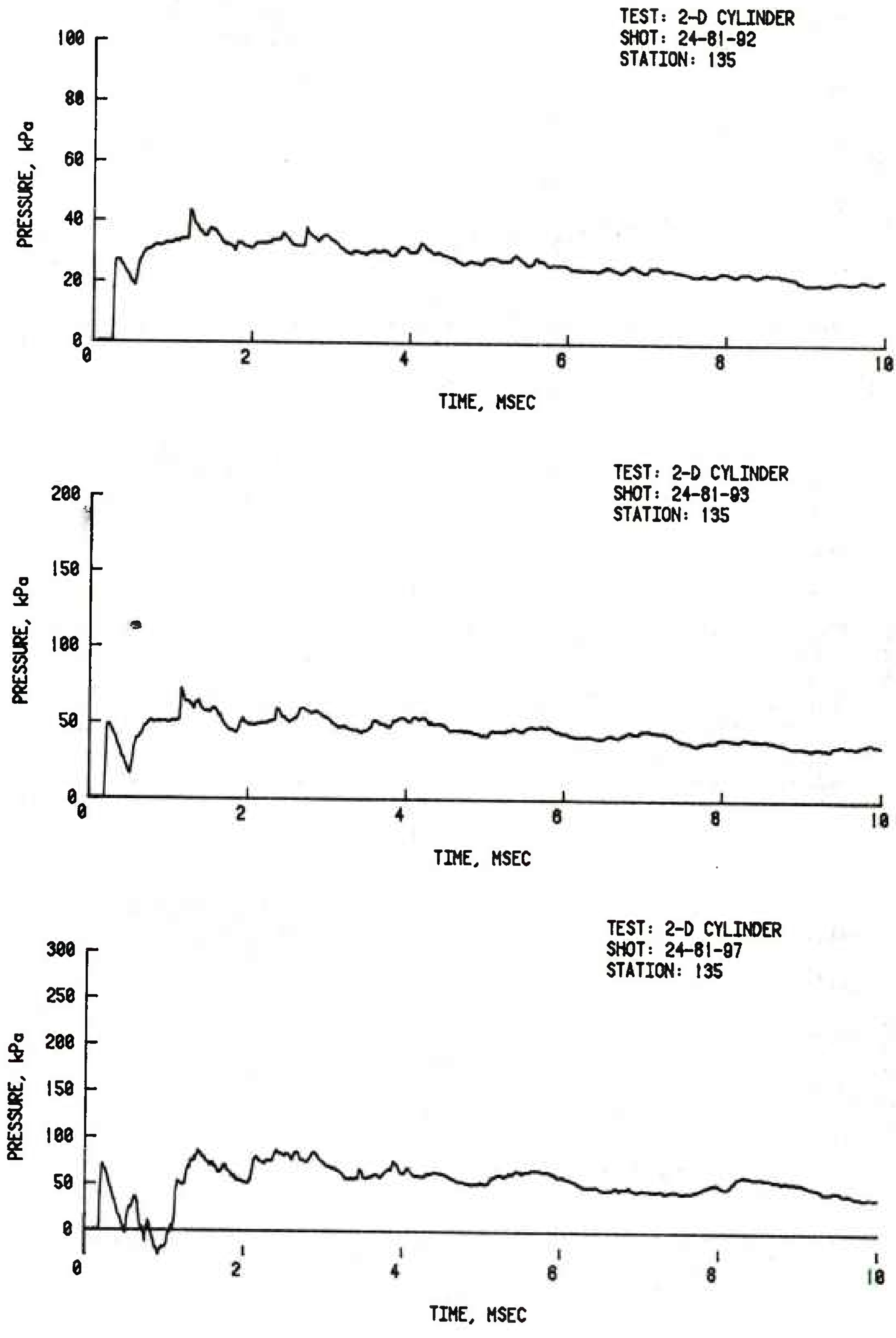

Figure 15. Pressure-time records for 135 degrees.

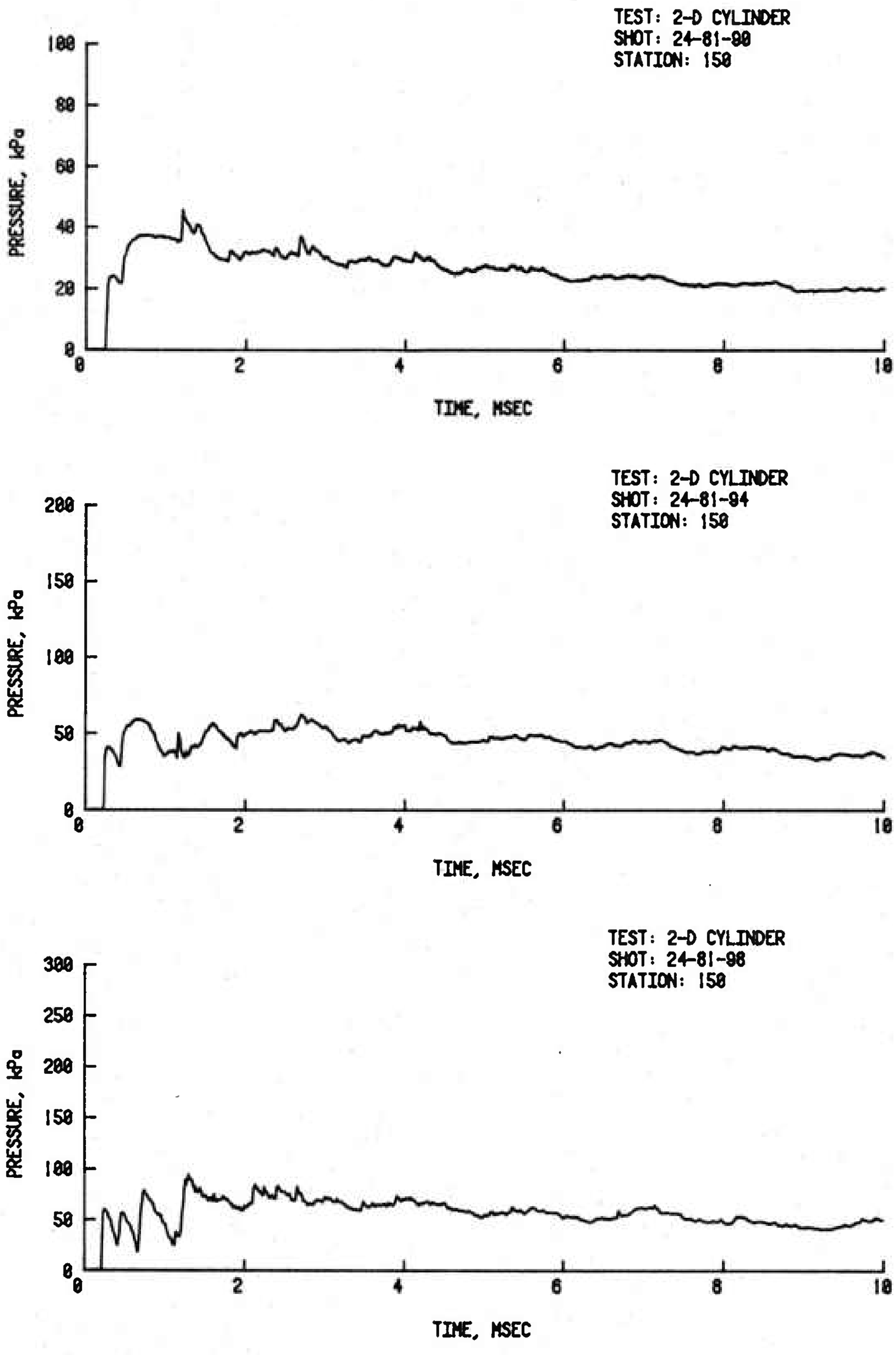

Figure 16. Pressure-time records for 150 degrees.

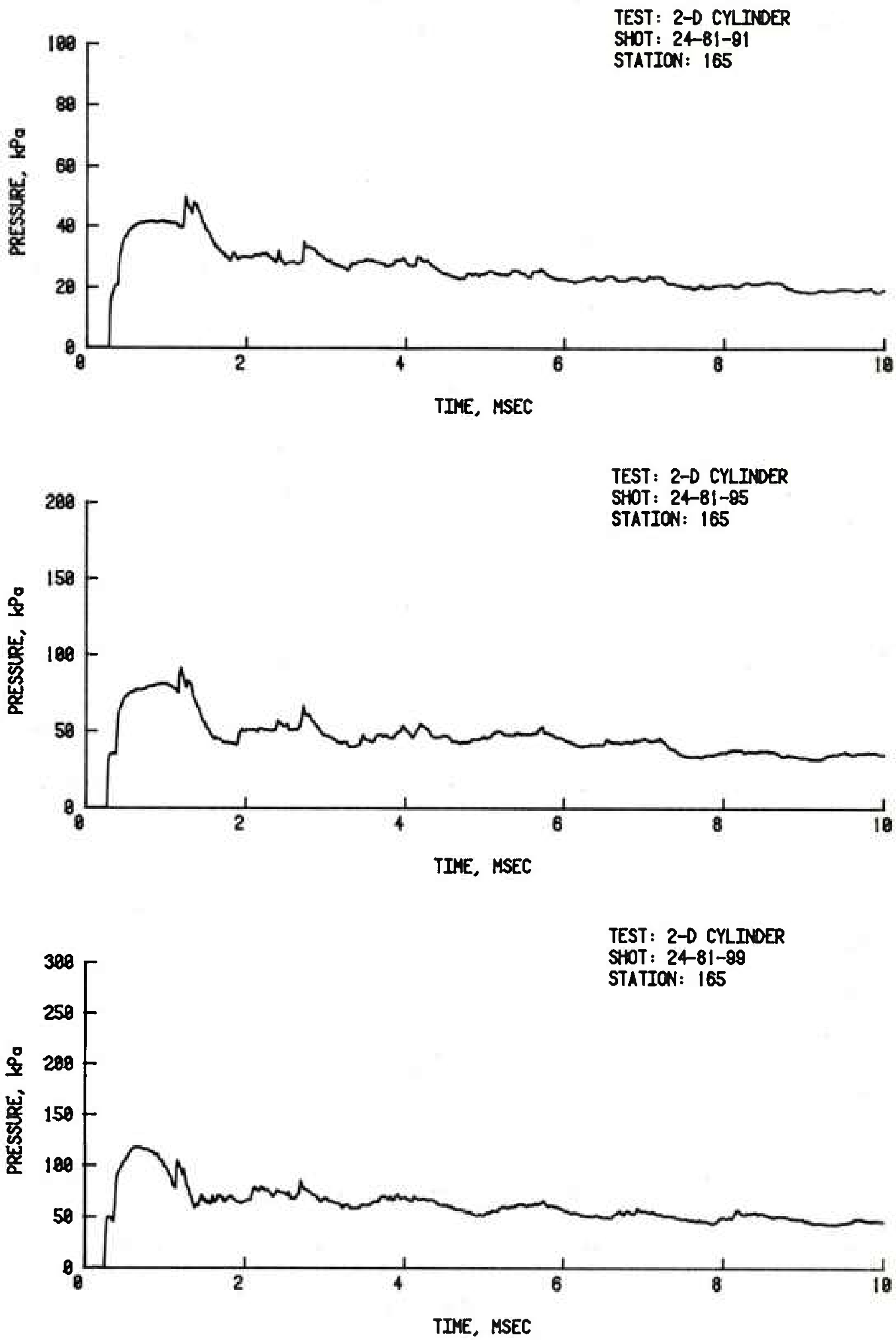

Figure 17. Pressure-time records for 165 degrees.

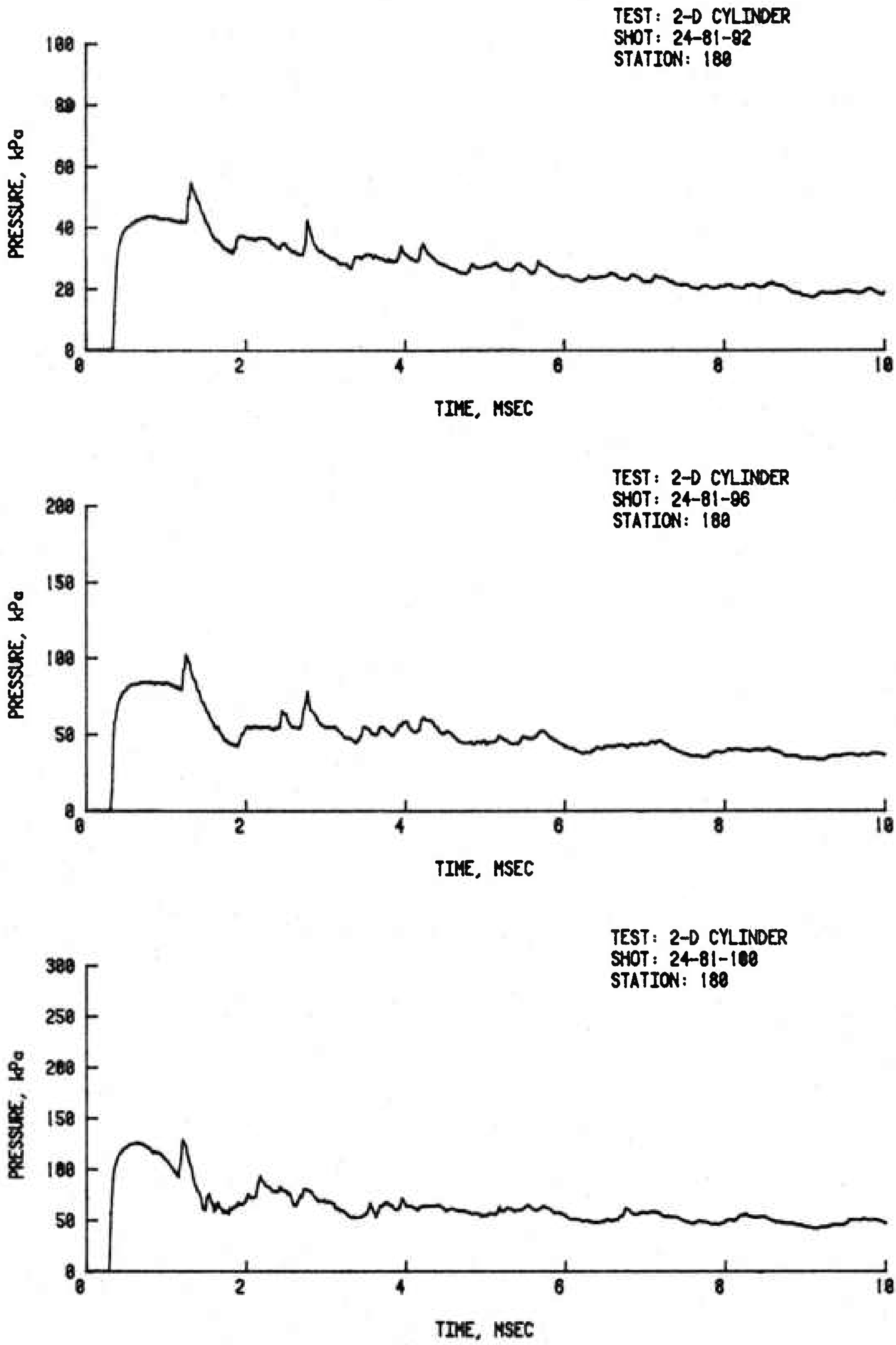

Figure 18. Pressure-time records for 180 degrees.

A. Equivalent Charge Weight

Cube root scaling[11] allows the blast parameters from one high explosive yield of TNT to be found for another yield. For the same atmospheric test conditions, the scaling relationships are given by Equation 1 where the scaling is from charge (1) to charge (2).

$$\frac{D_2}{D_1} = \frac{TA_1}{TA_2} = \frac{t_2}{t_1} = \frac{I_2}{I_1} = \left(\frac{W_2}{W_1}\right)^{1/3} \text{, where} \qquad (1)$$

D, TA, t, I, and W are the station distance, time of arrival, positive duration, positive impulse and charge mass of the explosive. Subscript (1) parameter values are taken from Reference 12 and are listed in Table 4 for Cases I, II, and III.

The equivalent charge mass to be found may be obtained by rewriting a portion of Equation 1 as Equation 2.

$$W_2 = W_1 \left(\frac{I_2}{I_1}\right)^3 \text{, where} \qquad (2)$$

W_2 is the equivalent weight of TNT needed to reproduce a blast wave with the same side-on overpressure and impulse, I_2. Table 4 lists these average values for each set of test shots for the shock tube cases. The values used for I, are listed for Cases I, II, and III correspond to average side-on pressure values obtained during the shock tube tests.

After equivalent values of W_2 are calculated (last column of Table 4)the remaining parameter of distance, arrival time, and positive duration may be calculated by use of Equation 1 above. For example, for free-air, a blast equal in pressure (75.88 kPa) and positive impulse (1118.6 kPa-ms) to the middle group of shock tube shots (24-81-93 to 24-81-96) would be produced by an equivalent mass of 4,244 kg of TNT. The pressure would occur at a distance of 48.2 m from the charge center of detonation. It would arrive 63.2 ms after detonation with a positive duration of 34.8 ms and with the required 1118.6 kPa-ms of positive impulse.

---

[11] *Samuel Gladstone and Philip J. Dolan-Editors, "The Effects of Nuclear Weapons," Dept. of Army Pamphlet No. 50-3- Hdq. Dept. of Army, March 1977.*

[12] *"Structures to Resist the Effects of Accidental Explosions," TM 5-1300, Dept. of Army, June 1969.*

TABLE 4. FREE-AIR BLAST PARAMETERS FOR TNT EQUIVALENT

Case or Shot Number	Peak Overpressure kPa	Station Distance m	Arrival Time ms	Positive Duration ms	Positive Impulse kPa-ms	Ambient Pressure kPa	Ambient Temperature °K	Charge Weight TNT, kg
Case I	42.25	3.05	4.75	2.05	41.4	101.35	288.0	0.454[a]
Case II	75.88	2.29	3.00	1.65	53.1	101.35	288.0	0.454
Case III	112.2	1.92	2.25	1.42	63.4	101.35	288.0	0.454
Shots 24-81-87 to 24-81-92	42.25	35.4	55.2	23.8	481.0	101.35	288.0	712.0
Shots 24-81-93 to 24-81-96	75.88	48.2	63.2	34.8	1118.6	101.35	288.0	4,244
Shots 24-81-97 to 24-81-100	112.2	57.0	66.8	42.2	1883.2	101.35	288.0	11,898

[a]Scaling was from standard conditions of an atmosphere of 101.35 kPa at a temperature of 288°K.

Table 4 above summarizes the calculations for the three blast overpressure levels used during the cylinder tests.

B. Coefficient of Drag

It is customary[13] to present loading data for a test object in a form such that a coefficient of drag, C_D, might be found for the object. It will be assumed that the net horizontal load (in the diffraction as well as the drag phase) across the test structure can be found from the appropriate measured pressure-time profile multiplied by a normal projected area. The sum of these loads over the normal area will be the total horizontal load exerted on the object by the pressure from the blast wave. Equation 3 expresses these relationships for the coefficient of drag, C_D.

$$C_D = \frac{F}{qA} = \frac{2\delta A \sum_{\Theta=0^\circ}^{180^\circ} P(\Theta)}{qA} , \qquad (3)$$

where the drag force, F, is obtained from the summation of the net pressure difference across the cylinder for the projected normal surface, A. δA (See Table 5.) is the incremental projected normal surface calculated for 7.5° each side of a transducer position. $P(\Theta)$ is the pressure as a function of angle. C_D changes as a function of time with pressure changes in the dynamic pressure, corresponding to variations in the free-field blast wave.

Equation 4 gives the relationship used to calculate q.

$$q = \frac{2.5\ P_s^2}{7P_1 + P_s} , \qquad (4)$$

where P_s is the side-on overpressure and P_1 is the ambient pressure. Equation 4 is strictly correct only at the front of the blast wave but will be used throughout the entire blast wave's positive duration for calculations of q as a function of time. This method agrees well with the exponential decay of q as given in Reference 14. The method used here was considerably more convenient to the data processing method used than the more exact method given in Reference 14.

---

[13] *Sighard F. Hoerner, Fluid-Dynamic Drag, Published by author, 148 Busteed Drive, Midland Park, NJ, 1965.*

[14] *"Design of Structures to Resist Effects of Atomic Weapons, Weapons Effect Data," Dept. of Army Technical Manual TM 5-856-1, November 1960.*

Figure 19 shows the force-time curves computed from the side-on blast wave after being multiplied by the total normal area/length, m. The pressure records used were smoothed through the small pressure peaks propagated upstream from the cylinder. This was done to better represent undisturbed free-stream flow.

Table 5 lists the pertinent parameters needed for the calculation of total drag force, F, as a function of time. This function is displayed in Figure 20. Substituting the data from Figure 19, force versus time, (from q versus time) and Figure 20 (for drag F, versus time) into Equation 3, the coefficients of drag versus time can be computed for the cylinder. This was done and is presented in Figure 21.

It should be noted from Figure 21 that the initial loading of the cylinder during the diffraction phase caused coefficients of drag several times the average value after the diffraction phase. A second point of interest is that Figures 21-A and 21-B show negative values for the coefficients for the interval 1 to 1.5 ms. The remainder of the records show oscillations in the drag coefficients.

Vortex shedding (Reference 15, 16, and 17) could account for the oscillations present. A meaningful average value is a bit difficult to determine; however, Table 6 and Figure 22 attempt to relate an average early time coefficient (2-6 ms) for the present work and that reported in References 15 and 16 with steady state values from Hoerner (Reference 13). Table 6 lists the average coefficients determined for early times after the diffraction phase as a function of Reynolds number (using diameter of the cylinder) and flow Mach number behind the shock front.

The present results and the shock tube results reported in Reference 15 tend to cluster about the upper curve of Figure 22 indicating Reynolds numbers below transition flow. Whereas, the field data reported from the Dice Throw Event (Reference 16) clusters about the lower curve of Figure 22, indicating flows above transition Reynolds numbers. To predict accurately the coefficient of drag, it is necessary for the test structure to be clearly in one or the other of the two flow regions. In the Mach number region 0.45 to 0.50, one's

---

[15] *Valerie C. Martin, K.F. Mead, and J.E. Uppard, "The Drag on a Circular Cylinder in a Shock Wave," AWRE Report No. 0-34/67, May 1967.*

[16] *A.W.M. Gibb and D.A. Hill, "Free Flight Measurement of the Drag Forces on Cylinders in Event Dice Throw," Suffield Tech Paper No. 453, February 1979.*

[17] *Valerie C. Martin, K.F. Mead, and J.E. Uppard, "Blast Loading on a Right Circular Cylinder," AWRE Report No. 0-93/65, November 1965.*

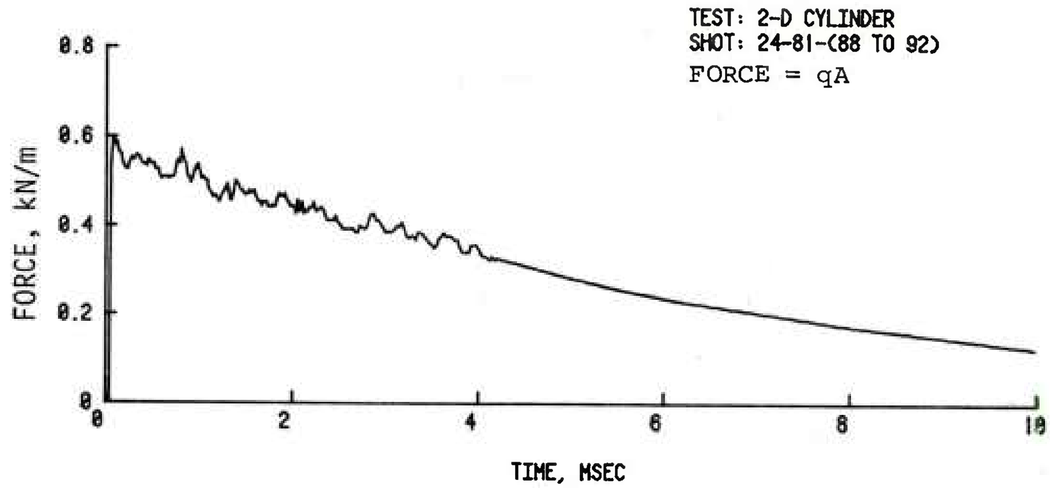

A. Input of 42.3 kPa

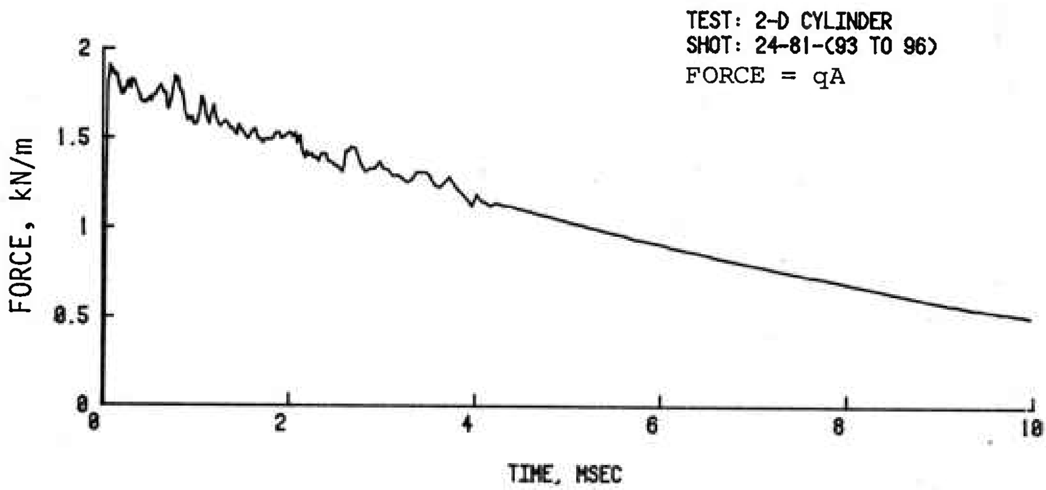

B. Input of 75.9 kPa

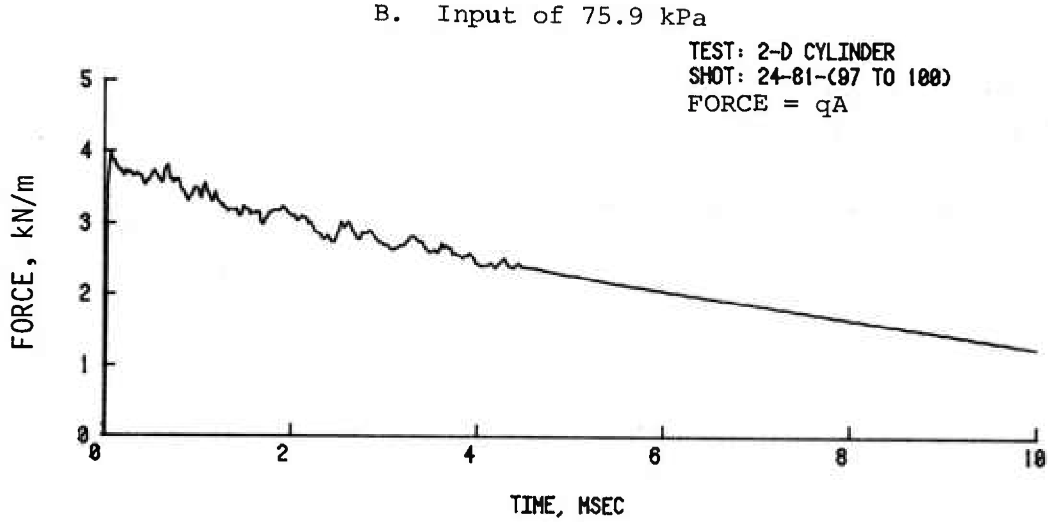

C. Input of 112.2 kPa

Figure 19. Net horizontal force-time functions computed from the side-on pressure-time records.

TABLE 5. DRAG PARAMETERS

Positions	Ambient Pressure kPa	Area/Length m	Shots
0 - 180[a]	102.7	.0132[b]	24-81-88 - 24-81-92[c]
15 - 165	102.7	.0256	24-81-90 - 24-81-91
30 - 150	102.7	.0230	24-81-91 - 24-81-90
45 - 135	102.7	.0187	24-81-88 - 24-81-88
60 - 120	102.7	.0132	24-81-90 - 24-81-91
75 - 105	102.7	.0077	24-81-91 - 24-81-90
P_s = 42.25 kPa, P_1 = 102.7 kPa, T_1 = 20.9°C			
0 - 180	102.9	.0132	24-81-93 - 24-81-96
15 - 165	102.9	.0256	24-81-94 - 24-81-95
30 - 150	192.9	.0230	24-81-95 - 24-81-94
45 - 135	102.9	.0187	24-81-93 - 24-81-96
60 - 120	102.9	.0132	24-81-94 - 24-81-95
75 - 105	102.9	.0077	24-81-95 - 24-81-94
P_s = 75.88 kPa, P_1 = 102.9 kPa, T_1 = 21.0°C			
0 - 180	102.9	.0132	24-81-97 - 24-81-100
15 - 165	102.9	.0256	24-81-98 - 24-81-99
30 - 150	102.9	.0230	24-81-99 - 24-81-98
45 - 135	102.9	.0187	24-81-97 - 24-81-97
60 - 120	102.9	.0132	24-81-98 - 24-81-99
75 - 105	102.9	.0077	24-81-99 - 24-81-98
P_s = 112.2 kPa, P_1 = 102.9 kPa, T_1 = 21.2°C			

[a] Area includes factor of two to include both instrumented and uninstrumented sections of model.

[b] Normal projected areas were calculated for 7.5 degrees each side of transducer position except for 75 and 105 degree positions. Area to the 90 degree point was included for these two positions.

[c] Total projected normal area, A, for all shots is 0.1016 m^2/length.

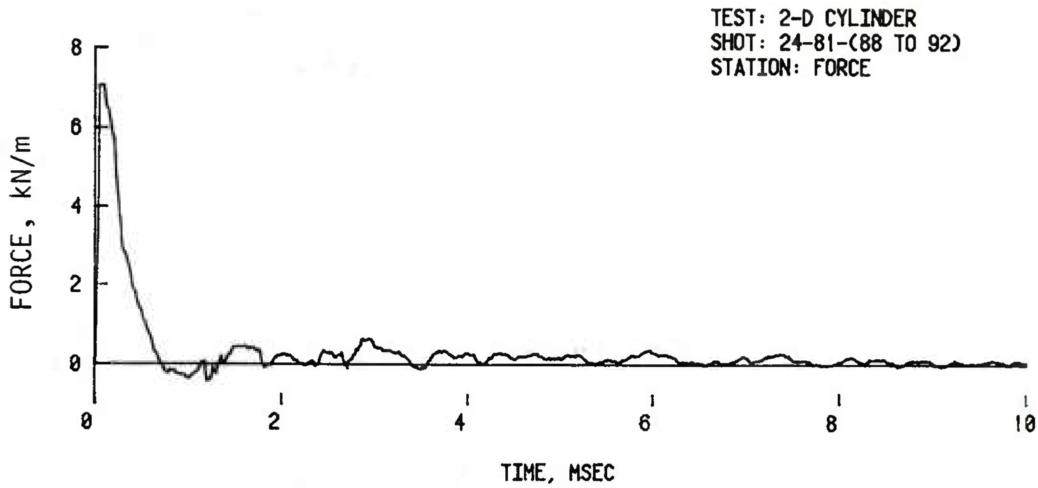

A. Input of 42.3 kPa

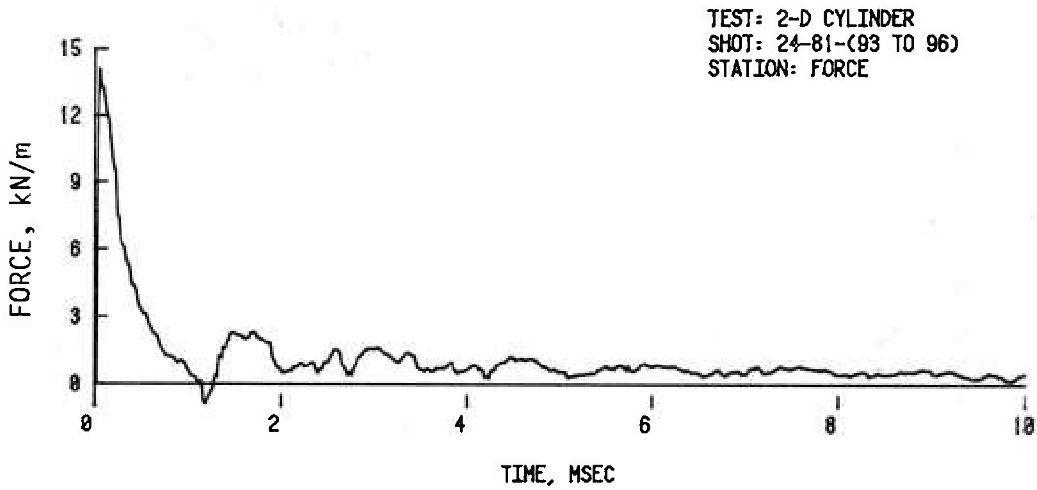

B. Input of 75.9 kPa

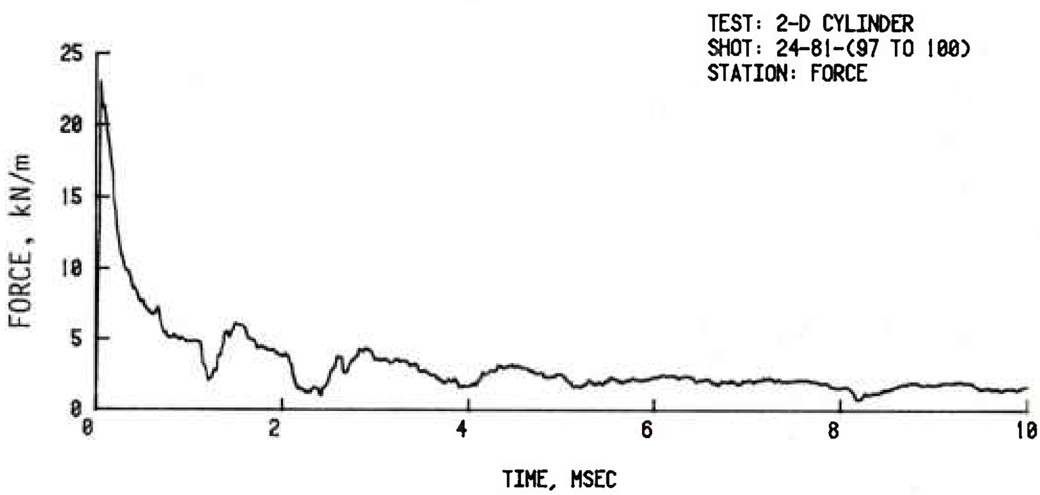

C. Input of 112.2 kPa

Figure 20. Net horizontal force/length of model as a function of time.

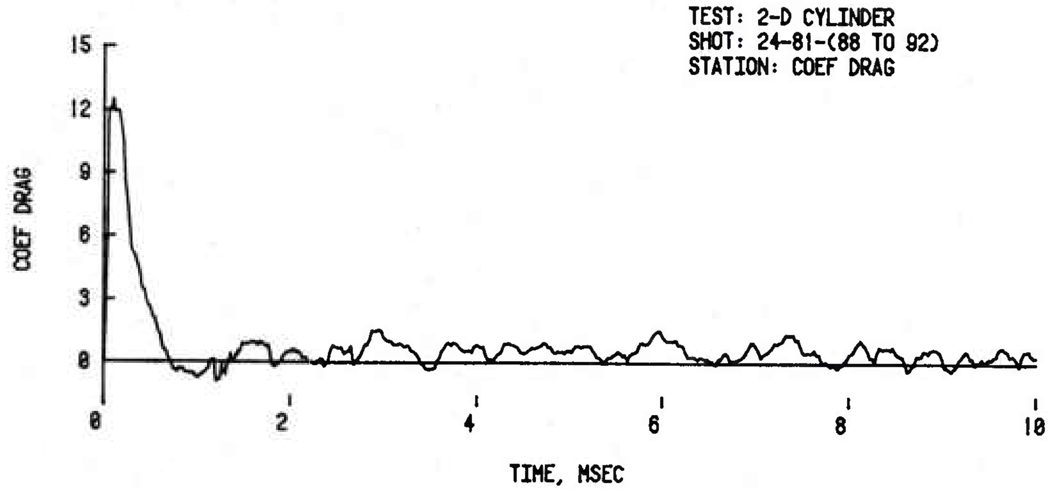

A. Input of 42.3 kPa

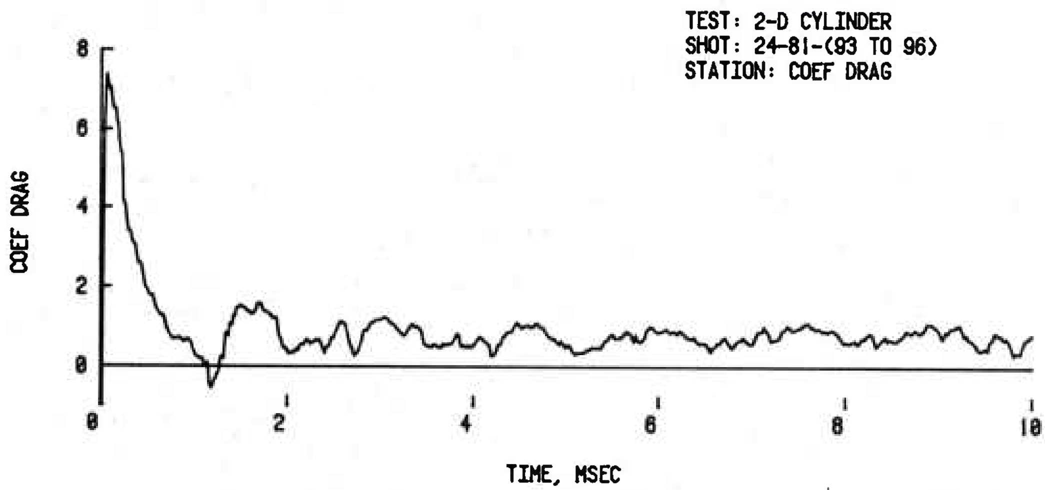

B. Input of 75.9 kPa

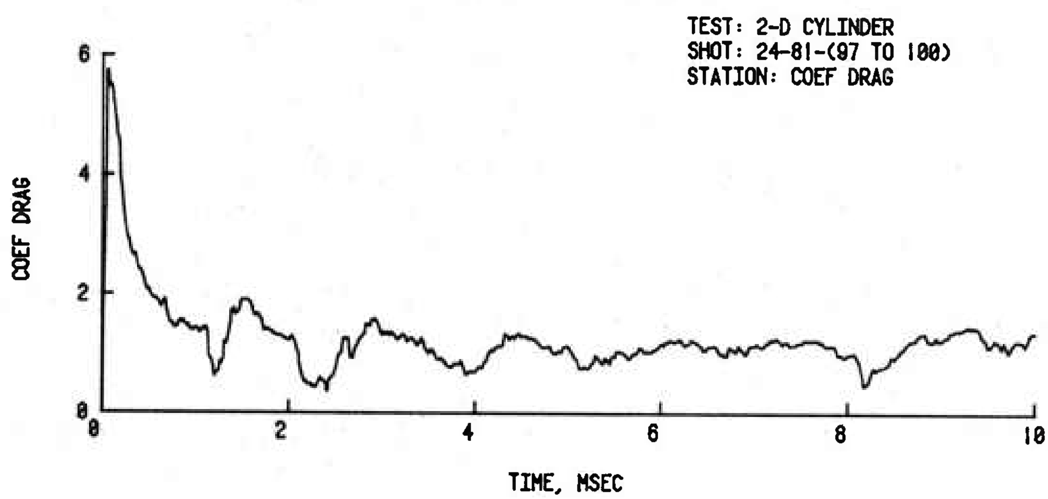

C. Input of 112.2 kPa

Figure 21. Coefficients of drag computed for the net horizontal loads.

TABLE 6. COEFFICIENT OF DRAG, 2-D CYLINDER PARAMETERS

Source Reference	Diameter cm	Pressure kPa	Reynolds No.*	Mach No.	Coefficient Drag (av)
Hoerner, Ref. 13	---	---	>4 x 10	0.24	0.27
				0.30	0.30
				0.38	0.34
				0.50	1.14
				0.60	1.41
Present Work	---	---	$<4 \times 10^5$	0.10	1.17
				0.40	1.21
				0.50	1.28
				0.60	1.43
				0.70	1.60
Martin & Others, Ref. 15	10.2	55.2	9.2×10^5	0.30	1.10
	10.2	131.0	2.2×10^6	0.56	1.69
Gibb & Hill, Ref. 16	8.9	66.9	8.1×10^5	0.38	0.34
	8.9	137.9	1.3×10^6	0.60	0.70
	24.1	46.2	1.6×10^6	0.29	0.43
	45.7	66.9	4.2×10^6	0.38	0.29
Present Work	10.2	42.3	6.8×10^5	0.24	0.90
	10.2	75.9	1.3×10^6	0.38	1.15
	10.2	112.2	1.8×10^6	0.50	1.27

*Average values of Reynolds No., Mach No., and coefficient of drag over 2-6 millisecond of record time.

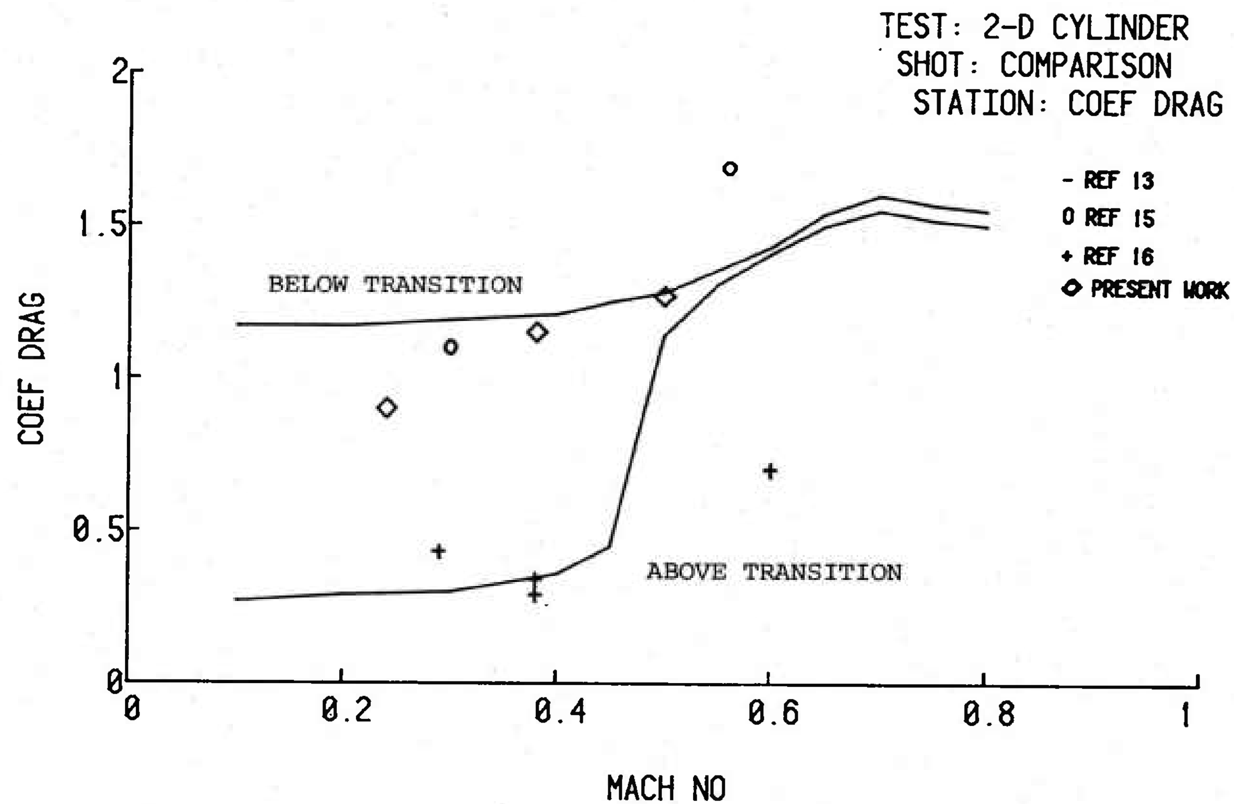

Figure 22. Average coefficient of drag as a function of Mach number.

predictions might range from the low curve value for C_D of 0.34 to 1.20 for the high curve. Great care is needed for accurate prediction of drag coefficients for test structures.

C. Pressure Coefficient versus Angle

Also of interest in determining the response of a structure is knowing the enhancement of the side-on pressure as a function of angle of incidence. The reflected pressures P_r divided by side-on pressures P_s taken from Table 2 are plotted in Figure 23. Values of P_r/P_s overlap at 45 degrees, and beyond 45 degrees can be represented by a single curve.

V. SUMMARY AND CONCLUSIONS

A two-dimensional non-responding cylinder was tested in the BRL 57.5 cm shock tube at nominal overpressure levels of 42.3, 75.9, and 112.2 kPa. Pressure-time loading records were obtained at 15° increments of the cylinder for each of the pressure levels for a decaying input shock wave. These blast parameters scaled to those that would be produced by detonation of 712, 4244, and 11898 kg of TNT high explosive.

Total loads from the pressure loading were obtained by summation of the pressure over the projected normal area of the cylinder. Coefficients of drag as a function of time were computed from the net horizontal drag forces and the free-field input waves from which the dynamic pressures, q, had been calculated.

The resulting coefficients of drag curves were presented for the three pressures tested. A great variation of several times for the coefficient was seen from the values of the diffraction portion to the values of the semi-steady state portion of the curves. An early time (2-6 ms) average coefficient was compared to the steady state coefficients listed in Hoerner (Reference 13).

It is seen from these comparisons that the flow region to which the cylinder is exposed, has to be clearly defined in order to make accurate predictions of transient drag coefficients.

ACKNOWLEDGMENTS

The author wishes to thank Mr. Richard Thane for the modification to the driver section of the BRL 57.5 cm shock tube and its operation during the tests. The author wishes to thank Mr. Charles Fisher for the careful electronic recording of the test results.

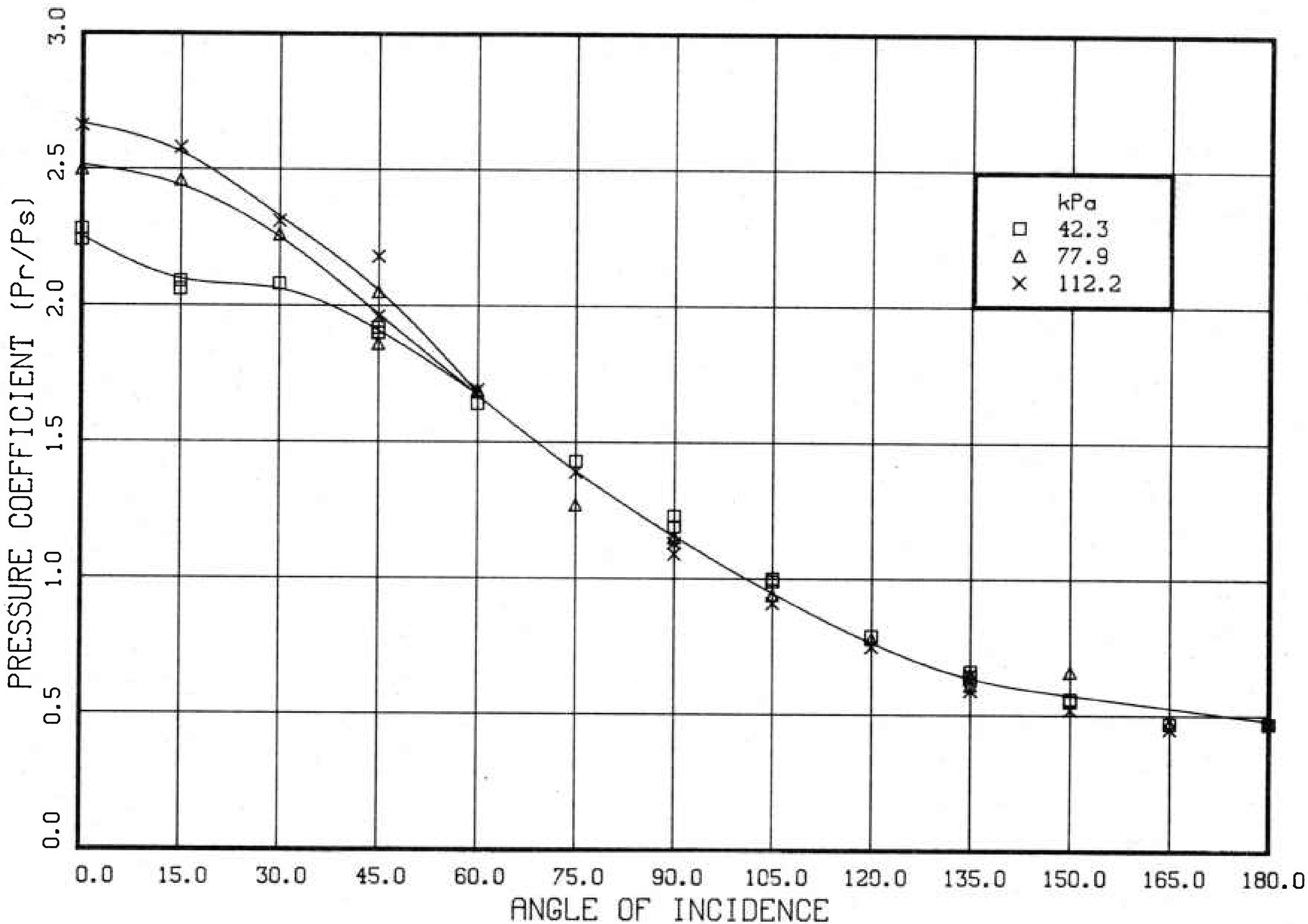

Figure 23. Pressure coefficient versus angle.

LIST OF REFERENCES

1. S.H. J. Allen and W.G. Vincenti, "Wall Interference in a Two-Dimensional Flow Wind Tunnel with Consideration of the Effect of Compressibility," Nat. Adv. Comm. for Aeronautics Report 782, 1944.

2. R.N. Hollyer and R.E. Duff, "The Effect of Wall Boundary Layer on the Diffraction of Shock Waves around Cylindrical and Rectangular Obstacles," Univ. of Michigan Report 50-2, 1950.

3. W. Bleakney and D.R. White, "Shock Loading of Rectangular Obstacles," Dept. of Physics Technical Report II, 11, Princeton Univ., January 1953.

4. N.K. Delany and N.E. Sorensen, "Low Speed Drag of Cylinders of Various Shapes," Nat. Adv. Comm. Aeronautics Technical Note 3038, Was., DC, 1953.

5. George A. Coulter and William T. Matthews, "Coefficients of Drag Measured with a Force Balance," BRL Tech. Note No. 1155, December 1954.

6. M.A. Fry and others, "The HULL Hydro-Dynamics Computer Code," AFWL-TR-76-183, U.S. Air Force Weapons Lab, Kirtland Air Force Base, NM, September 1976.

7. Richard E. Lottero, "A Detailed Comparison of 3-D Hydrocode Computations for Shock Diffraction Loading on an S-280 Electrical Equipment Shelter," BRL Tech. Report ARBRL-TR-02334, June 1981.

8. John D. Wortman, "Blast Computations over a Hemicylindrical Aircraft Shelter," BRL Memo. Report ARBRL-MR-03115, July 1981.

9. George A. Coulter and Brian P. Bertrand, "BRL Shock Tube Facility for the Simulation of Air Blast Effects," BRL Memo. Report No. 1685, August 1965.

10. C.W. Lampson, "Résumé of the Theory of Plane Shock and Adiabatic Waves with Applications to the Theory of the Shock Tube," BRL Tech. Note No. 139, March 1950.

11. Samuel Gladstone and Philip, J. Dolan, "The Effects of Nuclear Weapons," Dept. of Army Pamphlet No. 50-3, Hdq. Dept. of Army, March 1977.

12. "Structures to Resist the Effects of Accidental Explosions," TM 5-1300, Dept. ofArmy, June 1969.

13. Sighard F. Hoerner, <u>Fluid-Dynamic Drag</u>, Published by author, 148 Busteed Drive, Midland Park, NJ, 1965.

14. "Design of Structures to Resist Effects of Atomic Weapons, Weapons Effect Data," Dept. of Army Tech. Manual TM 5-856-1, November 1960.

15. Valerie C. Martin, K.F. Mead, and J.E. Uppard, "The Drag on a Circular Cylinder in a Shock Wave," AWRE Report No. 0-34/67, May 1967.

16. A.W.M. Gibb and D.A. Hill, "Free Flight Measurement of the Drag Forces on Cylinders in Event Dice Throw," Suffield Tech. paper No. 453, February 1979.

17. Valerie C. Martin, K.F. Mead, and J.E. Uppard, "Blast Loading on a Right Circular Cylinder," AWRE Report No. 0-93/65, November 1965.

APPENDIX A

DRAWINGS FOR CYLINDER

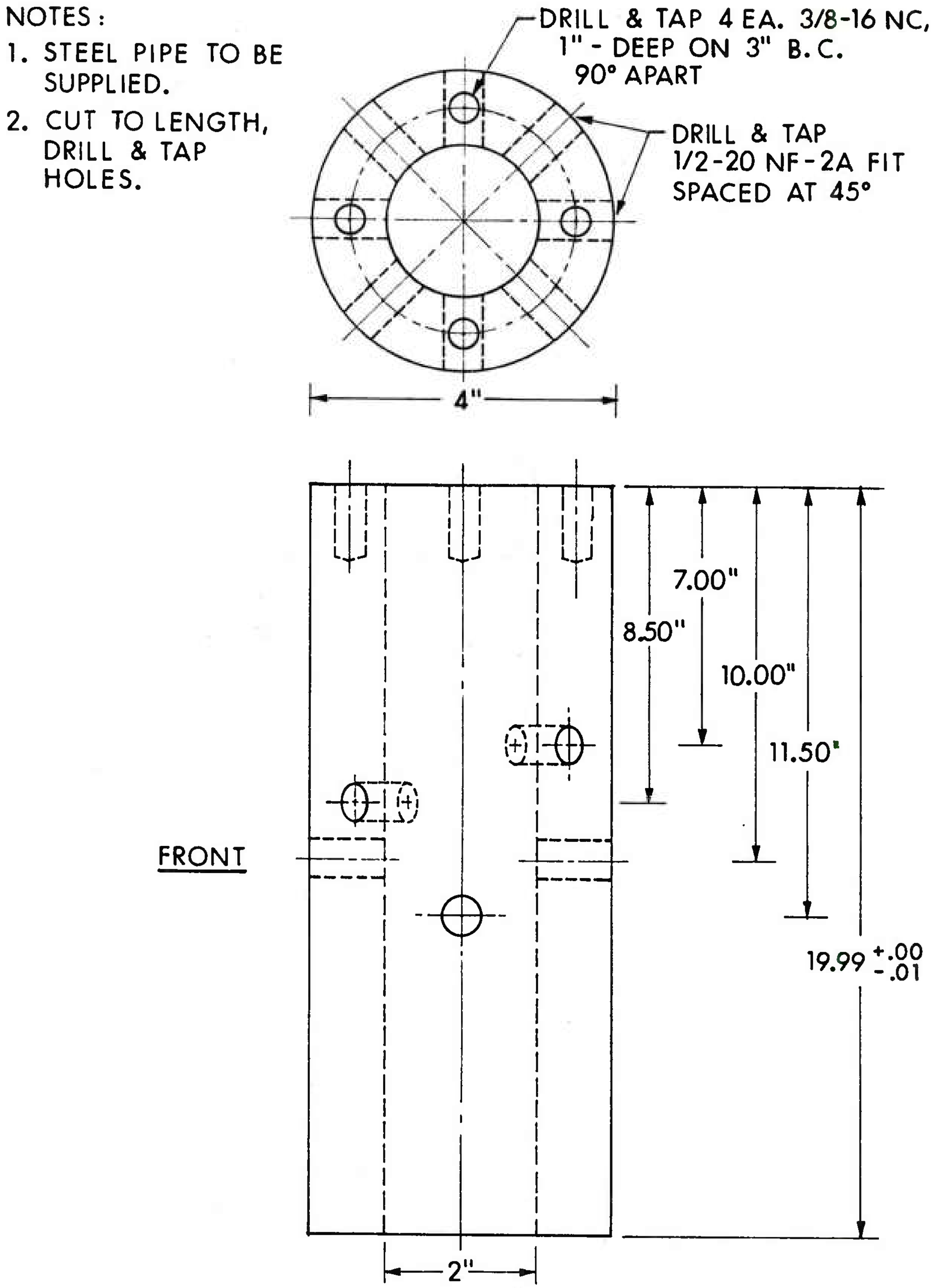

Figure A-1. Sketch of two-dimensional model cylinder.

NOTES:

1. MTL - STEEL
2. MACHINE CENTER POINT ON PLUG.
3. MAKE ONE.

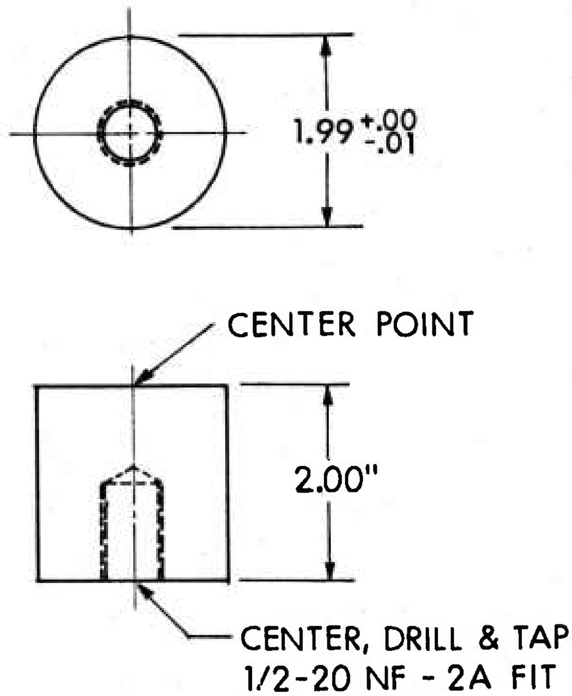

Figure A-2. Bottom plug for model.

NOTES:

1. MOUNTING PLATE TO BE FURNISHED.
2. TRY BOTTOM PLUG FOR FIT.
3. FURNISH 3/8-2 3/4 LONG MOUNTING BOLTS.
4. SCRIBE MOUNTING PLATE AT FRONT - 0°.

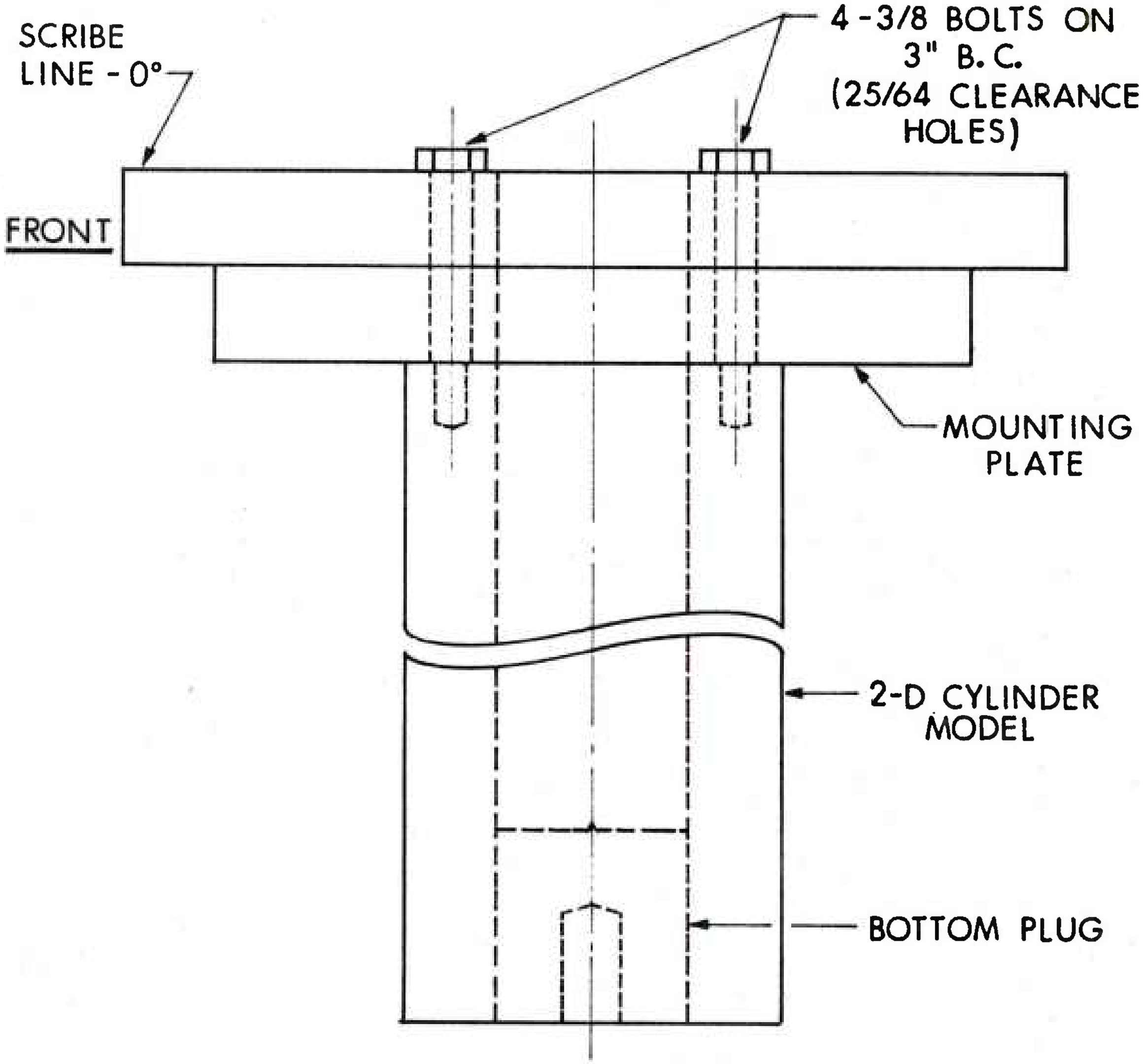

Figure A-3. Assembly drawing.

APPENDIX B

PRESSURE-TIME RECORDS

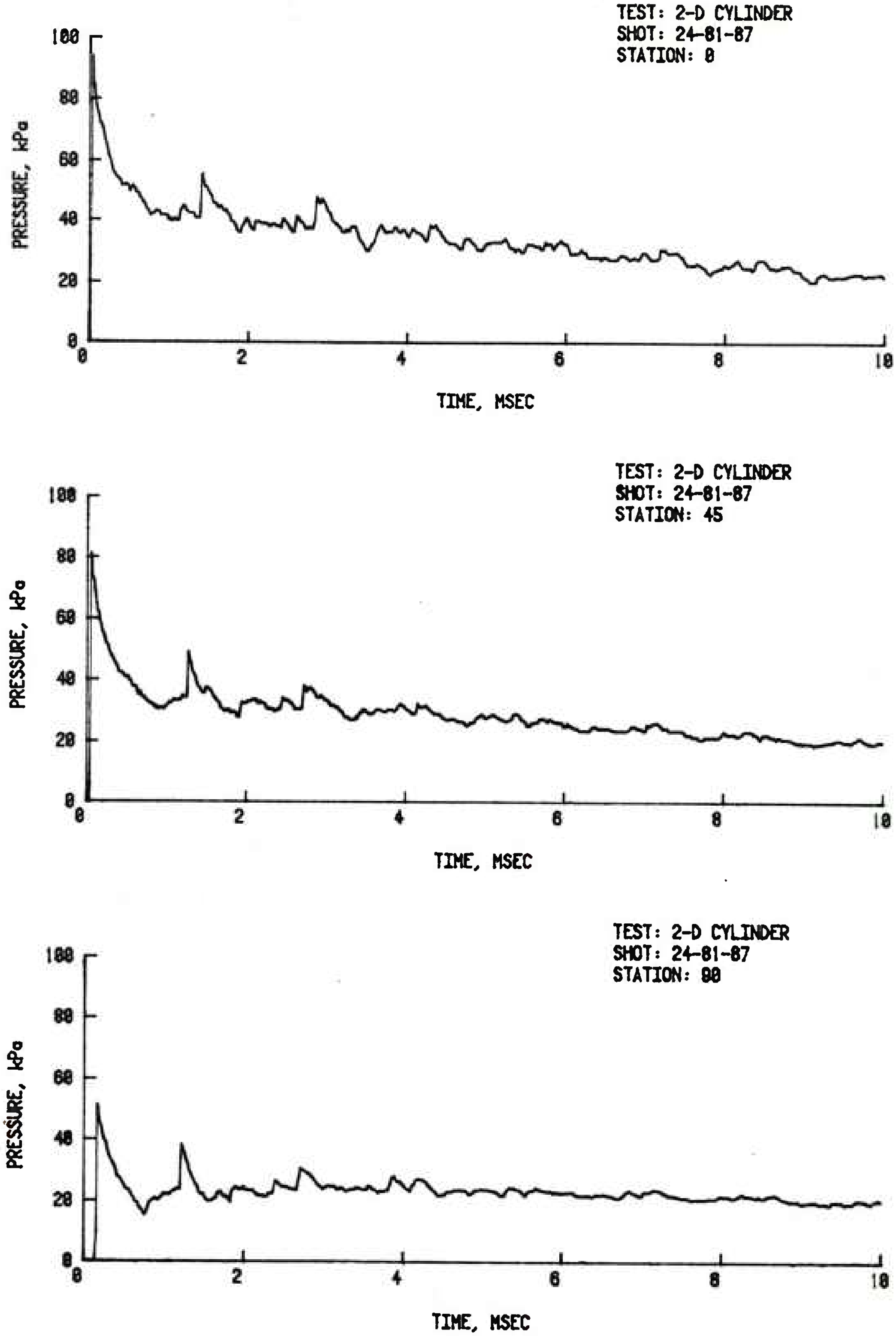

Figure B-1. Pressure-time records from cylinder for input overpressure of 42.3 kPa.

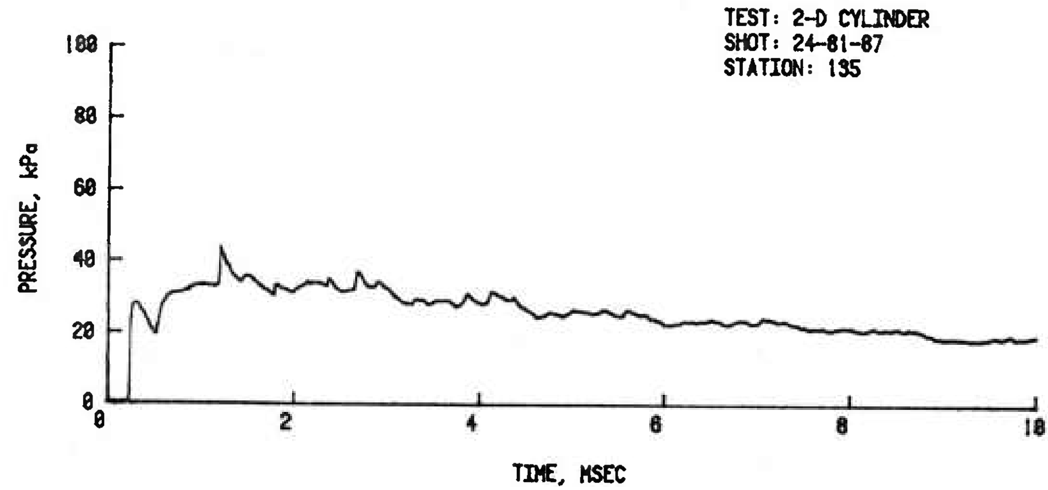

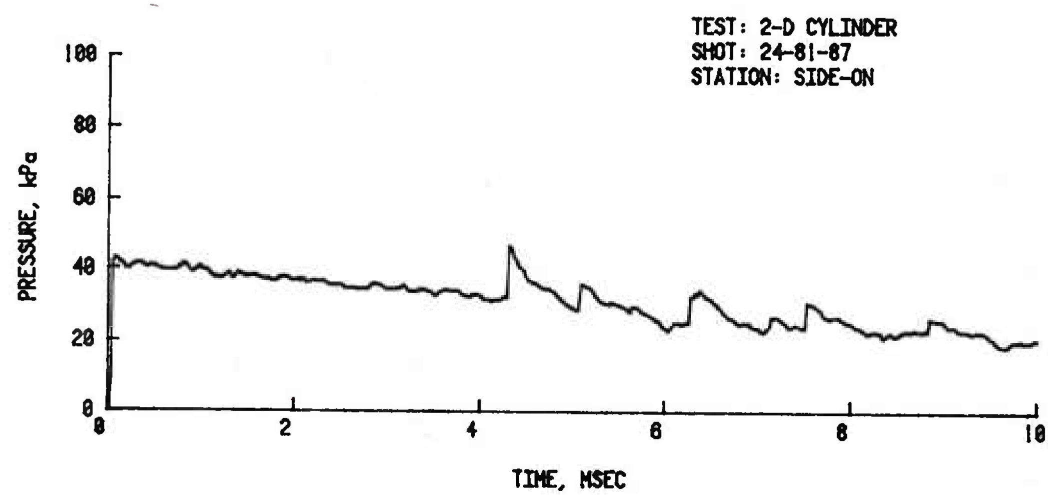

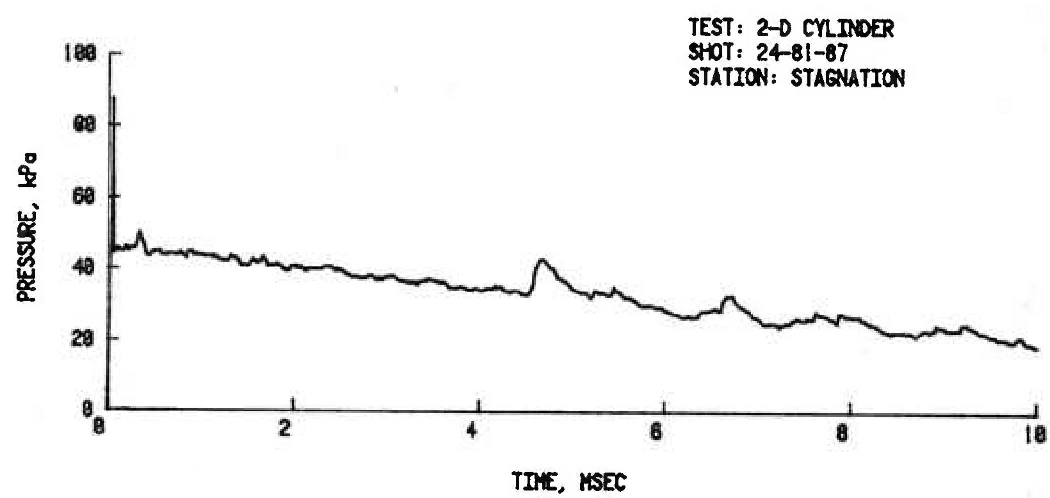

Figure B-1. Pressure-time records from cylinder for input overpressure of 42.3 kPa. (cont'd)

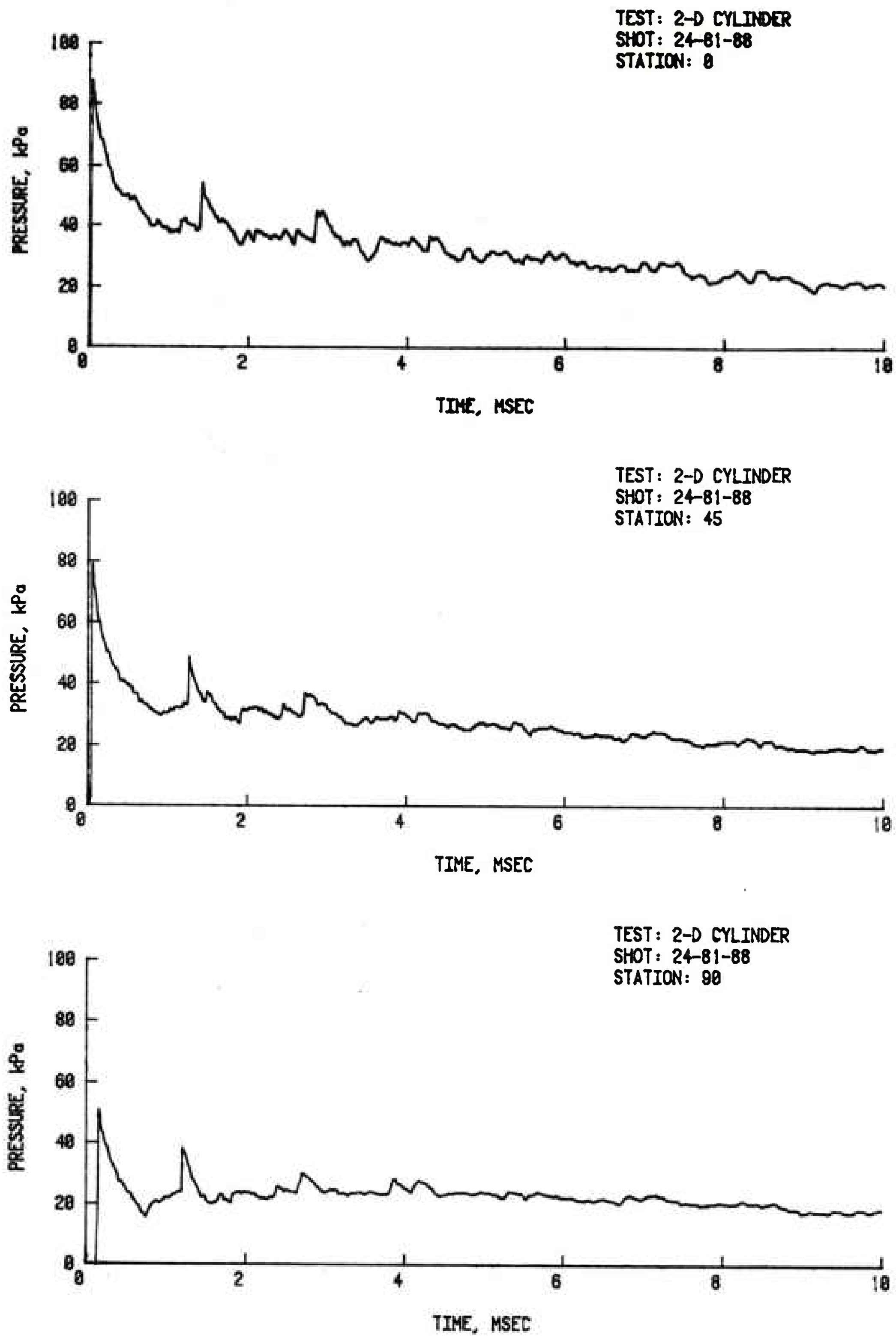

Figure B-1. Pressure-time records from cylinder for input overpressure of 42.3 kPa. (cont'd)

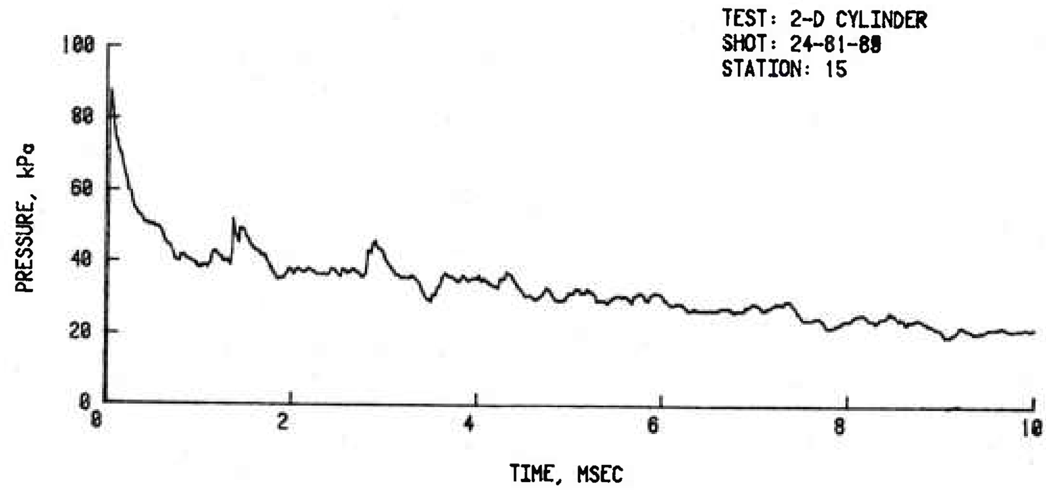

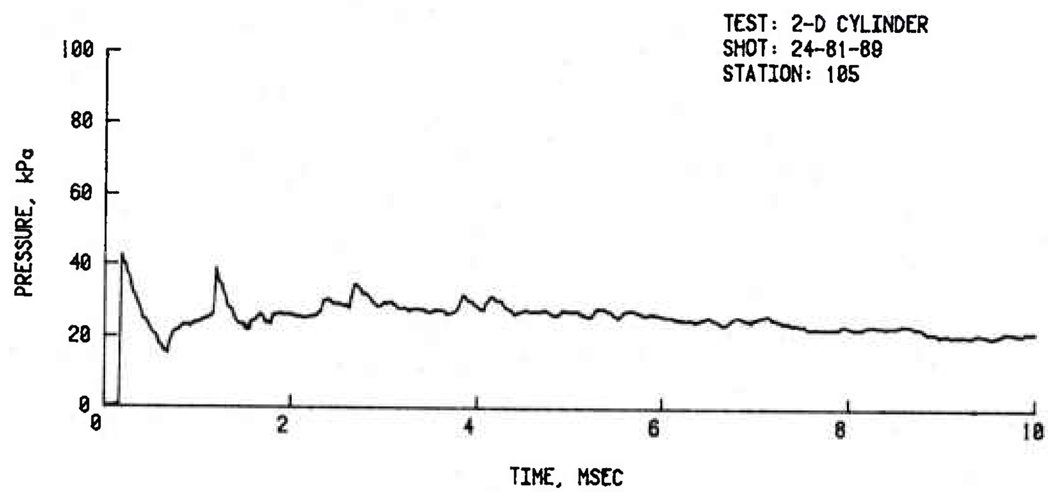

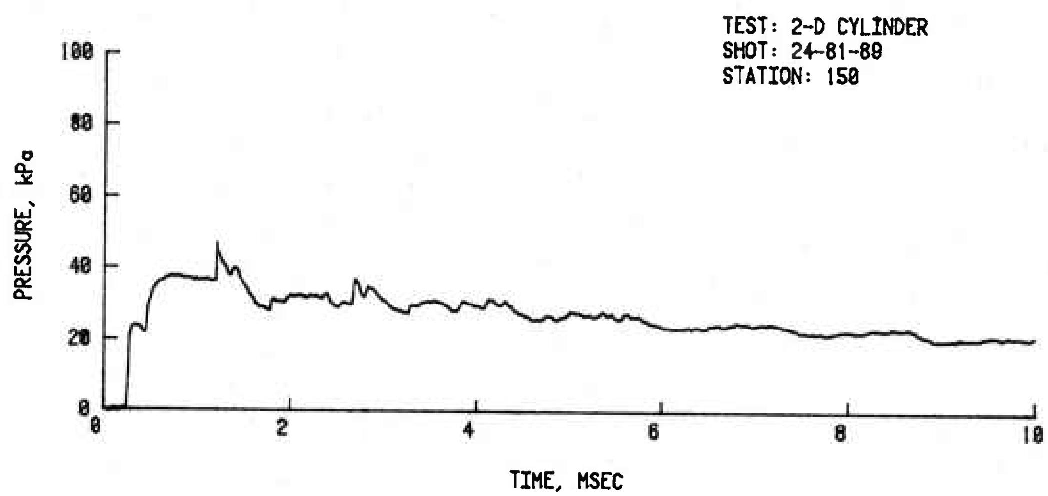

Figure B-1. Pressure-time records from cylinder for input overpressure of 42.3 kPa. (cont'd)

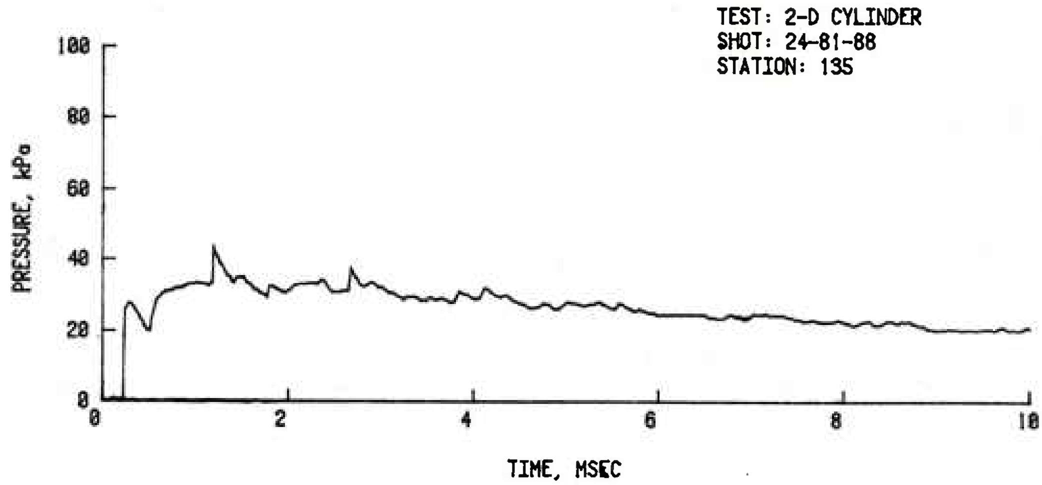

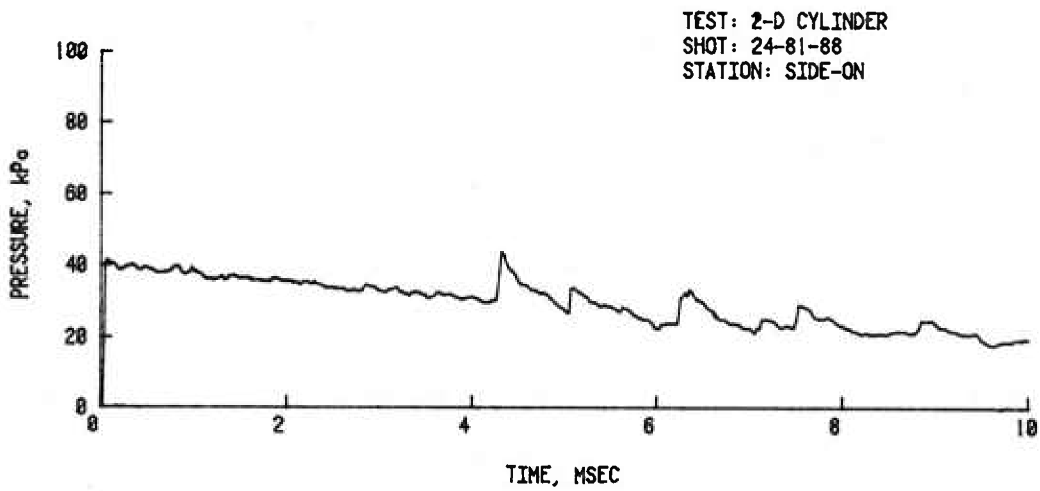

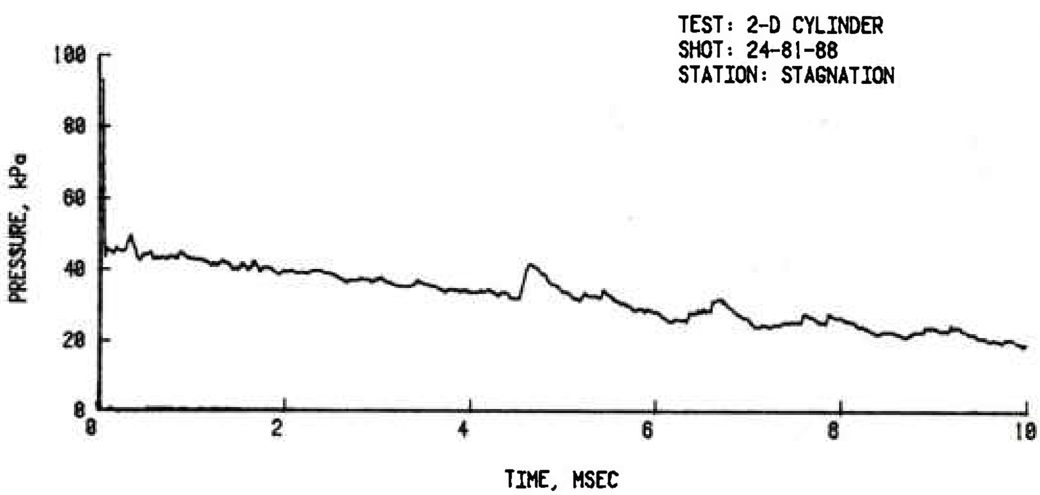

Figure B-1. Pressure-time records from cylinder for input overpressure of 42.3 kPa. (cont'd)

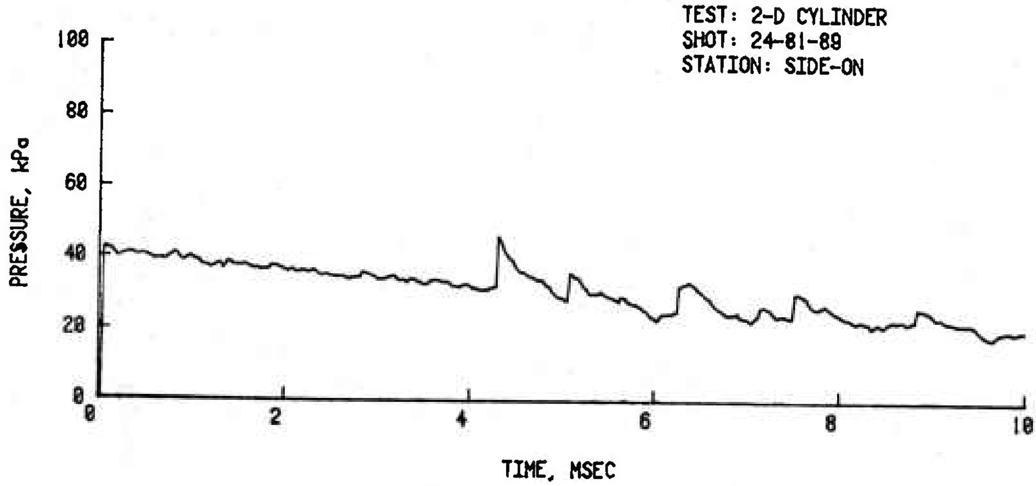

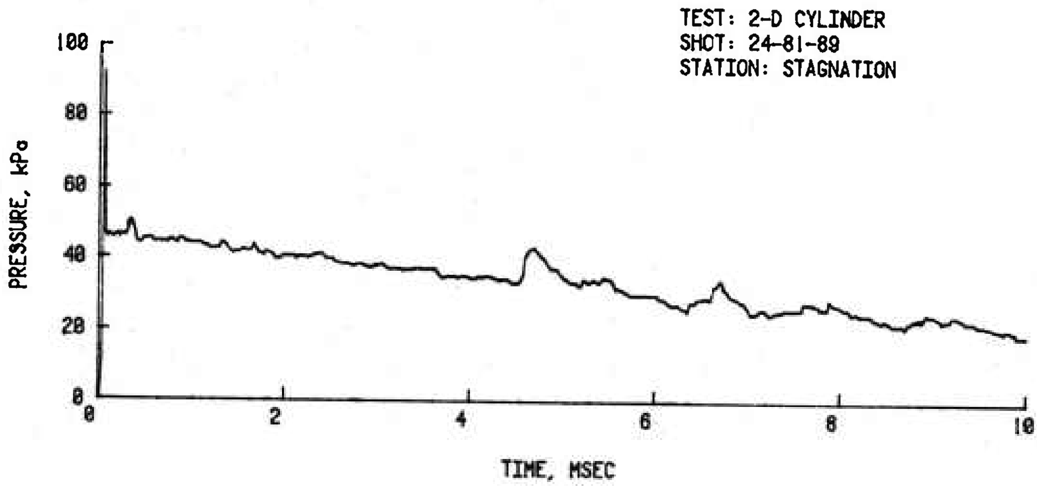

Figure B-1. Pressure-time records from cylinder for input overpressure of 42.3 kPa. (cont'd)

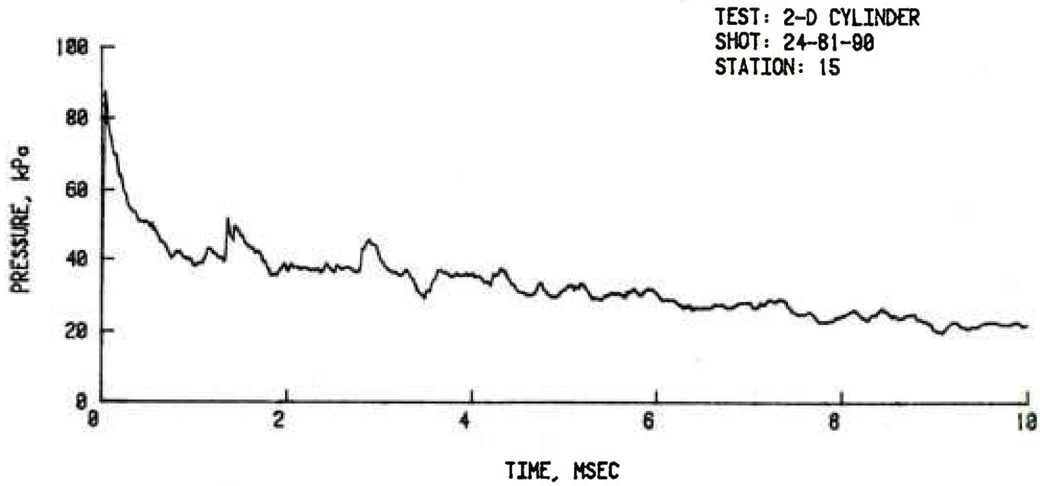

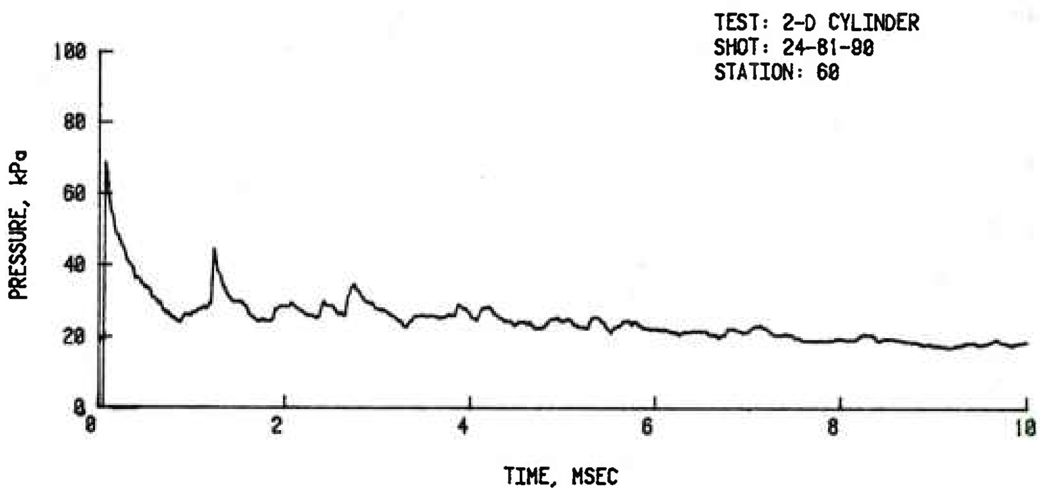

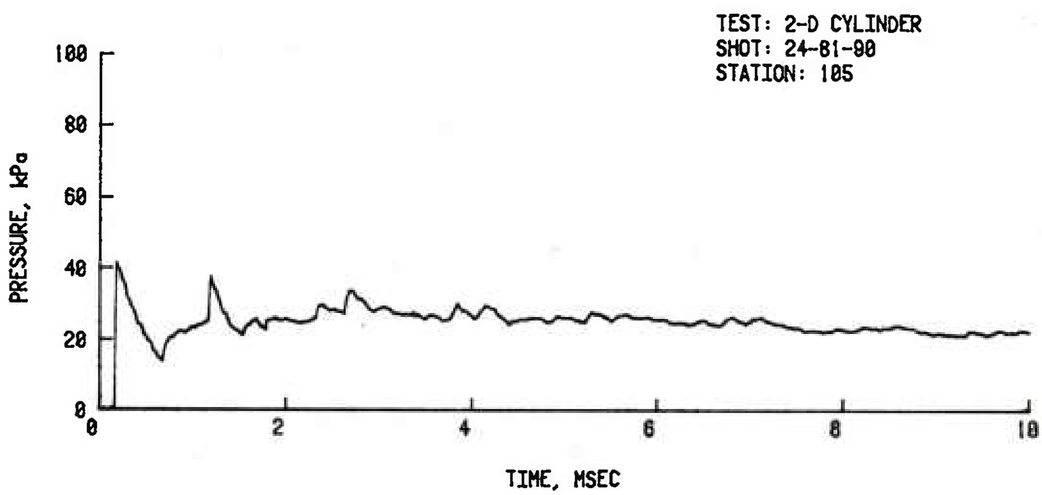

Figure B-1. Pressure-time records from cylinder for input overpressure of 42.3 kPa. (cont'd)

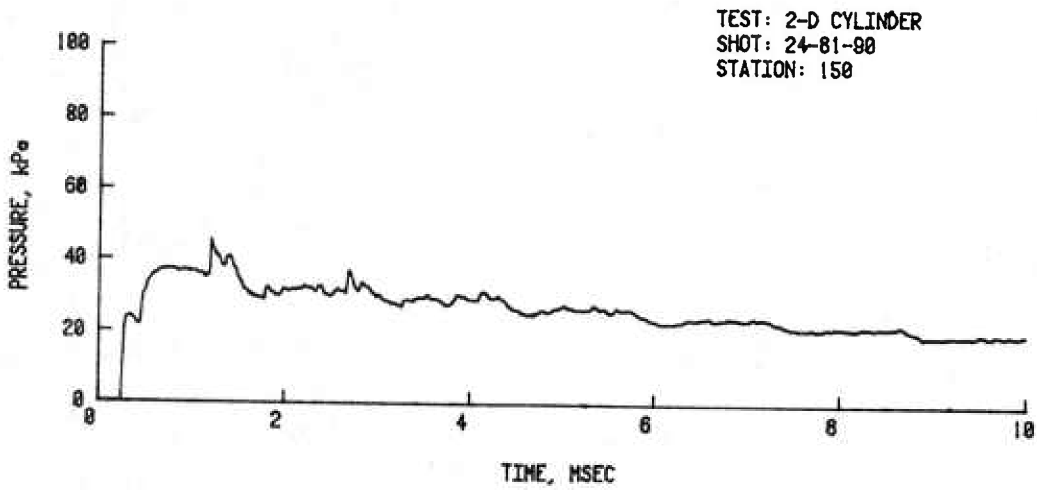

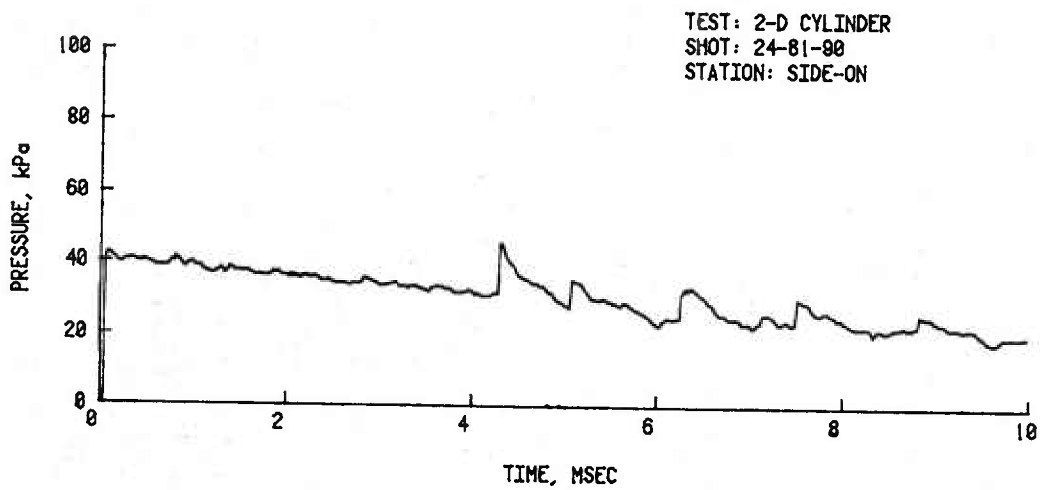

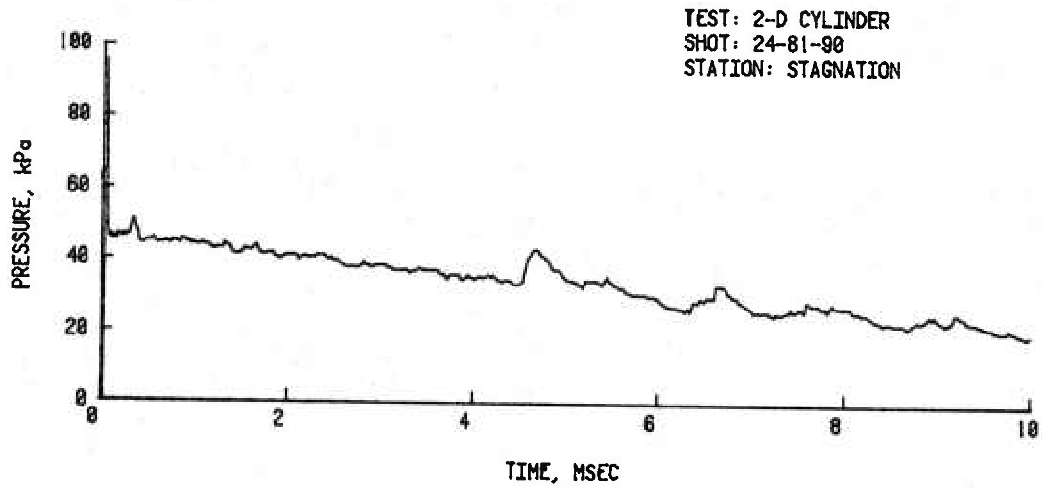

Figure B-1. Pressure-time records from cylinder for input overpressure of 42.3 kPa. (cont'd)

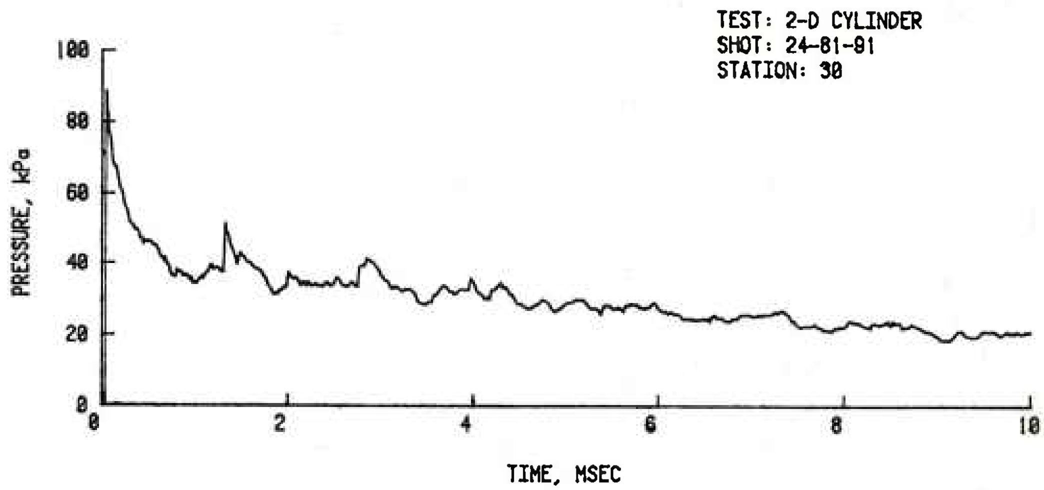

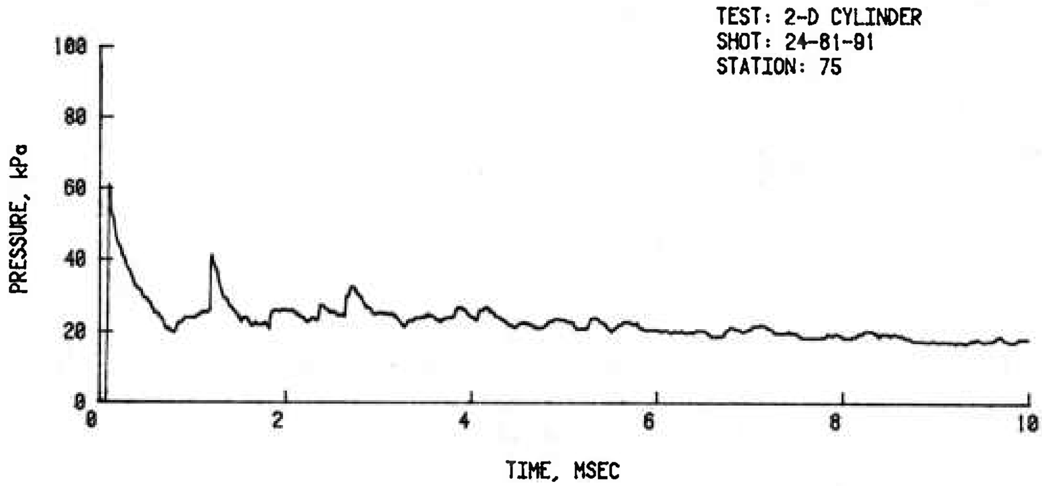

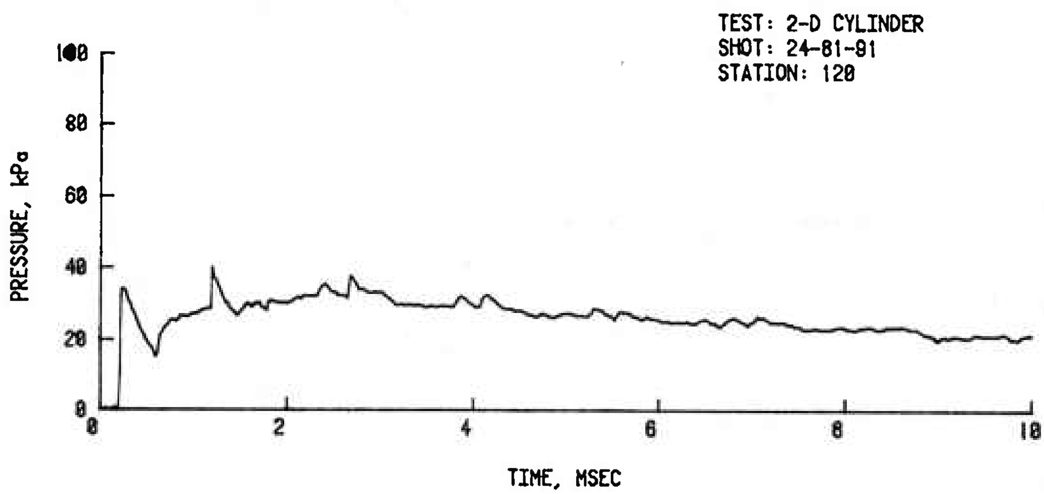

Figure B-1. Pressure-time records from cylinder for input overpressure of 42.3 kPa. (cont'd)

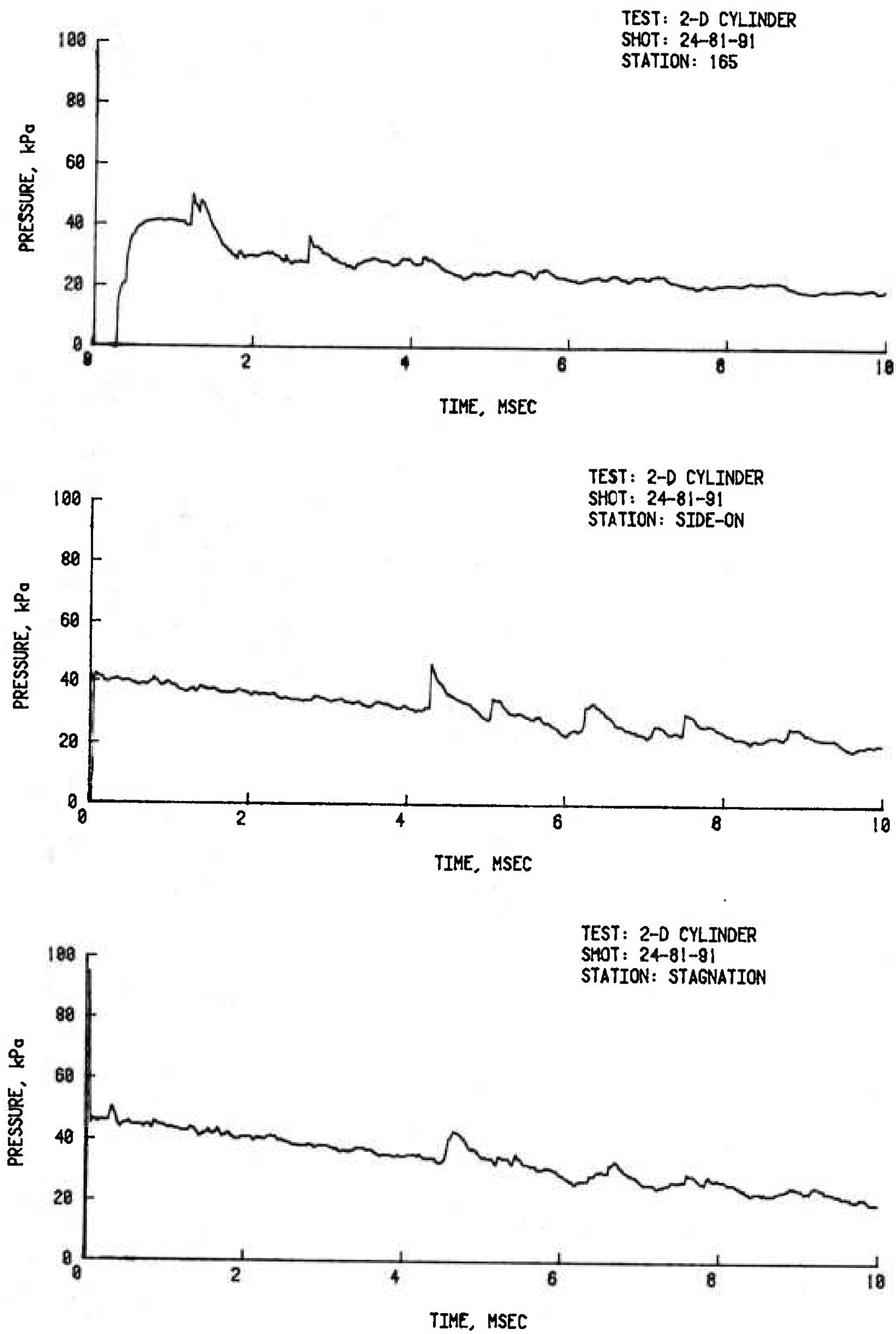

Figure B-1. Pressure-time records from cylinder for input overpressure of 42.3 kPa. (cont'd)

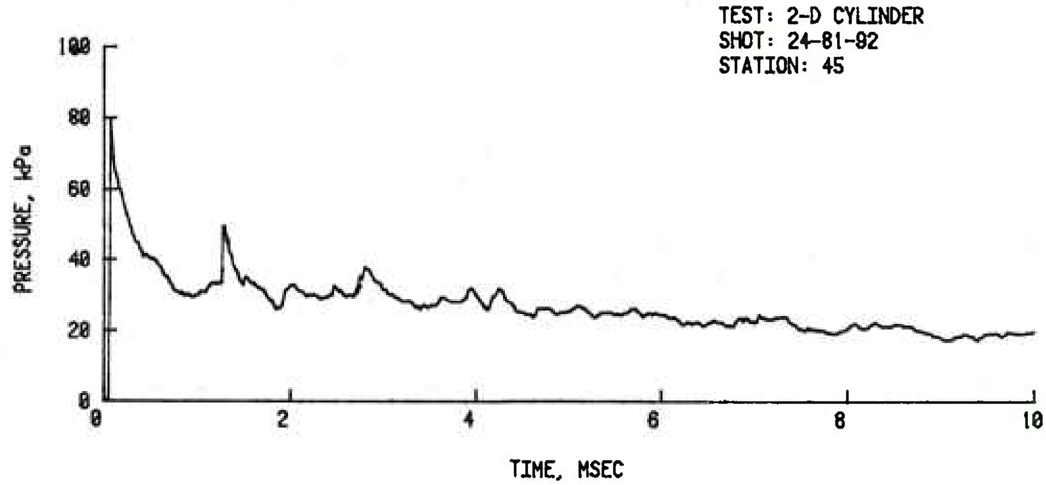

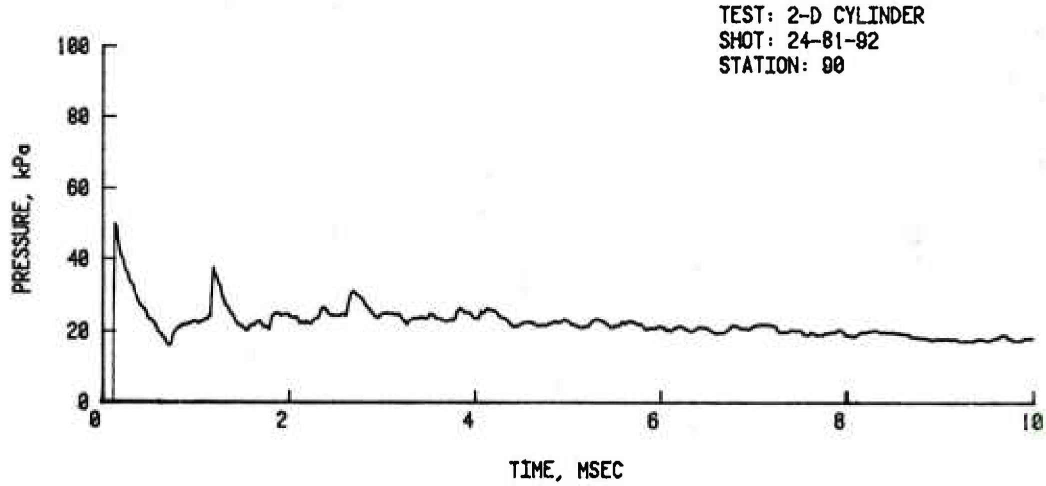

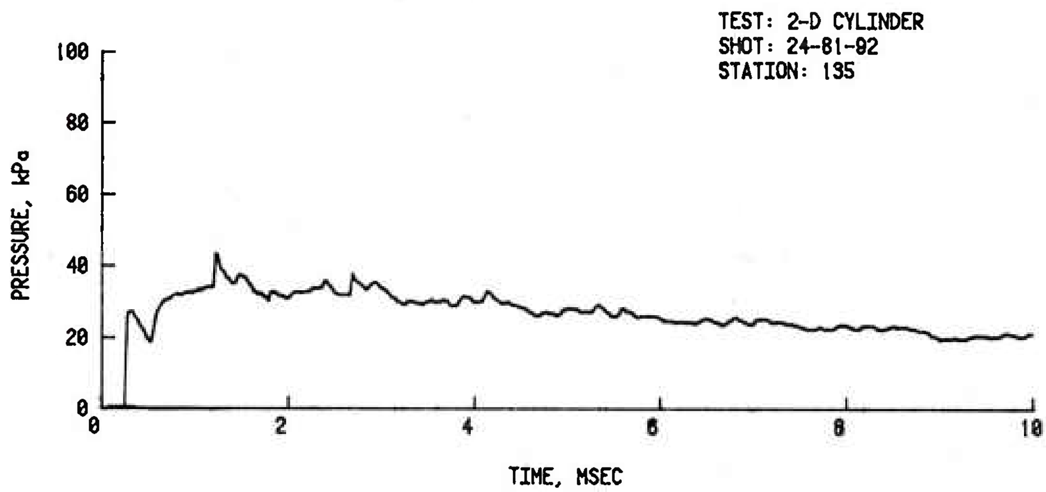

Figure B-1. Pressure-time records from cylinder for input overpressure of 42.3 kPa. (cont'd)

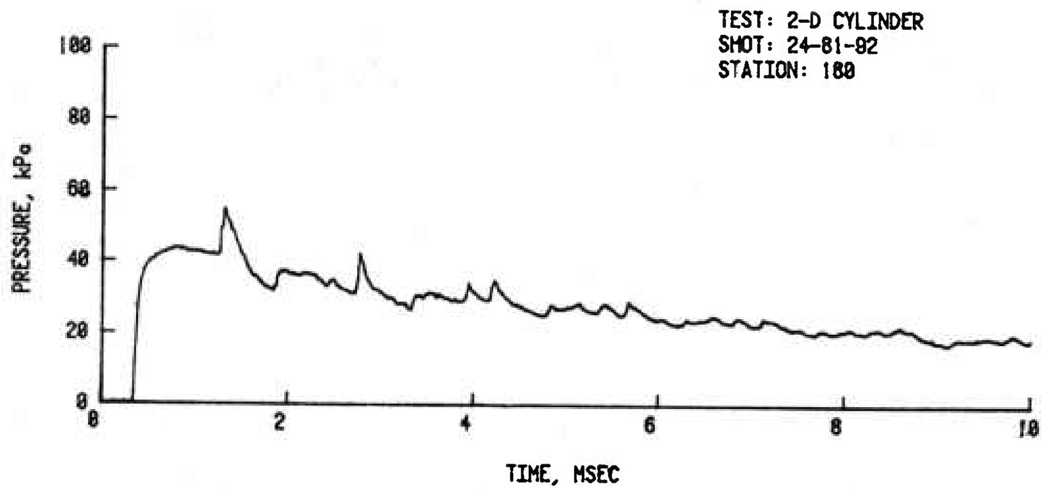

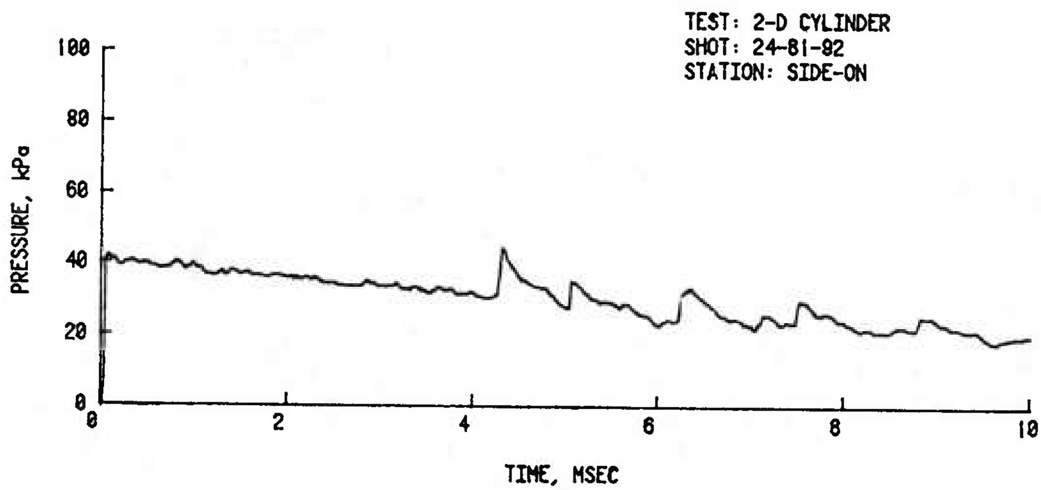

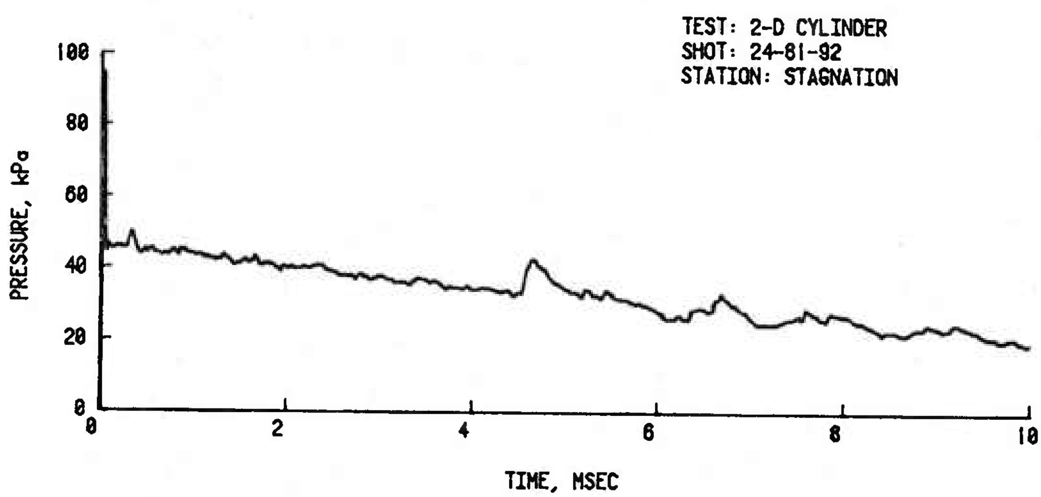

Figure B-1. Pressure-time records from cylinder for input overpressure of 42.3 kPa. (cont'd)

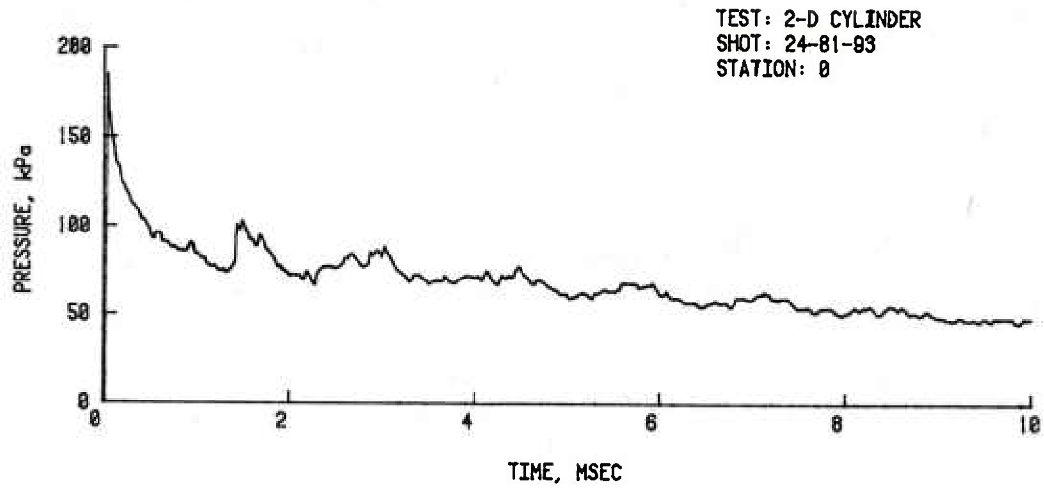

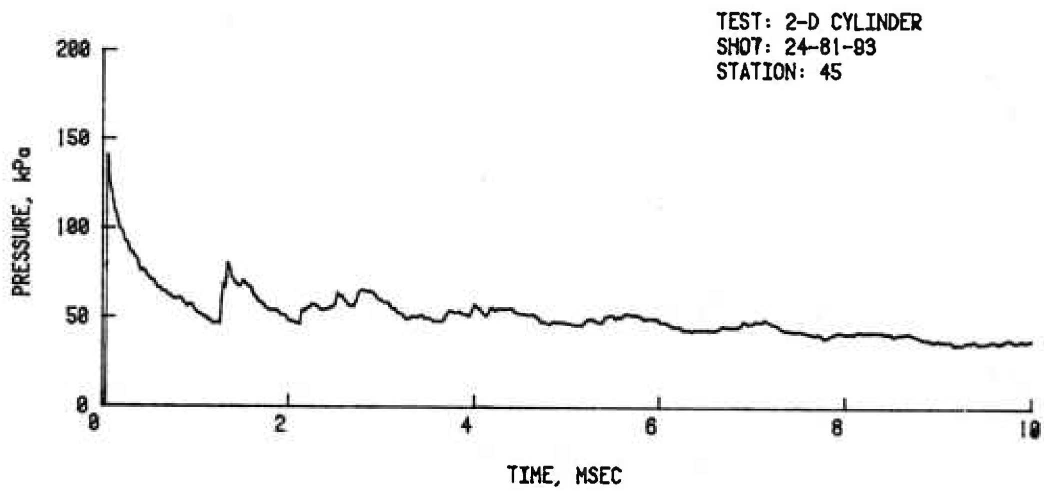

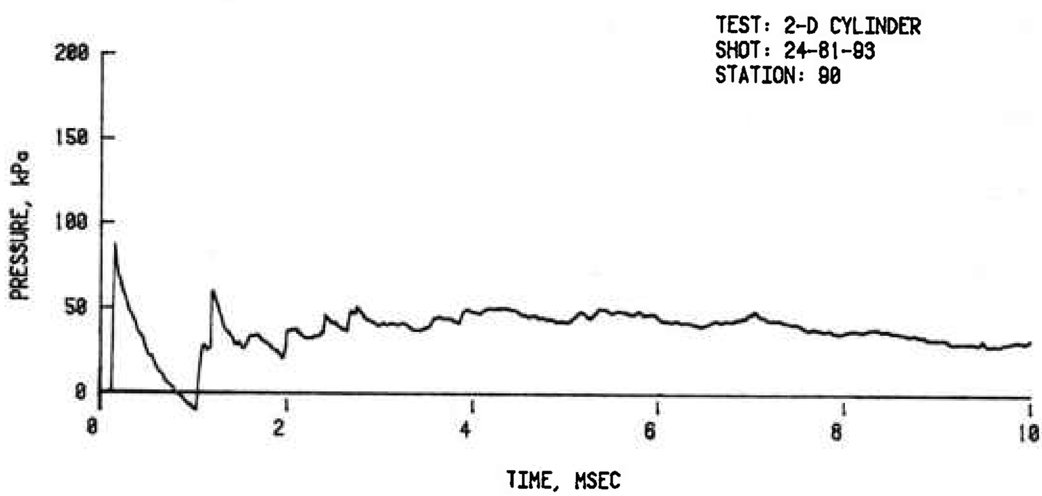

Figure B-2. Pressure-time records from cylinder for input overpressure of 75.9 kPa.

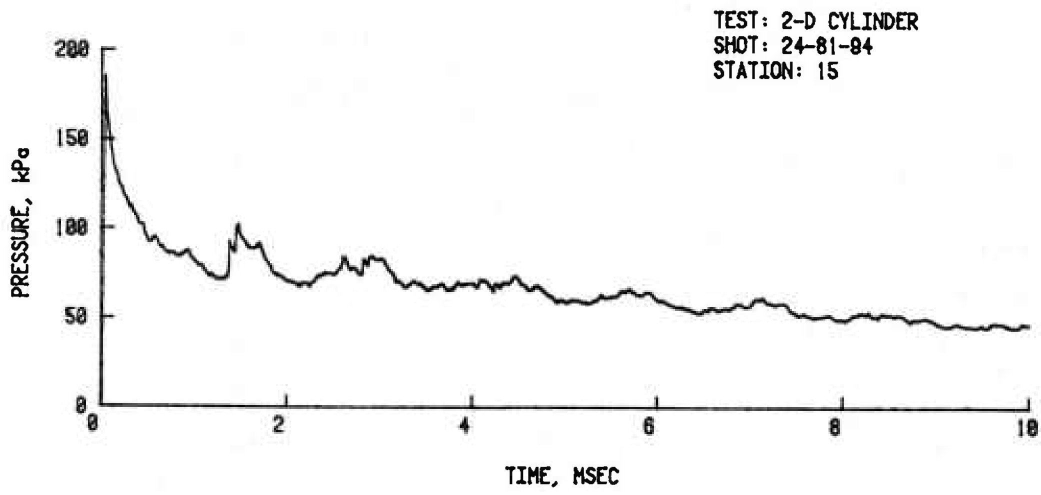

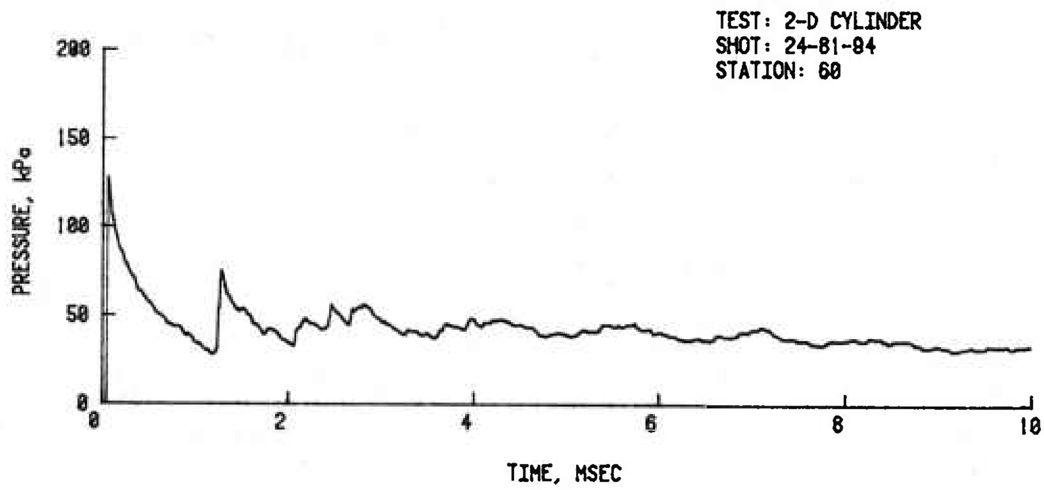

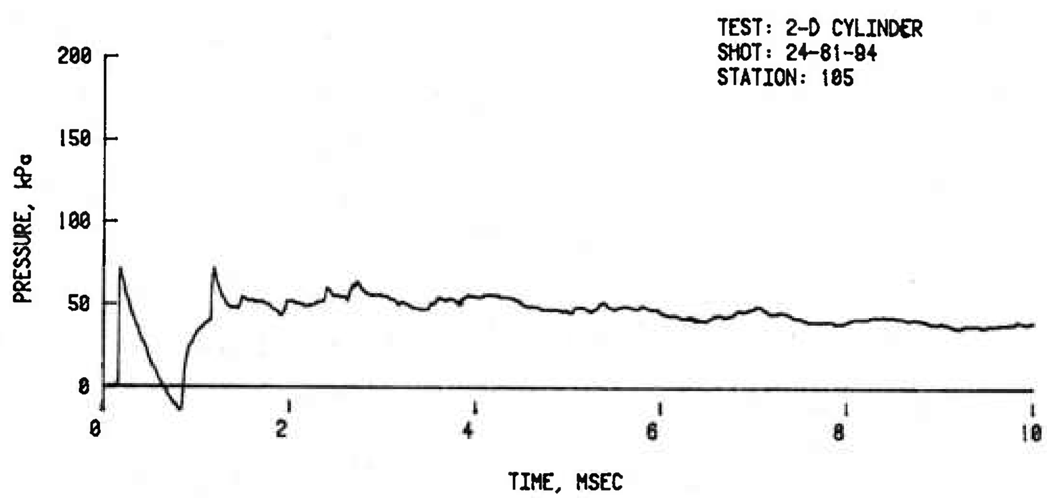

Figure B-2. Pressure-time records from cylinder for input overpressure of 75.9 kPa. (cont'd)

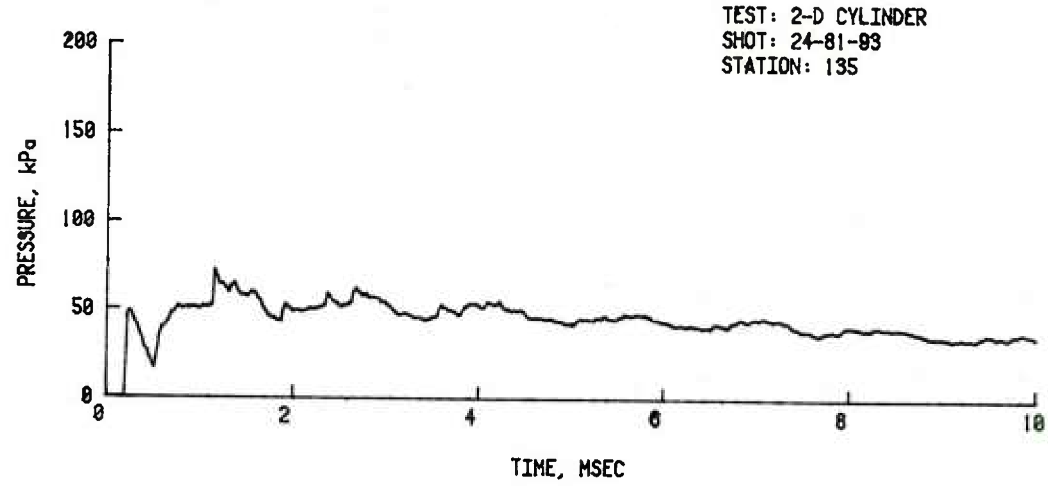

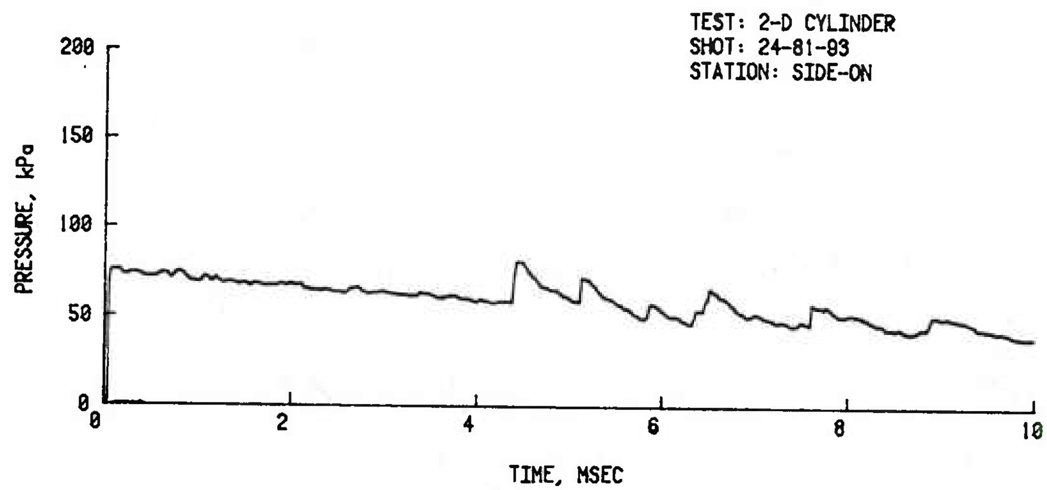

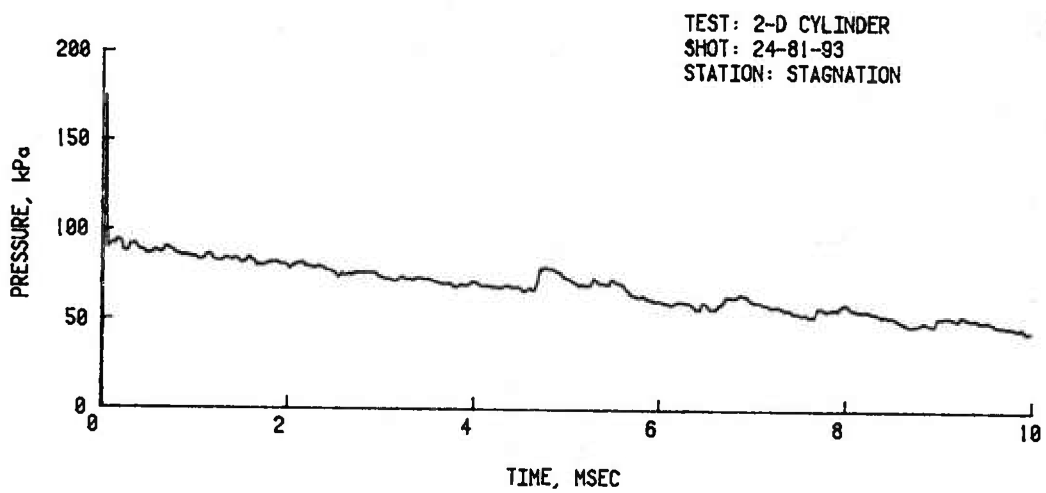

Figure B-2. Pressure-time records from cylinder for input overpressure of 75.9 kPa. (cont'd)

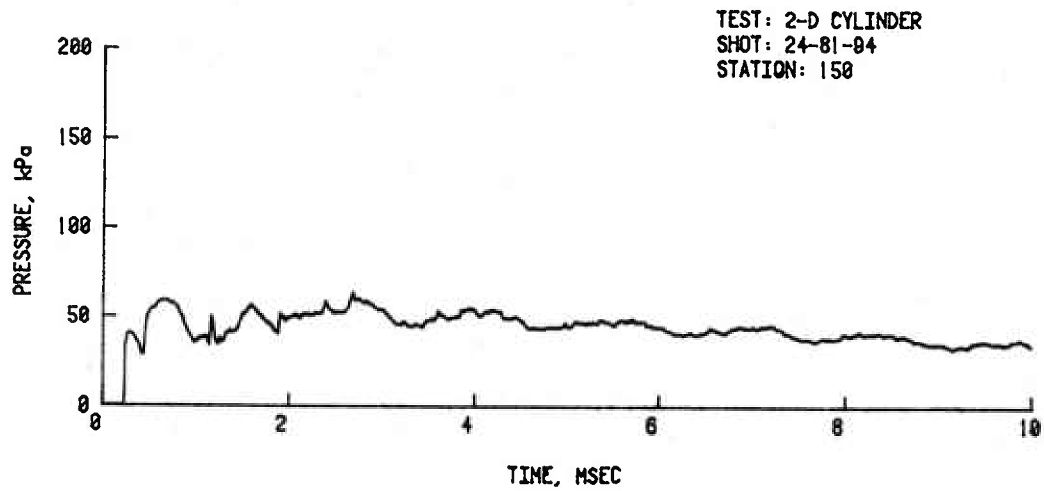

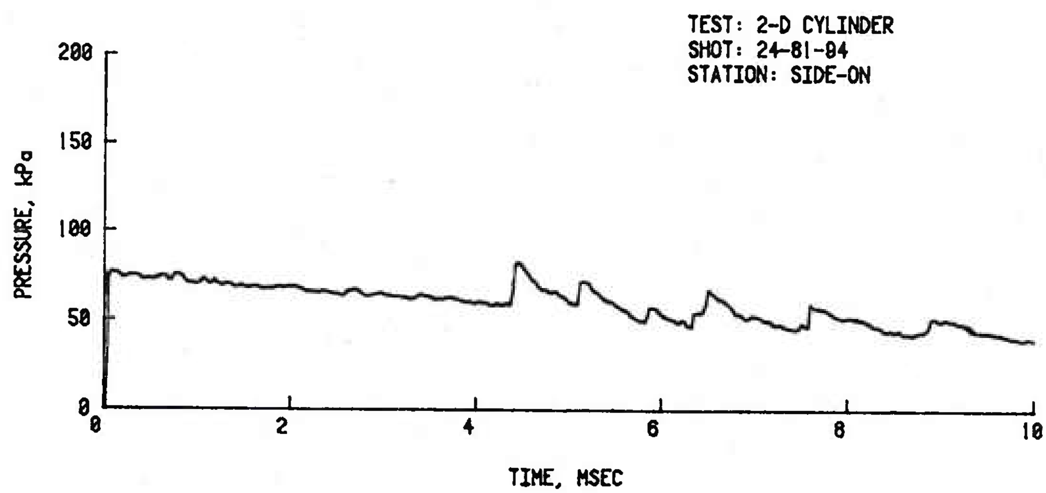

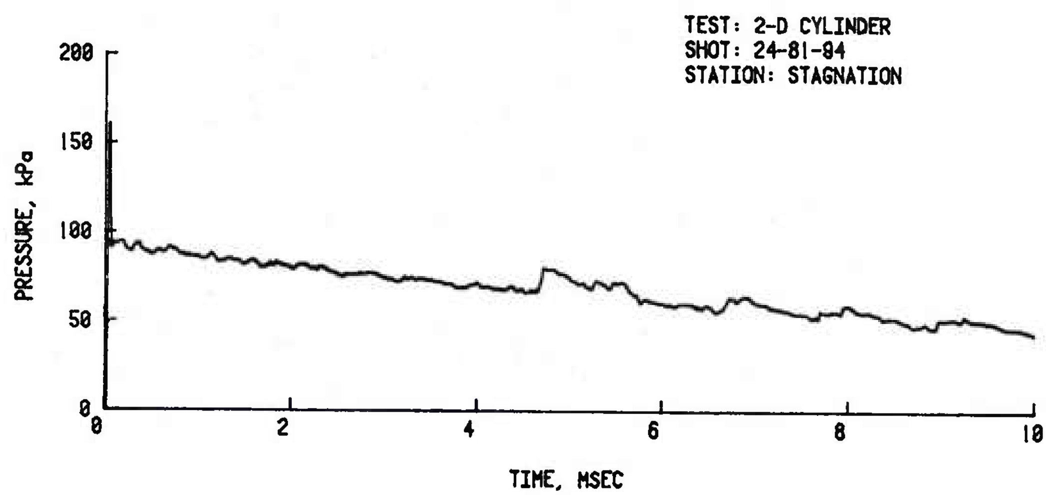

Figure B-2. Pressure-time records from cylinder for input overpressure of 75.9 kPa. (cont'd)

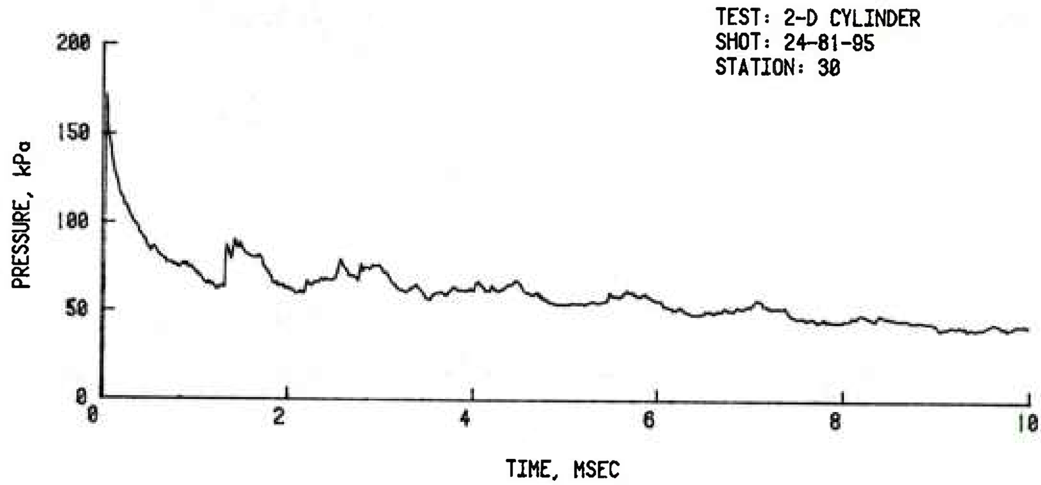

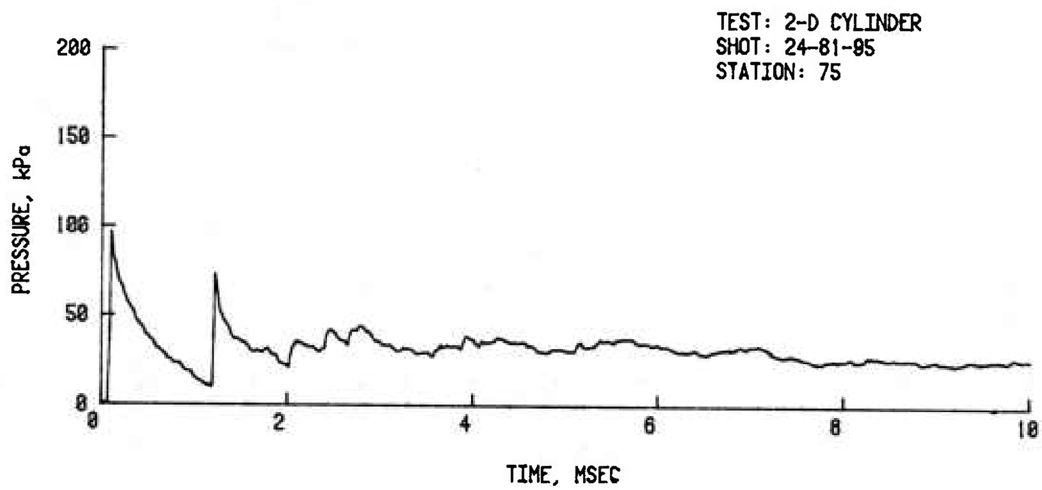

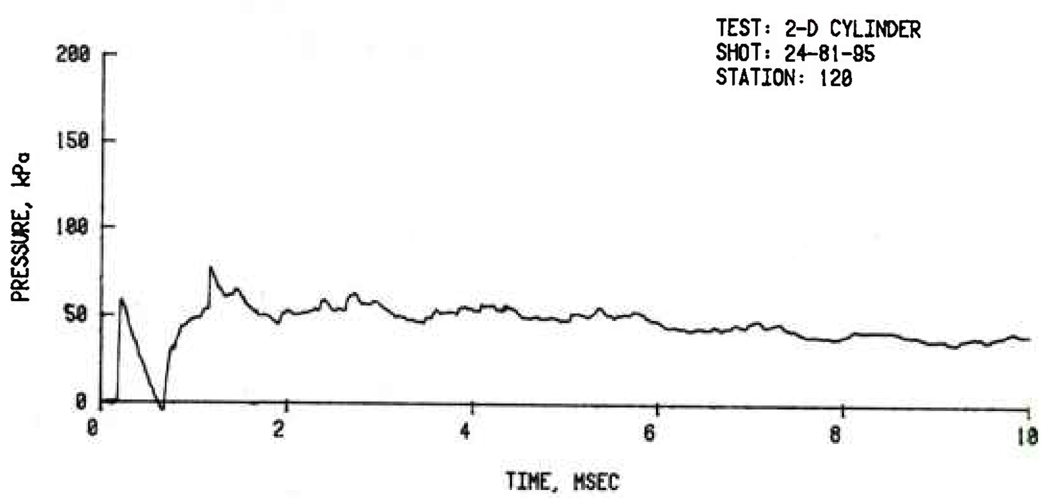

Figure B-2. Pressure-time records from cylinder for input overpressure of 75.9 kPa. (cont'd)

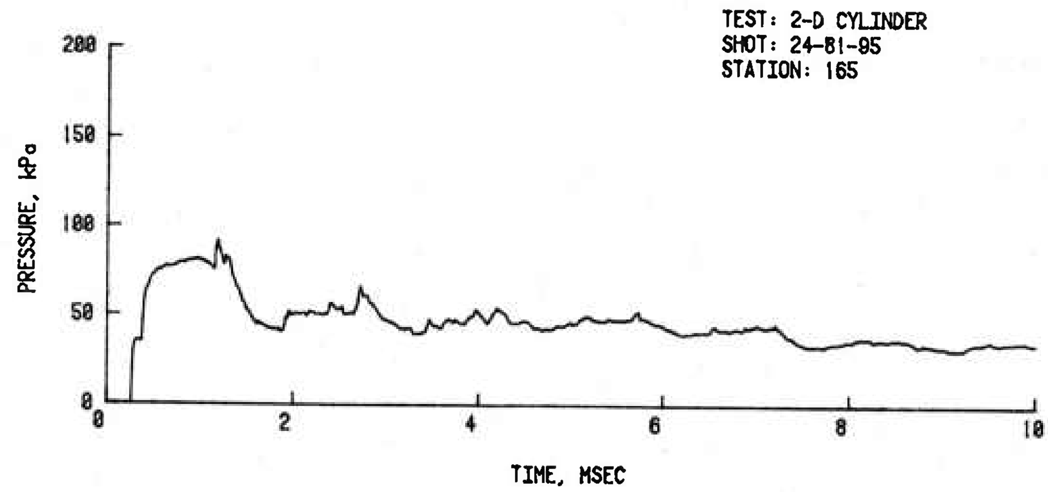

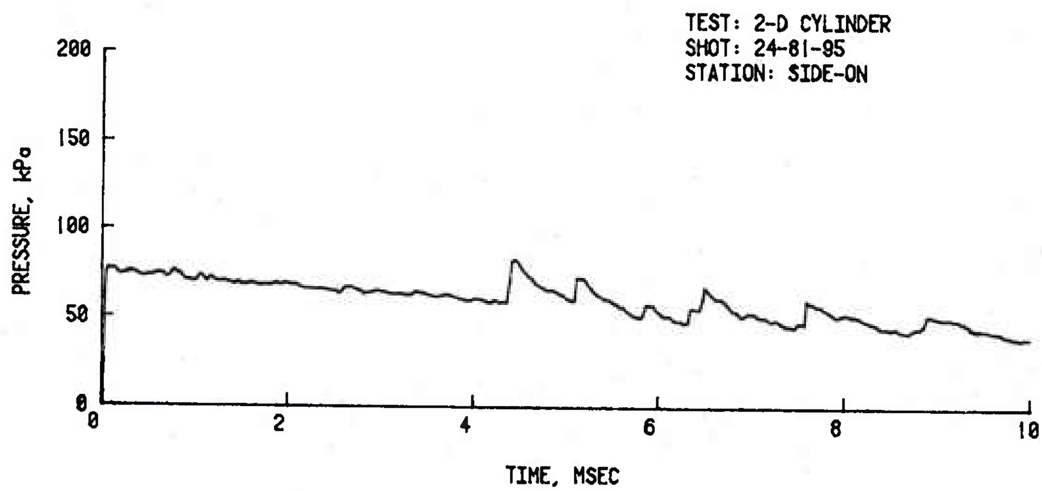

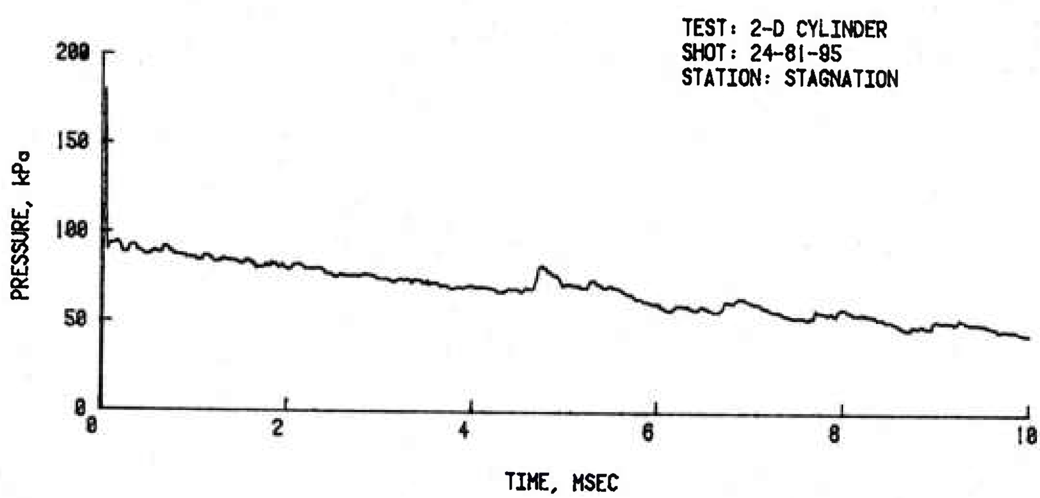

Figure B-2. Pressure-time records from cylinder for input overpressure of 75.9 kPa. (cont'd)

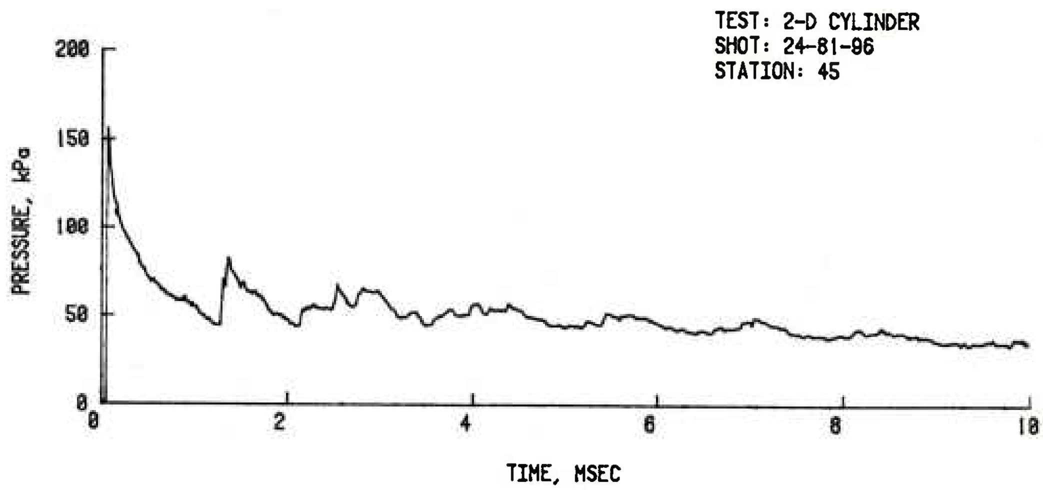

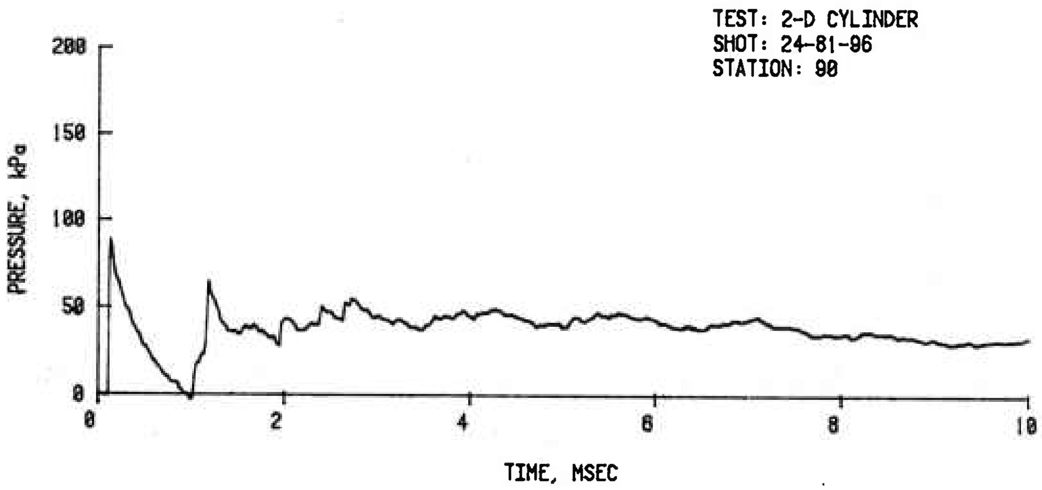

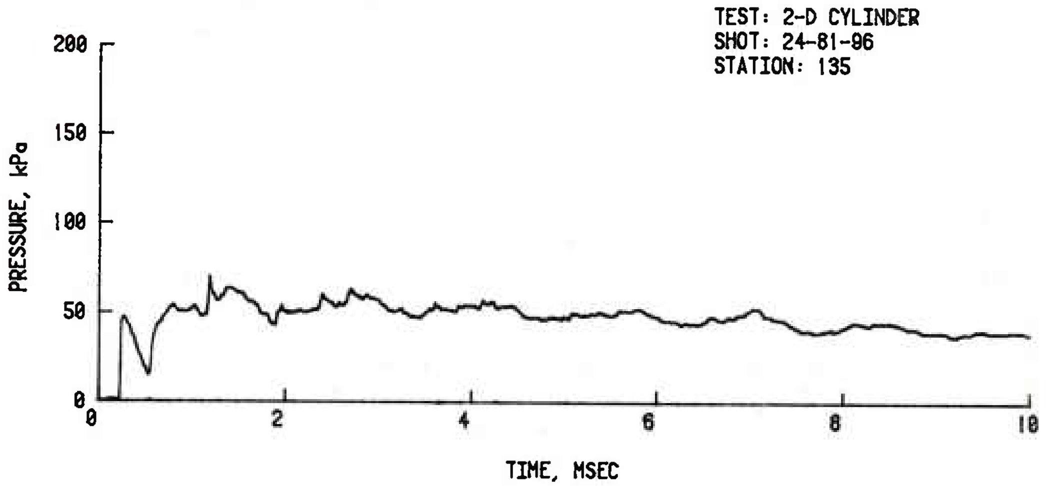

Figure B-2. Pressure-time records from cylinder for input overpressure of 75.9 kPa. (cont'd)

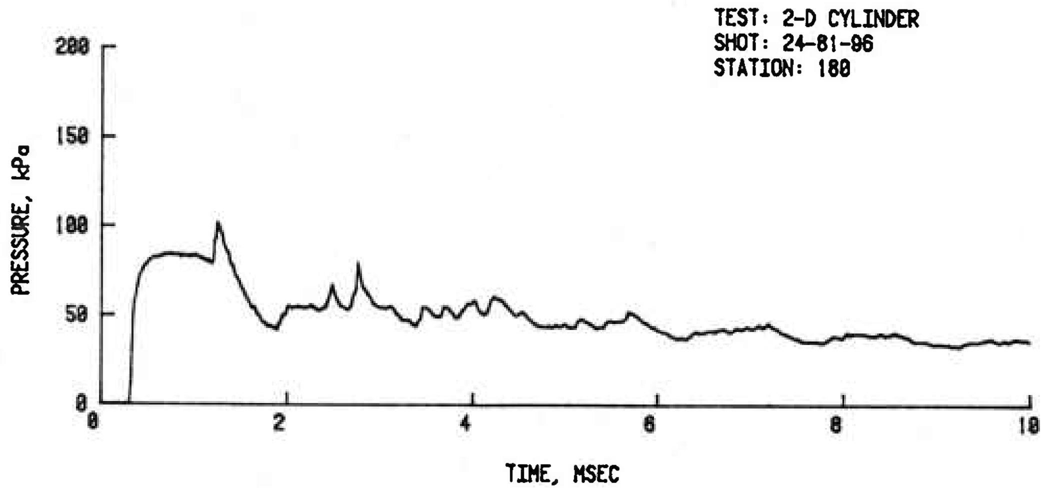

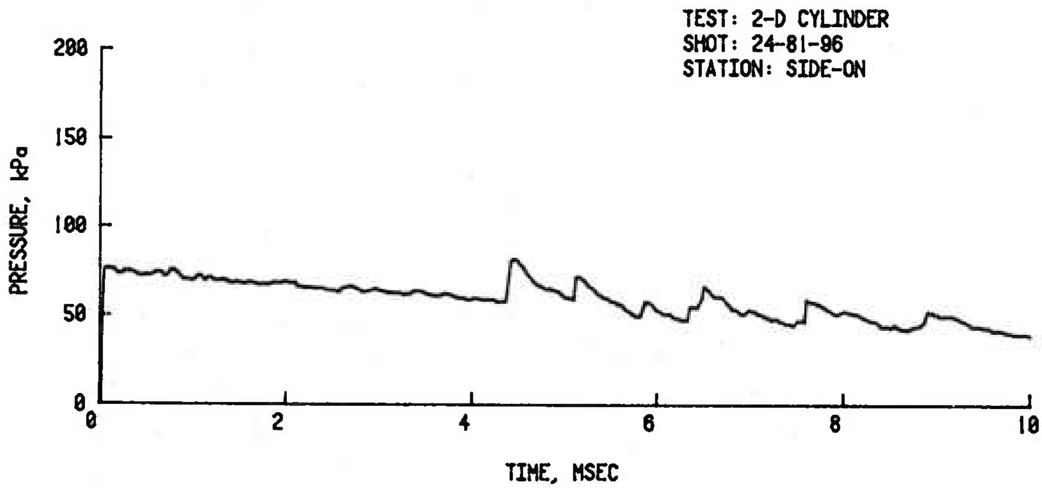

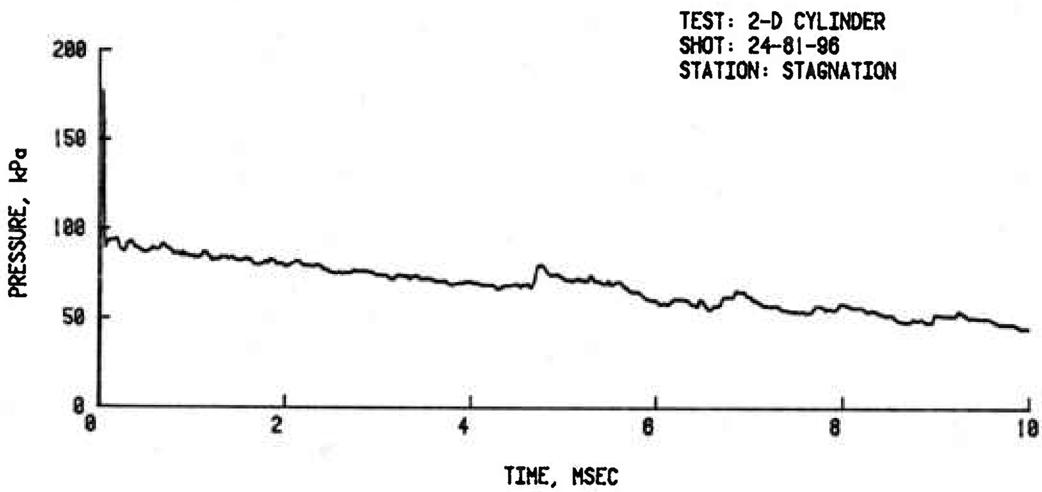

Figure B-2. Pressure-time records from cylinder for input overpressure of 75.9 kPa. (cont'd)

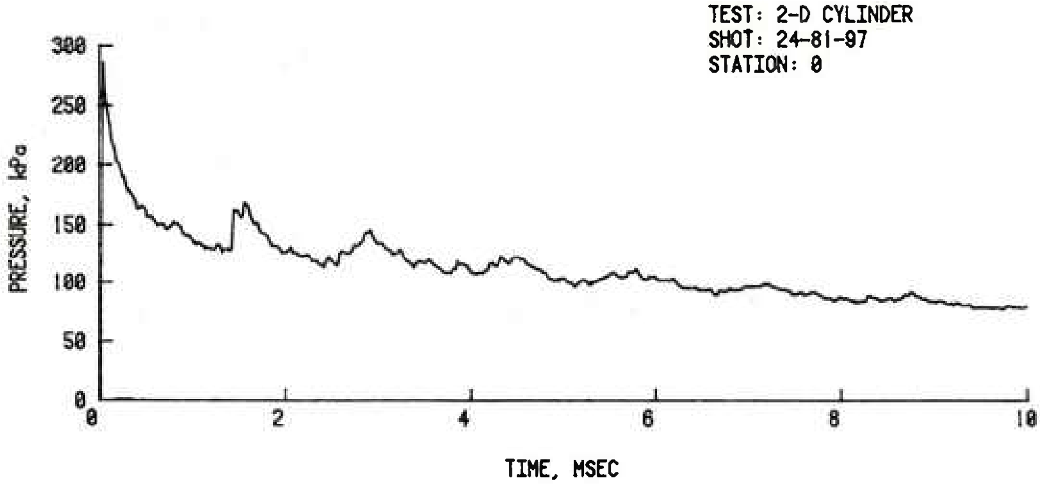

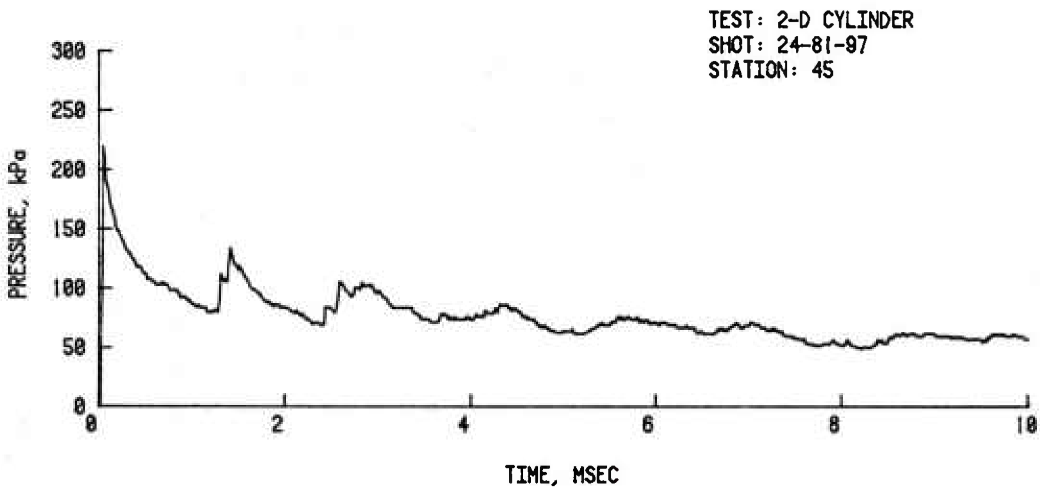

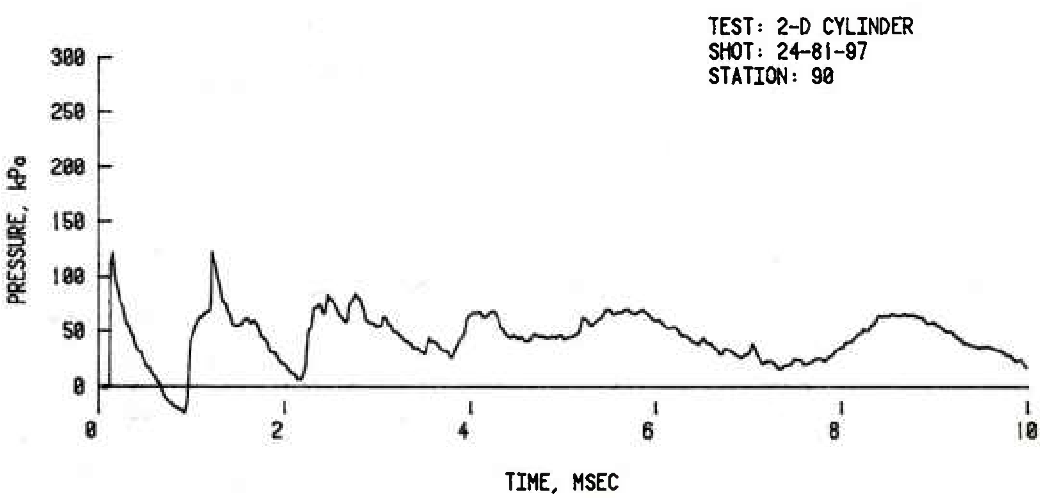

Figure B-3. Pressure-time records from cylinder for input overpressure of 112.2 kPa.

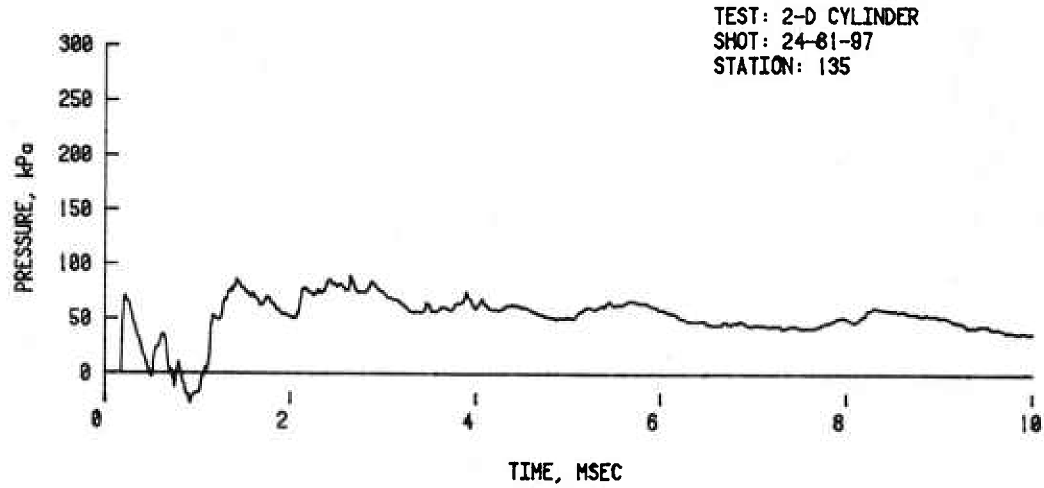

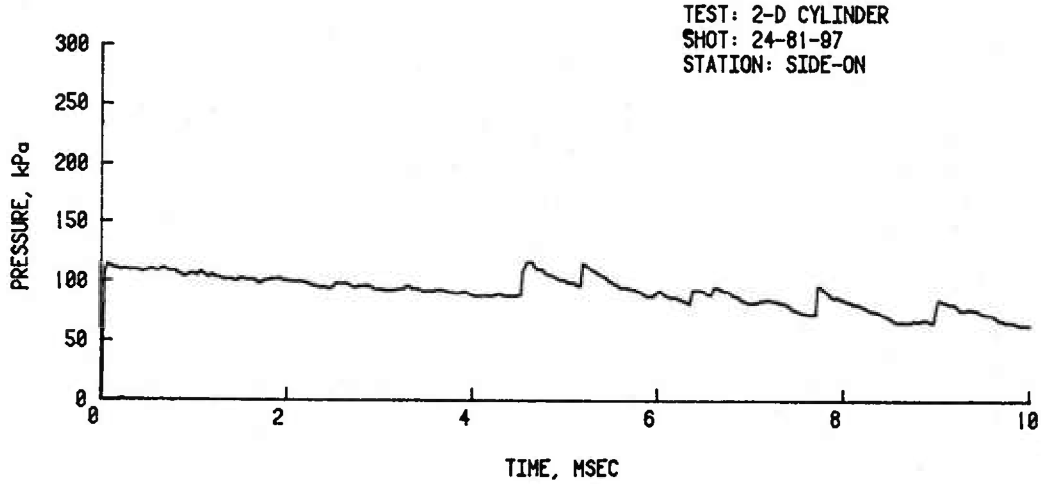

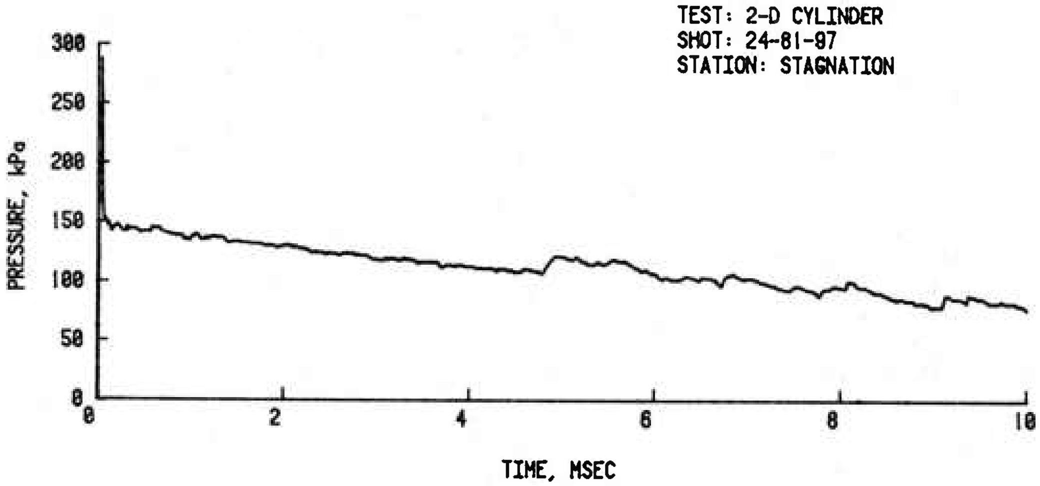

Figure B-3. Pressure-time records from cylinder for input overpressure of 112.2 kPa. (cont'd)

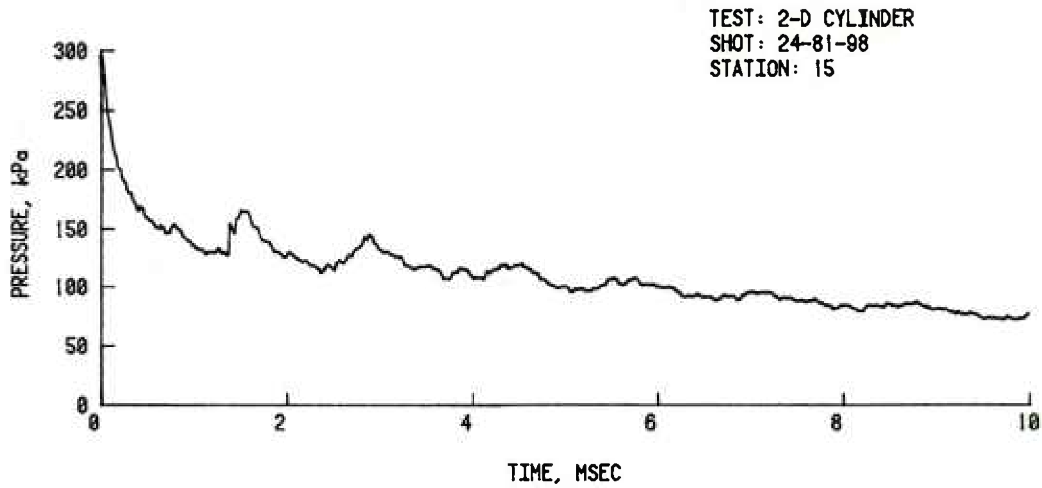

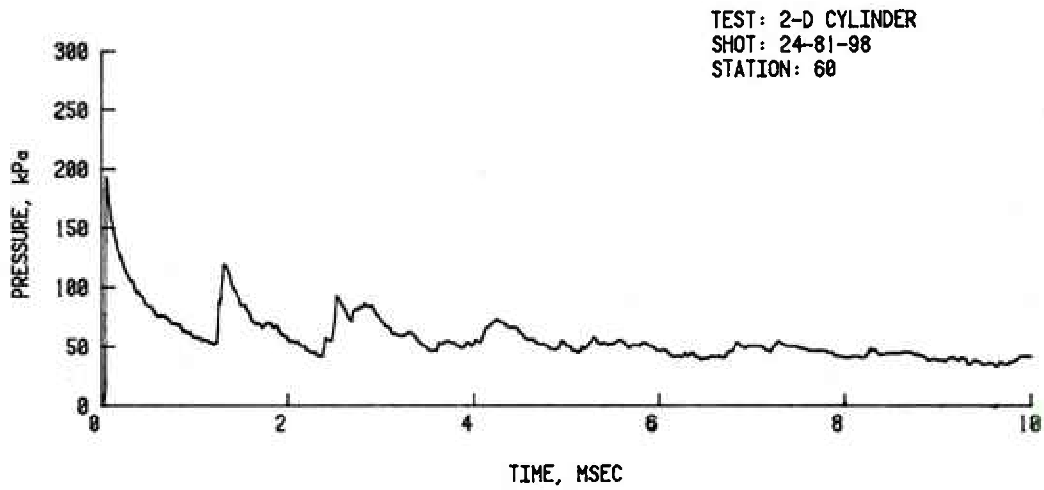

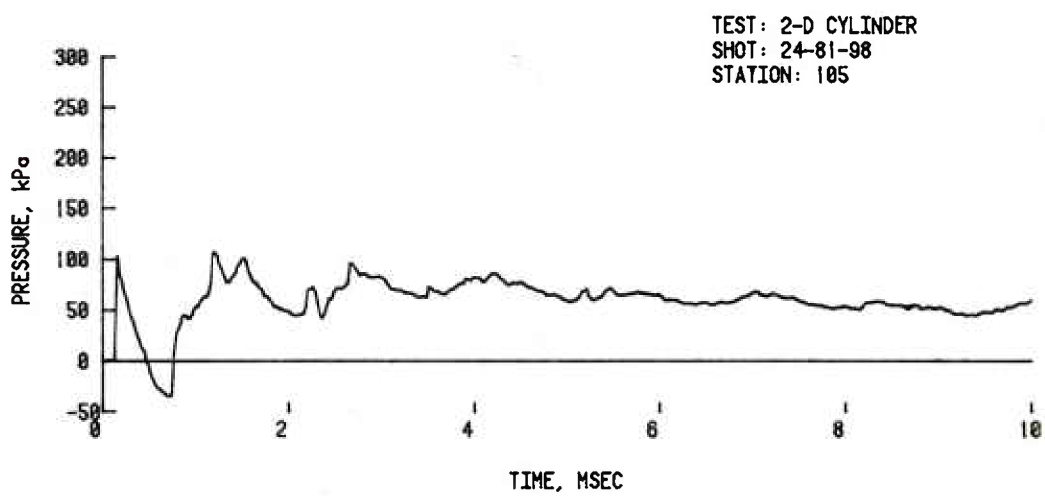

Figure B-3. Pressure-time records from cylinder for input overpressure of 112.2 kPa. (cont'd)

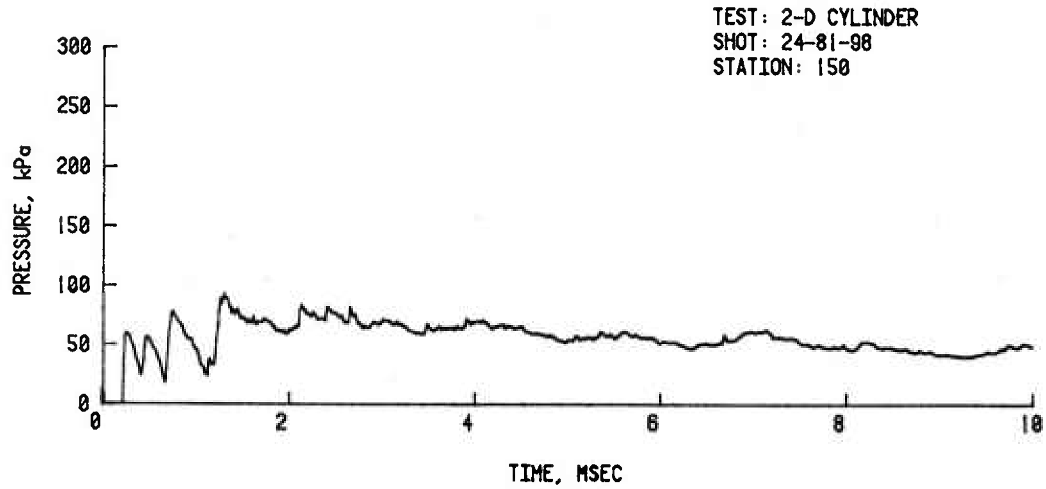

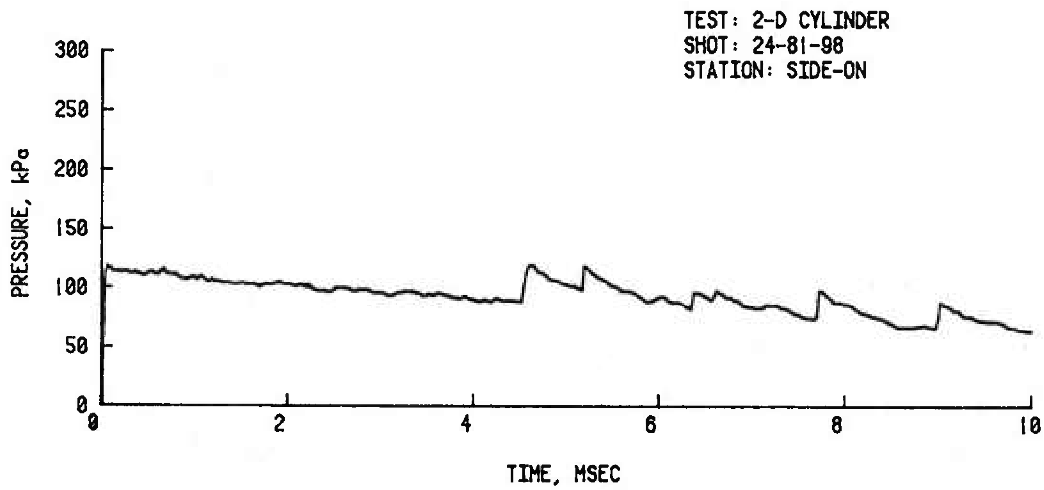

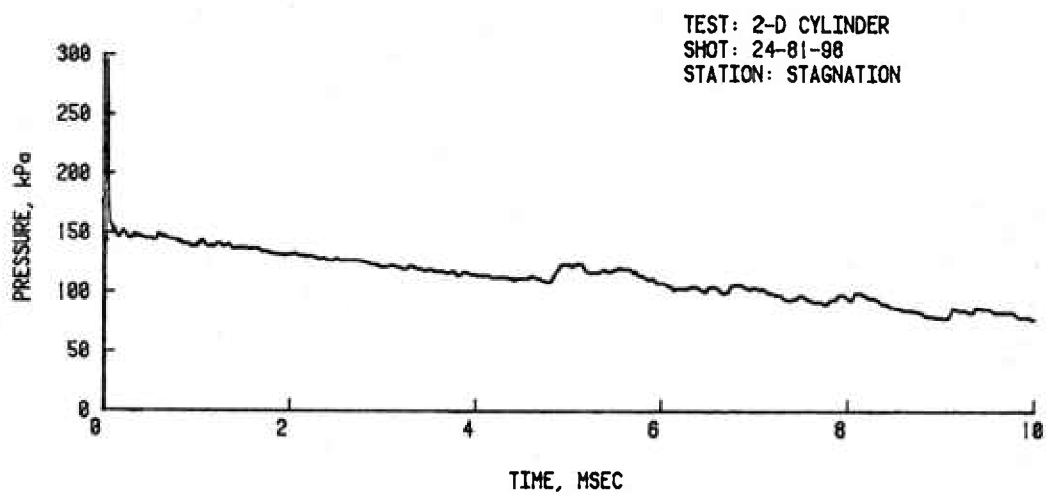

Figure B-3. Pressure-time records from cylinder for input overpressure of 112.2 kPa. (cont'd)

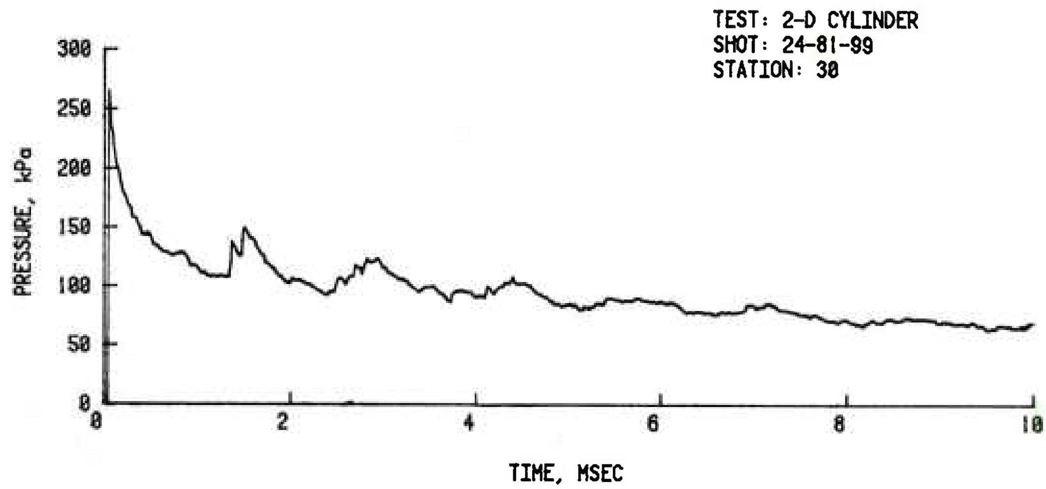

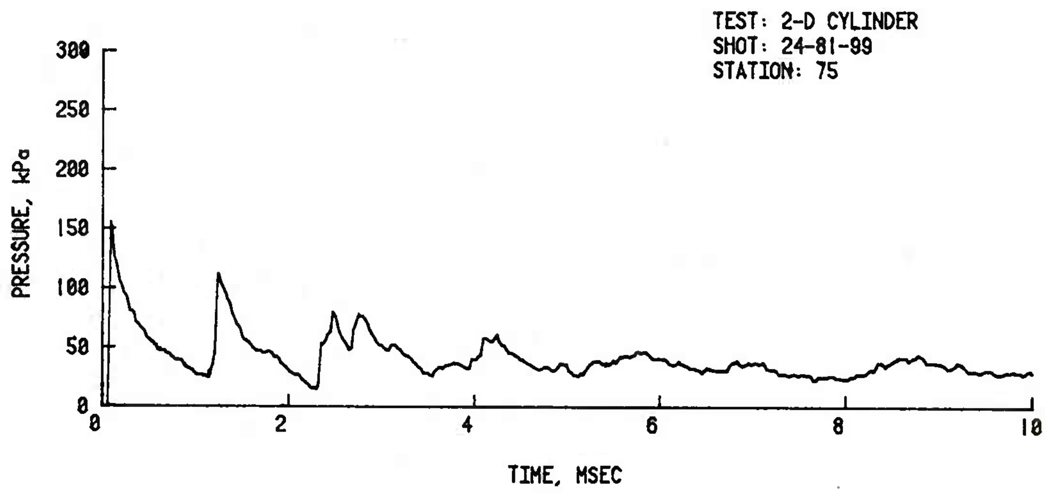

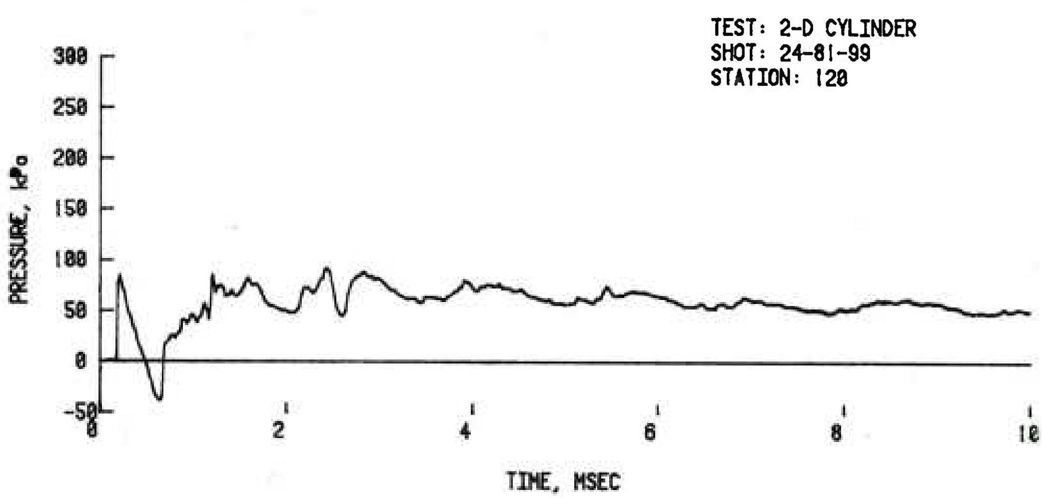

Figure B-3. Pressure-time records from cylinder for input overpressure of 112.2 kPa. (cont'd)

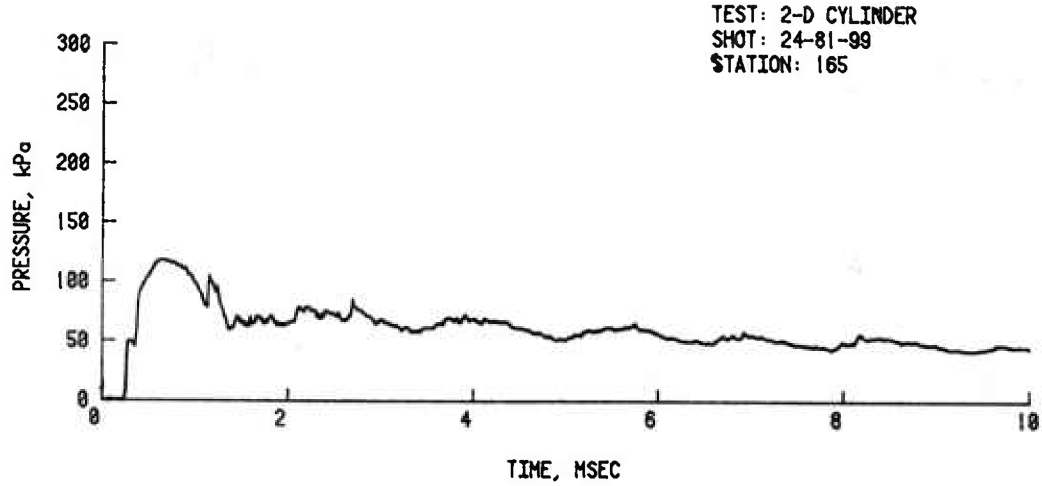

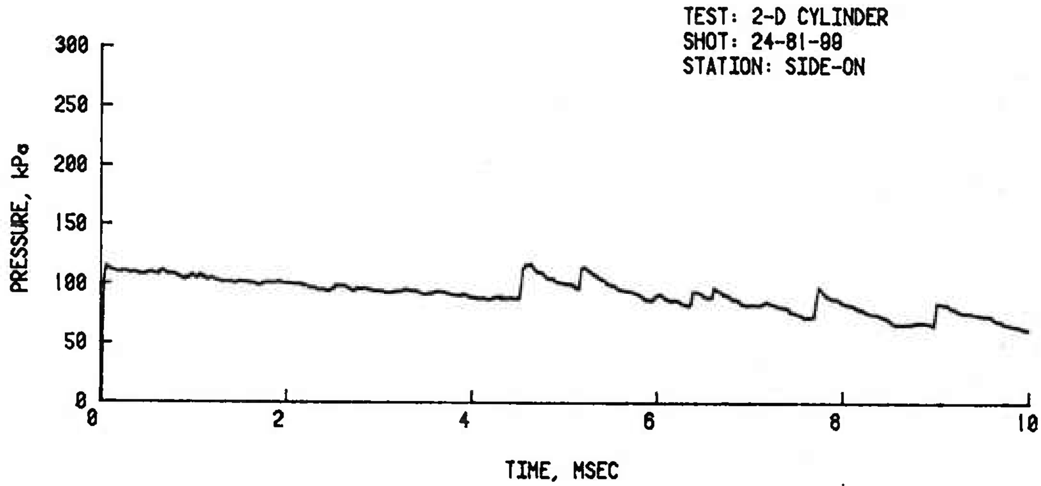

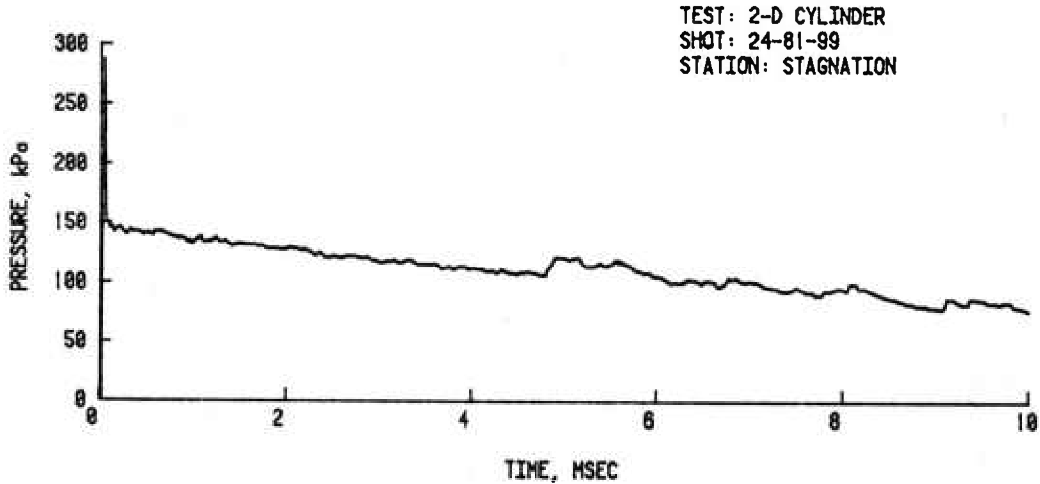

Figure B-3. Pressure-time records from cylinder for input overpressure of 112.2 kPa. (cont'd)

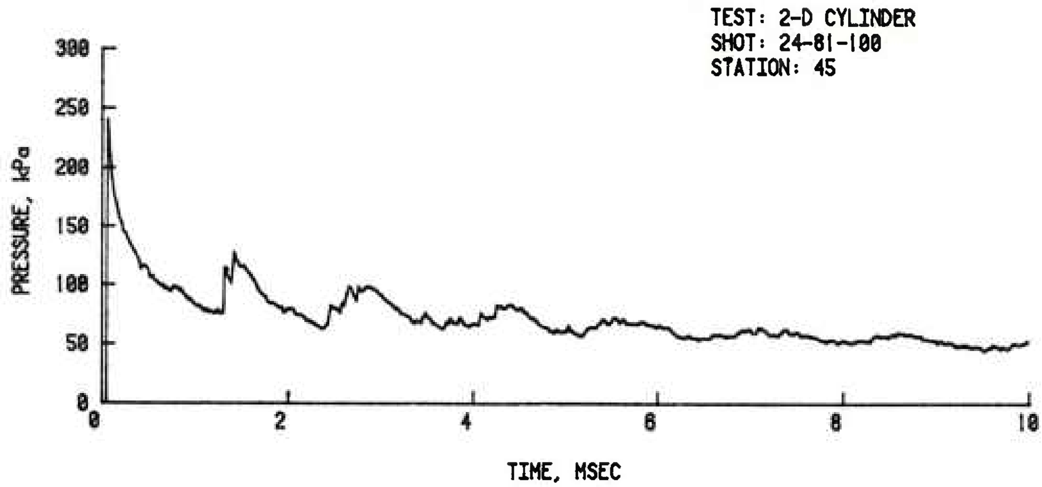

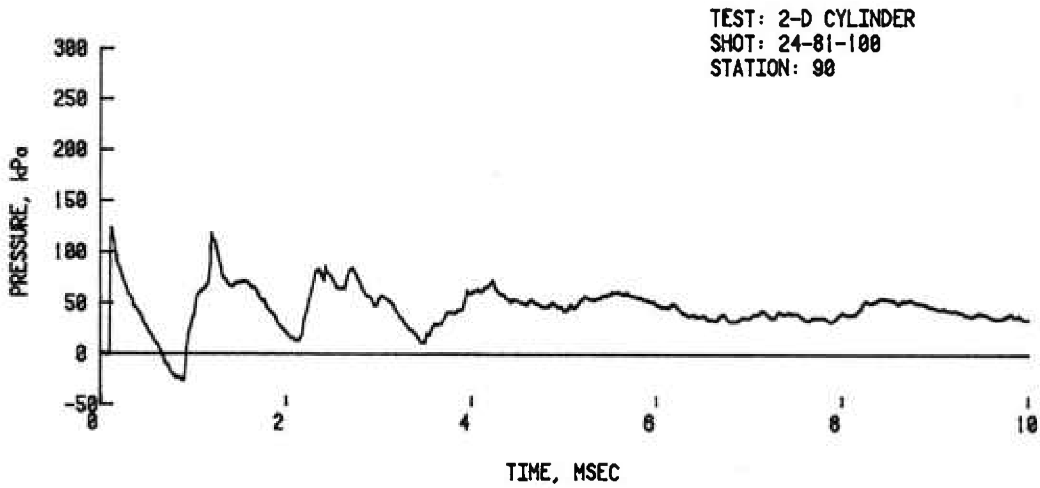

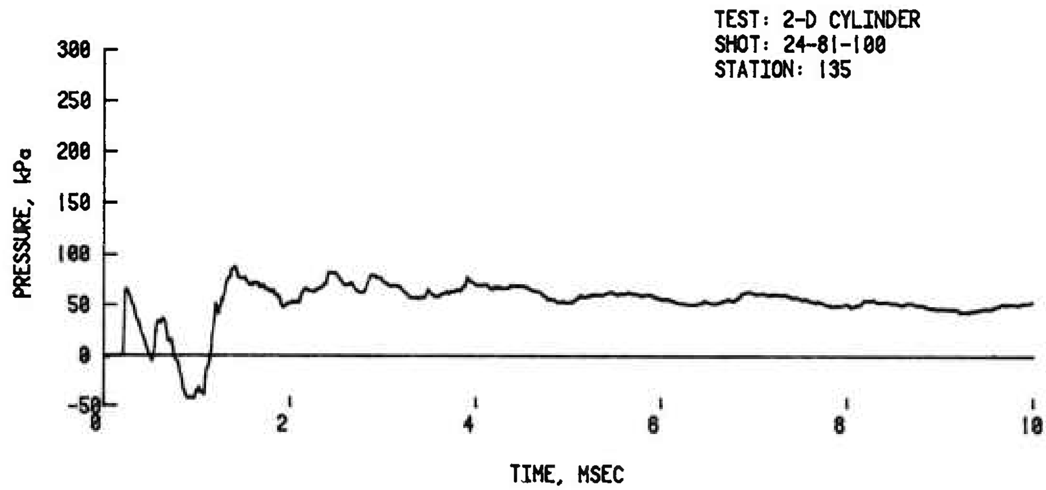

Figure B-3. Pressure-time records from cylinder for input overpressure of 112.2 kPa. (cont'd)

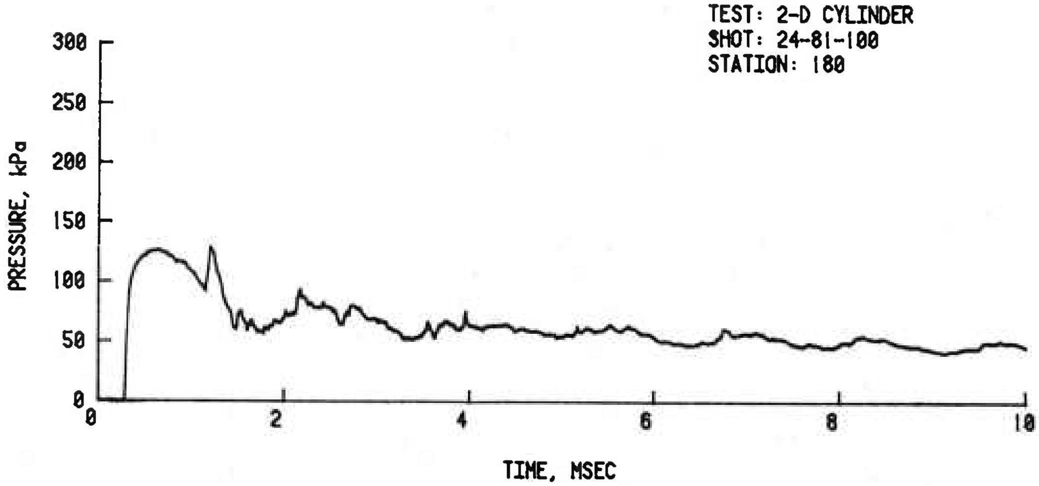

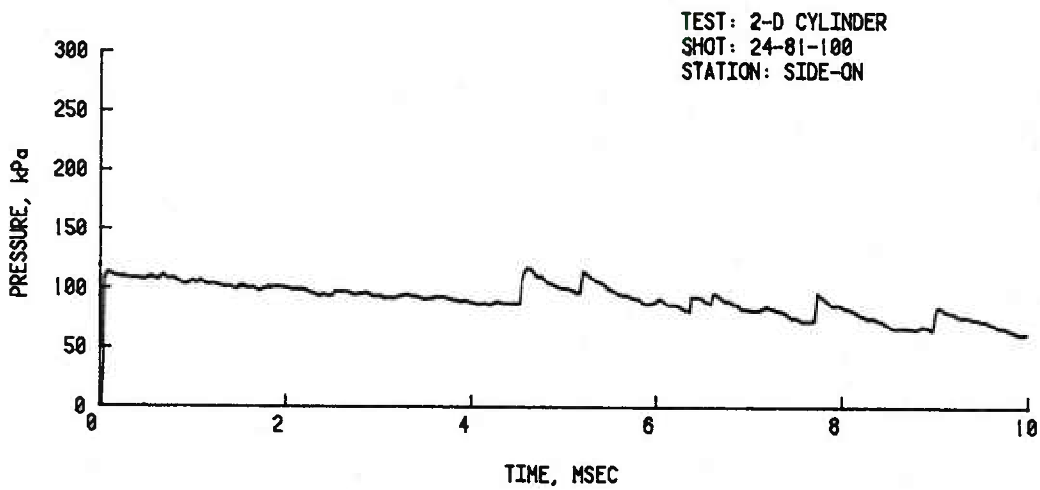

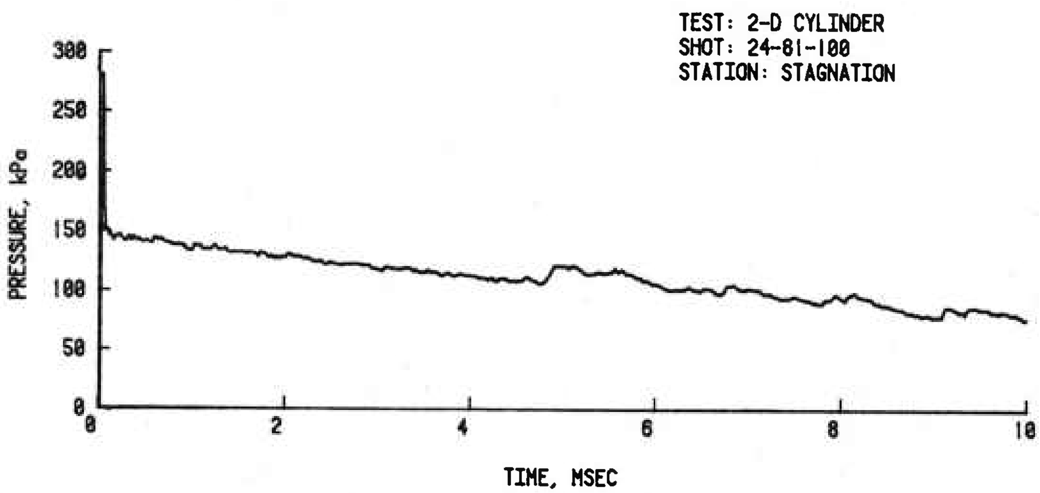

Figure B-3. Pressure-time records from cylinder for input overpressure of 112.2 kPa. (cont'd)

DISTRIBUTION LIST

No. of Copies	Organization
12	Administrator Defense Technical Info Center ATTN: DTIC-DDA Cameron Station Alexandria, VA 22314
4	Director of Defense Research and Engineering ATTN: DD/TWP DD/S&SS DD/I&SS AD/SW Washington, DC 20301
3	Director Defense Advanced Research Project Agency ATTN: Technical Library NMRO PMO 1400 Wilson Boulevard Arlington, VA 22209
1	Director Defense Intelligence Agency ATTN: Mr. C. Wiehle Washington, DC 20301
8	Director Defense Nuclear Agency ATTN: STTL (Tech Lib, 2cys) SPSS, Dr. K. Goering Dr. G. Ullrich DDST, COL Frankhouser (3 cys) SPAS, Mr. D. Kohler Washington, DC 20305
2	Commander Field Command, DNA ATTN: FCTMOF Kirtland AFB, NM 87115

No. of Copies	Organization
1	Chairman DOD Explosives Safety Board ATTN: T. Zaker Rm 856-C, Hoffman Bldg. I 2461 Eisenhower Avenue Alexandria, VA 22331
1	HQDA (DAMA-AR, NCB Division) Washington, DC 20310
1	Commander US Army Ballistic Missile Defense Program Office ATTN: DACS-SAE-S, J. Shea 5001 Eisenhower Avenue Alexandria, VA 22333
1	Commander US Army Ballistic Missile Defense Systems Command ATTN: SSC-DH P.O. Box 1500 Huntsville, AL 35804
3	Director US Army BMD Advanced Technology Ctr. ATTN: Mr. B. E. Kelley Mr. M. Capps Mr. Marcus Whiteford P.O. Box 1500 Huntsville, AL 35804
2	Commander US Army Engineer Waterways Experiment Station ATTN: Library W. Flateau P.O. Box 631 Vicksburg, MS 29181
1	Commander Fleet Marine Force, Atlantic ATTN: G-4 (NSAP) Norfolk, VA 23511

DISTRIBUTION LIST

No. of Copies	Organization
1	Commander US Army Materiel Development and Readiness Command ATTN: DRCDMD-ST 5001 Eisenhower Avenue Alexandria, VA 22333
1	Commander US Army Armament Research and Development Command ATTN: DRDAR-TDC Dover, NJ 07801
2	Commander US Army Armament Research and Development Command ATTN: DRDAR-TSS (2cys) Dover, NJ 07801
1	Commander US Army Armament Materiel Readiness Command ATTN: DRSAR-LEP-L, Tech Lib Rock Island, IL 61299
1	Director US Army ARRADCOM Benet Weapons Laboratory ATTN: DRDAR-LCB-TL Watervliet, NY 12189
1	Commander US Army Aviation Research ATTN: DRDAV-E 4300 Goodfellow Boulevard St. Louis, MO 63120
1	Director US Army Air Mobility Research and Development Laboratory Ames Research Center Moffett Field, CA 94035
1	Commander US Army Communications Rsch and Development Command ATTN: DRDCO-PPA-SA Fort Monmouth, NJ 07703
1	Commander US Army Electronics Research and Development Command Technical Support Activity ATTN: DELSD-L Fort Monmouth, NJ 07703
4	Commander US Army Harry Diamond Lab ATTN: DRXDO-TI/012 DRXDO-NP, F. Wimenitz J. Gaul J. Gwaltney 2800 Powder Mill Road Adelphi, MD 20783
1	Commander US Army Missile Command ATTN: DRSMI-R Redstone Arsenal, AL 35898
1	Commander US Army Missile Command ATTN: DRSMI-YDL Redstone Arsenal, AL 35898
1	Commander US Army Tank Automotive Research and Development Command ATTN: DRDTA-UL Warren, MI 48090
1	Commander US Army Foreign Science & Technology Center ATTN: Research & Data Branch 220 7th Street, NE Charlottesville, VA 22901
1	Director US Army Materials and Mechanics Research Center ATTN: Technical Library Watertown, MA 02172

DISTRIBUTION LIST

No. of Copies	Organization
3	Commander US Army Nuclear & Chemical Agency ATTN: ATCN-W CDINS-E Technical Library 7500 Backlick Rd, Bldg. 2073 Springfield, VA 22150
1	Director US Army TRADOC Systems Analysis Activity ATTN: ATAA-SL, Tech Lib White Sands Missile Range, NM 88002
2	Chief of Naval Research Department of the Navy ATTN: T. Quinn, Code 461 J.L. Warner, Code 461 Washington, DC 20360
4	Commander Naval Surface Weapons Center ATTN: Code 1224, Navy Nuclear Programs Office Code 241 Code 730, Tech Library J. Pittman Silver Spring, MD 20910
1	Commander Naval Weapons Evaluation Fac ATTN: Document Control Kirtland AFB, NM 87117
1	Officer in Charge (Code L31) Civil Engineering Lab Naval Construction Battalion Center ATTN: Dr. W.A. Shaw, Code L31 Port Hueneme, CA 93041
3	Commander Naval Research Laboratory ATTN: M. Persechino G. Cooperstein Tech Lib, Code 2027 Washington, DC 20375

No. of Copies	Organization
1	HQ AFSC (DLCAW, Tech Lib) Andrews AFB Washington, DC 20331
1	AFOSR (OAR) Bolling AFB, DC 20332
1	RADC (Document Lib, FMTLD) Griffiss AFB, NY 13440
5	AFWL (CA, Dr. A. Guenther; DYT, 4 cys) Kirtland AFB, NM 87117
1	SAMSO (Library) P.O. Box 92960 Los Angeles, CA 90009
2	AFTAC (K. Rosenlof; G. Leies) Patrick AFB, FL 32925
2	AFML (G. Schmitt, MAS; MBC, D. Schmidt) Wright-Patterson AFB, OH 45433
2	Headquarters Dept. of Energy Dept of Military Applications ATTN: R & D Branch Library Branch, G-043 Washington, DC 20545
2	Director Los Alamos Scientific Lab ATTN: Dr. J. Taylor Technical Library P.O. Box 1663 Los Alamos, NM 87544
1	Director National Aeronautics and Space Administration ATTN: Code 04.000 Langley Research Center Langley Station Hampton, VA 23365

DISTRIBUTION LIST

No. of Copies	Organization
1	Director NASA Scientific & Technical Information Facility ATTN: SAK/DL P.O. Box 8757 Baltimore/Washington International Airport, MD 21240
1	National Academy of Sciences Advisor Committee on Civil Defense ATTN: Dr. Donald Groves 2101 Constitution Avenue, NW Washington, DC 20418
1	Aerospace Corporation ATTN: Tech Information Svcs Building 105, Room 2220 P.O. Box 92957 Los Angeles, CA 90009
1	Agbabian Associates ATTN: Dr. J. Malthan 250 N. Nash Street El Segundo, CA 90245
1	AVCO Systems Div ATTN: Dr. W. Bade 201 Lowell Street Wilmington, MA 01887
1	AVCO-Everett Research Lab ATTN: Technical Library 2385 Revere Beach Parkway Everett, MA 02149
1	John A. Blume & Associates ATTN: Dr. John A. Blume Sheraton-Palace Hotel 100 Jessie Street San Francisco, CA 94105
1	Center for Planning and Research Inc. ATTN: John R. Rempel 2483 East Bayshore Road Palo Alto, CA 94303

No. of Copies	Organization
1	Effects Technology, Inc. ATTN: E. Anderson 5383 Holister Avenue Santa Barbara, CA 93105
1	General Electric Co. - TEMPO ATTN: DASIAC 816 State Street, Drawer QQ Santa Barbara, CA 93102
1	General Electric Co. - TEMPO 7800 Marble Avenue, NE Suite 5 Albuquerque, NM 87110
1	H-Tech Laboratories, Inc. ATTN: B. Hartenbaum P.O. Box 1686 Santa Monica, CA 90406
1	Hughes Aircraft Company Systems Development Lab ATTN: Dr. A. Puckett Centinela & Teale Streets Culver City, CA 90230
1	Ion Physics Corporation ATTN: Technical Library South Bedford Street Burlington, MA 01803
1	Kaman Sciences Corporation ATTN: Dr. D. Sachs 1500 Garden of the Gods Road Colorado Springs, CO 80907
1	Kaman Avidyne, Division of Kaman Sciences ATTN: Dr. J. Ray Ruetenik 83 2nd Ave, NW Industrial Park Burlington, MA 01830
1	KTECH Corporation ATTN: Dr. Donald V. Keller 911 Pennsylvania NE Albuquerque, NM 87110

DISTRIBUTION LIST

No. of Copies	Organization
1	Lockheed Missiles & Space Co, Inc. Div of Lockheed Aircraft Corp ATTN: J. Nickell P.O. Box 504 Sunnyvale, CA 94086
1	Management Science Associates ATTN: Kenneth Kaplan P.O. Box 239 Los Altos, CA 94022
1	Martin Marietta Aerospace Orlando Divsion ATTN: A. Ossin P.O. Box 5837 Orlando, FL 32805
1	Maxwell Laboratories, Inc. ATTN: A. Kolb 9244 Balboa Avenue San Diego, CA 92123
1	McDonnell Douglas Astronautics Company 5301 Bolsa Avenue Huntington Beach, CA 92647
1	H.L. Murphy Associates Box 1727 San Mateo, CA 94401
1	Philco Ford Corporation Aeronutronic Division ATTN: L.K. Goodwin Fort Road Newport Beach, CA 92663
1	Physics International Company ATTN: Document Control 2700 Merced Street San Leandro, CA 94577
3	R&D Associates ATTN: Technical Library Jerry Carpenter Allen Kuhl P.O. Box 9695 Marina del Rey, CA 90291
1	Sandia Laboratories ATTN: Dr. J. Kennedy Albuquerque, NM 87115
2	Science Application, Inc. ATTN: Joseph McGahan Dr. John Cockayne 8400 West Park Drive McLean, VA 22102
1	Shock Hydrodynamics, Inc. ATTN: L. Zernow 4710-16 Vineland Avenue N. Hollywood, CA 91602
1	Systems, Science & Software ATTN: Technical Library P.O. Box 1620 La Jolla, CA 92037
1	Teledyne-Brown Engineering Cummings Research Park Huntsville, AL 35807
1	Union Carbide Corporation Oak Ridge National Lab ATTN: Technical Library P.O. Box X Oak Ridge, TN 37830
1	Battelle Memorial Institute ATTN: Technical Library 505 King Avenue Columbus, OH 43201
	Director Applied Physics Laboratory The Johns Hopkins University Johns Hopkins Road Laurel, MD 20707

DISTRIBUTION LIST

No. of Copies	Organization
1	Lovelace Research Institute ATTN: Dr. D. Richmond P.O. Box 5890 Albuquerque, NM 87108
1	Massachusetts Institute of Technology Aerophysics Laboratory 77 Massachusetts Avenue Cambridge, MA 02139
1	New Mexico Institute of Mining and Technology ATTN: Mr. P. McClain Socorro, NM 87801
1	Northwestern Michigan College Traverse City, MI 49584
1	Southwest Research Institute ATTN: Dr. W. Baker 8500 Culebra Road San Antonio, TX 78228
1	Research Institute of Temple University ATTN: Technical Library Philadelphia, PA 19144
1	Texas Tech University Dept of Civil Engineering ATTN: Mr. Joseph E. Minor Lubbock, TX 79409
1	University of Arkansas Department of Physics ATTN: Prof O. Zinke Fayetteville, AR 72701
1	University of California Lawrence Livermore Lab Technical Library Division ATTN: Technical Library Dr. Donald N. Montan P.O. Box 808 Livermore, CA 94550
2	University of Denver Denver Research Institute ATTN: Mr. John Wisotski 2390 S. University Blvd Denver, CO 80210
1	J. D. Haltiwanger Consulting Engineering Services B106a Civil Engineering Bldg. 208 N. Romine Street Urbana, IL 61801
1	The University of Maryland Department of Physics College Park, MD 20742
1	University of New Mexico Eric H. Wang Civil Eng'g Res Fac ATTN: Technical Library University Station, Box 188 Albuquerque, NM 87131
1	University of Oklahoma Department of Physics ATTN: Prof. R. Fowler 440 W. Brooks, Rm 131 Norman, OK 73069

Aberdeen Proving Ground

Director, USAMSAA
ATTN: DRXSY-D
DRXSY-MP, H. Cohen
Mr. R. Norman, GWD

Cdr, USATECOM
ATTN: DRSTE-TO-F

Dir, USACSL, Bldg. E3516, EA
ATTN: DRDAR-CLB-PA

USER EVALUATION OF REPORT

Please take a few minutes to answer the questions below; tear out this sheet, fold as indicated, staple or tape closed, and place in the mail. Your comments will provide us with information for improving future reports.

1. BRL Report Number ______________________________

2. Does this report satisfy a need? (Comment on purpose, related project, or other area of interest for which report will be used.)

____

____

____

3. How, specifically, is the report being used? (Information source, design data or procedure, management procedure, source of ideas, etc.) ______________________________

____

____

4. Has the information in this report led to any quantitative savings as far as man-hours/contract dollars saved, operating costs avoided, efficiencies achieved, etc.? If so, please elaborate.

____

____

5. General Comments (Indicate what you think should be changed to make this report and future reports of this type more responsive to your needs, more usable, improve readability, etc.) ______________

____

____

____

6. If you would like to be contacted by the personnel who prepared this report to raise specific questions or discuss the topic, please fill in the following information.

Name: ______________________________

Telephone Number: ______________________________

Organization Address: ______________________________

____

____